AFRL-DE-PS-TR-2004-1094

COMPARISON OF RADIOMETRIC AND CHEMOMETRIC SENSITIVITIES FOR HETERODYNE AND DIRECT DETECTION DIAL

Daniel C. Senft, et al.

July 2004

Final Report

APPROVED FOR PUBLIC RELEASE; DISTRIBUTION IS UNLIMITED

AIR FORCE RESEARCH LABORATORY
Directed Energy Directorate
3550 Aberdeen Ave SE
AIR FORCE MATERIEL COMMAND
KIRTLAND AIR FORCE BASE, NM 87117-5776

AFRL-DE-PS-TR-2004-1094

This report has been approved for publication.

// signed on original //

DANIEL C. SENFT, DR-III
Project Manager

// signed on original //

// signed on original //

GREGORY J. VANSUCH, LtCol, USAF	L. BRUCE SIMPSON, SES
Chief, Optics Division	Director, Directed Energy Directorate

REPORT DOCUMENTATION PAGE

Form Approved
OMB No. 0704-0188

1. REPORT DATE *(DD-MM-YYYY)*	**2. REPORT TYPE**	**3. DATES COVERED** *(From - To)*
16-07-2004	Final Report	1 Oct 2001 – 30 Sep 2003

4. TITLE AND SUBTITLE
Comparison of Radiometric and Chemometric Sensitivities for Heterodyne and Direct Detection DIAL

5a. CONTRACT NUMBER
In-House

5b. GRANT NUMBER

5c. PROGRAM ELEMENT NUMBER
62605F

6. AUTHOR(S)
Daniel C. Senft, Diego F. Pierrottet, James A. Dowling, Brian T. Kelly, and Anthony P. Peredo

5d. PROJECT NUMBER
4866

5e. TASK NUMBER
LT

5f. WORK UNIT NUMBER
01

7. PERFORMING ORGANIZATION NAME(S) AND ADDRESS(ES)

Air Force Research Laboratory
Directed Energy Directorate
3550 Aberdeen Ave SE
Kirtland AFB, NM 87117-5776

8. PERFORMING ORGANIZATION REPORT

9. SPONSORING / MONITORING AGENCY NAME(S) AND ADDRESS(ES)
Air Force Research Laboratory/DE
3550 Aberdeen Ave SE
Kirtland AFB, NM 87117-5776

10. SPONSOR/MONITOR'S ACRONYM(S)

11. SPONSOR/MONITOR'S REPORT NUMBER(S)
AFRL-DE-PS-TR-2004-1094

12. DISTRIBUTION / AVAILABILITY STATEMENT

APPROVED FOR PUBLIC RELEASE; DISTRIBUTION IS UNLIMITED.

13. SUPPLEMENTARY NOTES

14. ABSTRACT
The heterodyne / direct detection DIAL comparison (HD/DD DC) experiment series was conducted at Kirtland AFB, NM, to simultaneously characterize and compare the radiometric and chemical detection sensitivities of heterodyne and direct detection DIAL systems. The system developed by the Air Force Research Laboratory Directed Energy Directorate demonstrated the first known programmable and shot-to-shot wavelength-agile heterodyne DIAL measurements. The experiments studied radiometric issues, speckle mitigation through spread spectrum (modelocked) operation, and chemical detection sensitivities. The measurements were performed over horizontal paths at standoff ranges from 4 to 15 km, using both natural and man-made targets. Heterodyne and direct detection radiometric and chemometric results are presented and contrasted, and are compared with predictions from simulations and models.

15. SUBJECT TERMS
Differential absorption lidar (DIAL), heterodyne lidar, wavelength agile DIAL, direct detection lidar, laser remote sensing, laser chemical detection

16. SECURITY CLASSIFICATION OF:			**17. LIMITATION OF ABSTRACT**	**18. NUMBER**	**19a. NAME OF RESPONSIBLE PERSON**
a. REPORT	**b. ABSTRACT**	**c. THIS PAGE**			**19b. TELEPHONE NUMBER** *(include area code)*
Unclassified	Unclassified	Unclassified	SAR	118	505-853-3257

Standard Form 298 (Rev. 8-98)
Prescribed by ANSI Std. 239.18

TABLE OF CONTENTS

LIST OF FIGURES

Abstract

The heterodyne / direct detection DIAL comparison (HD/DD DC) experiment series was conducted at Kirtland AFB, NM, to simultaneously characterize and compare the radiometric and chemical detection sensitivities of heterodyne and direct detection DIAL systems. The system developed by the Air Force Research Laboratory Directed Energy Directorate demonstrated the first known programmable and shot-to-shot wavelength-agile heterodyne DIAL measurements. The experiments studied radiometric issues, speckle mitigation through spread spectrum (modelocked) operation, and chemical detection sensitivities. The measurements were performed over horizontal paths at standoff ranges from 4 to 15 km, using both natural and man-made targets. Heterodyne and direct detection radiometric and chemometric results are presented and contrasted, and are compared with predictions from simulations and models.

Author Affiliations

At the time of report preparation, the authors' affiliations were:

Daniel C. Senft - Air Force Research Laboratory, Directed Energy Directorate
3550 Aberdeen Ave. SE
Kirtland AFB, NM 87117-5776

Diego F. Pierrottet - Coherent Applications, Inc.
7 Sandpiper Ct.
Hampton, VA 23669

James A. Dowling - Applied Technology Associates
1300 Britt St. SE
Albuquerque, NM 87123

Brian T. Kelly - ITT Industries, Advanced Engineering and Sciences Division
5901 Indian School Rd. NE
Albuquerque, NM 87110

Anthony P. Peredo - Textron Systems Corporation
201 Lowell St.
Wilmington, MA 01887

Acknowledgements

The authors would like to thank Textron Systems Corporation and employees for the loan of the modelocking hardware, and for numerous helpful discussions with Dr. Victor Hasson (currently with Trex), Dr. Mark Kovacs, and their colleagues.

1. Introduction

A. Overview

The Heterodyne / Direct Detection DIAL Comparison (HD/DD DC) experiments were designed to provide a direct, simultaneous comparison of the radiometric and chemical detection sensitivities of the two receiver techniques. From October 1998 to September 2003, the HD/DD DC measurements were a main component of the Laser Remote Optical Sensing (LROS) program at the Air Force Research Laboratory Directed Energy directorate (AFRL/DE). In general, it is expected that heterodyne detection will have a significant radiometric sensitivity advantage (by a factor of approximately 10^2 to 10^3) over direct detection.[1] A key issue for heterodyne detection, however, is the sensitivity of the process to speckle, which affects the chemical detection sensitivity. For a direct detection system, it is possible to spatially average multiple speckles across the receiver aperture, thereby reducing the speckle-induced fluctuation in the received signal. For a common single-mode heterodyne receiver, the requirement of having a coherent phase front over the receiver aperture results in a speckle-limited single shot SNR of unity. For the HD/DD DC experiments, a speckle mitigation technique was studied which uses a spread spectrum (modelocked) transmit waveform. In this technique, multiple laser longitudinal modes are transmitted, each of which is speckled independently when returned from a diffuse target with sufficient longitudinal extent. An illustration of the SNR characteristics versus range for each of these techniques is given in Figure 1. The values in the Figure were not calculated for specific systems, but are representative of heterodyne and direct detection systems with similar transmit energies and receiver apertures. A common characteristic of all of the techniques is that at short ranges the SNR will be speckle limited, and therefore mainly independent of range. At some distance, the SNR will become signal limited, and will decrease proportionally with the range squared (R^2), or faster. The heterodyne radiometric advantage is that the breakpoint between speckle-limited and signal-limited operation will occur at significantly greater ranges. The SNR advantage at short ranges in the speckle-limited regime seen for a direct detection system in comparison to a single-mode heterodyne system can be reduced or nearly eliminated by utilizing a spread spectrum transmit waveform. The cost of this improvement in comparison with the more common single-mode heterodyne systems is slightly more complexity in the front end of the heterodyne receiver, where a higher bandwidth capacity is required. This bandwidth can later be reduced by either analog or digital processing to a level similar to that of a single-mode heterodyne receiver. The complexity of the spread spectrum (modelocked) transmitter actually tends to be less than that of a wavelength-agile single-mode transmitter. At short ranges a direct detection system will always have an advantage over a heterodyne system, since direct detection can utilize both spatial averaging and spread spectrum operation to provide speckle mitigation, while heterodyne detection can utilize spread spectrum operation but not spatial averaging. The heterodyne system advantage will always occur for longer range operation, where heterodyning can continue to make measurements after the direct detection system return level has dropped below the system noise floor.

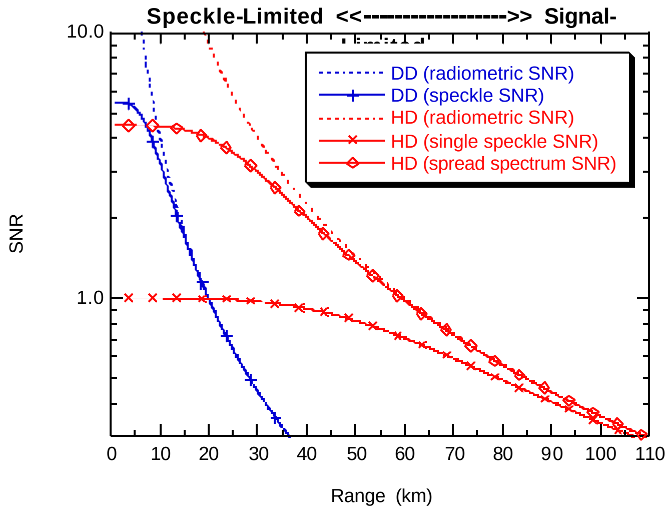

Figure 1. Illustration of spread spectrum heterodyne, single-mode heterodyne, and direct detection SNRs as a function of range.

B. Development Timeline

The Heterodyne / Direct Detection DIAL Comparison (HD/DD DC) experiments utilized components from two separate systems, the Laser Airborne Remote Sensing (LARS) and Coherent Remote Optical Sensing System (CROSS). The LARS program demonstrated the capability of direct detection DIAL measurements from an airborne platform, achieving multiple chemical detection at a one-way standoff slant range of greater than 30 km (see Figure 2)[2]. As the LARS program was concluding, the CROSS efforts began to develop a heterodyne DIAL capability, with the eventual goal of extending the operational range to a one-way standoff slant range of greater than 80 km. The development timeline for the LARS and CROSS systems is shown in Figure 3. The primary development required for the CROSS program was a wavelength agile, stable CO_2 local oscillator capable of high pulse repetition frequency (PRF) operation (with an eventual PRF goal of greater than 1 kHz). The Wavelength Agile Local Oscillator (WALO) was developed to meet the goals of the CROSS system[3], and is discussed in more detail later in this report.

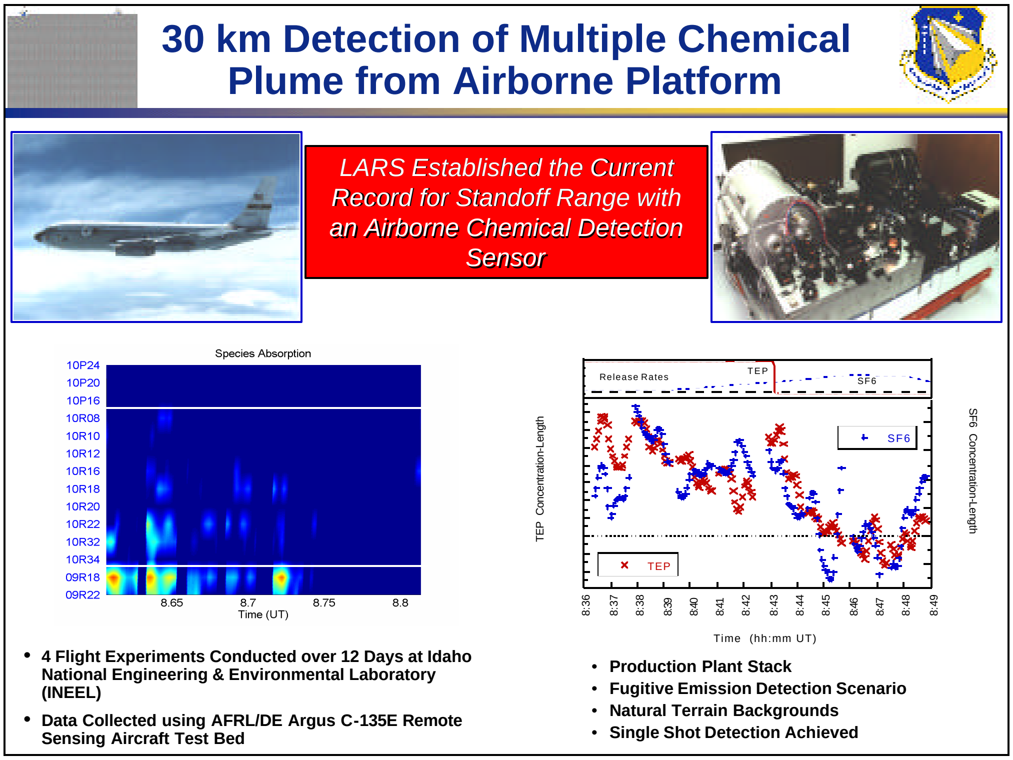

Figure 2.Airborne chemical detection at 30 km slant range using LARS direct detection system.

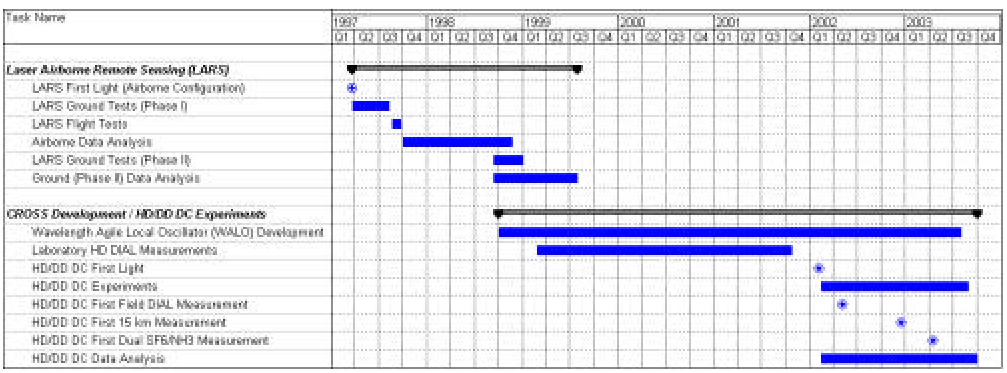

Figure 3. Development schedule for LARS, CROSS, and HD/DD DC experiments.

2. Experimental Information and Configuration

A. HD/DD DC Equipment Description

The layout of the equipment used in the HD/DD DC experiments is shown in Figure 4. The various subcomponents will be described in more detail in the following sections. A common transmitter was used as the illumination source for both the heterodyne and direct detection receivers. The transmitted light was passed through a gas absorption cell, and the optical return signal for both receivers also passed through the gas cell.

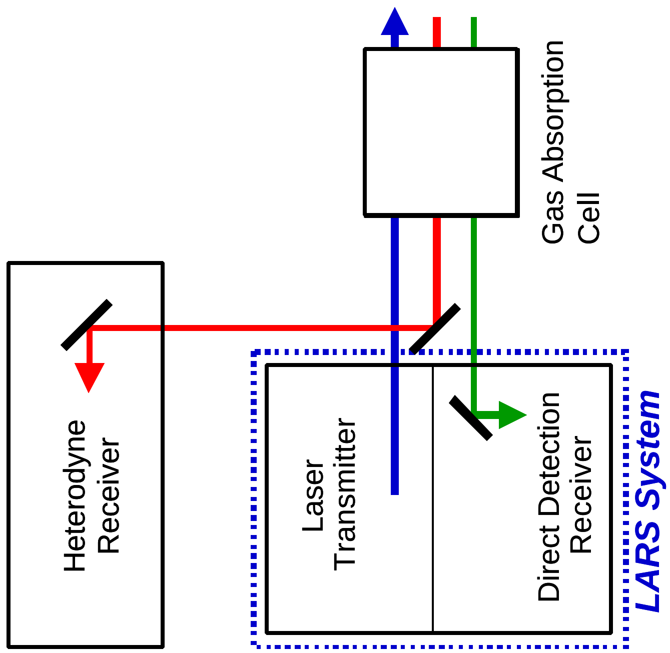

Figure 4. Layout of transmitter, direct detection receiver, and heterodyne receiver for Heterodyne / Direct Detection DIAL Comparison (HD/DD DC) experiments.

B. Transmitter System

The Breadboard Oscillator (BBO) CO_2 laser developed by Textron Systems Corporation was utilized as the transmitter for the Heterodyne / Direction Detection DIAL Comparison (HD/DD DC) experiments. The BBO laser was also used in the Laser Airborne Remote Sensing (LARS) program, which developed an airborne direct detection DIAL system that demonstrated simultaneous detection of multiple chemicals at ranges of greater than 30 km (see Figure 2). The laser and associated cavity optics are shown mounted on the left-hand side of the LARS airborne optical bench in Figure 5. The BBO laser is an RF-excited transverse electric

atmospheric (TEA) CO_2 laser with output pulse energies of greater than 4 J on strong CO_2 transition lines, and a pulse repetition frequency (PRF) of up to 30 Hz. For the HD/DD DC experiments the laser PRF was limited to approximately 1 Hz by the capabilities of the data acquisition and control system. The laser uses a mechanical grating to change the output wavelength in a programmed sequence. The HD/DD DC experiments commonly utilized sequences consisting of 12 to 13 of the approximately 60 laser lines accessible by the BBO using the $^{12}C^{16}O_2$ isotope in the laser gain medium. To investigate speckle mitigation the laser operation was often alternated between non-modelocked and modelocked configurations for successive data sets. In both configurations the laser had multiple longitudinal mode output, but modelocked operation resulted in more longitudinal modes, with higher and more stable amplitudes. The key parameters for the BBO laser are given in Table 1.

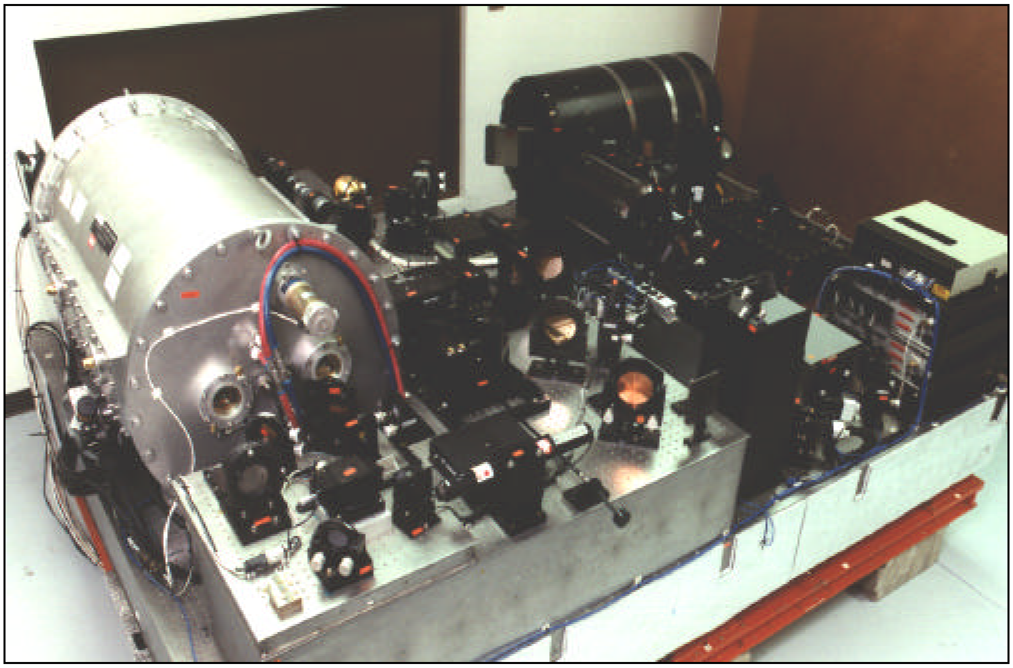

Figure 5. Photograph of BBO laser and system on Argus flight bench.

C. Direct Detection Receiver

A diagram of the LARS bench, comprising both the laser transmitter and the direct detection receiver, is shown in Figure 6. The transmit optical path is shown in blue, and is primarily on the left side of the optical bench. The direct detection receive signal is shown in purple on the right side of the optical bench. The direct detection receiver utilizes a 16" diameter reflective telescope, with a secondary / pickoff mirror obscuration. The receive light is focused onto a 0.500 mm diameter liquid nitrogen cooled HgCdTe detector with a bandwidth of 80 MHz. The

signal from the detector is sampled at 60 MSa/s, and stored by the LARS Acquisition and Processing System (LAPS) for use in both quick-look and offline analysis.

Table 1. BBO Laser Key Parameters

Parameter	Value
CO_2 Isotope	$^{12}C^{16}O_2$ $^{13}C^{16}O_2$
Pulse Energy	> 4 J (strong line, using $^{12}C^{16}O_2$) > 50 mJ (weak line)
Pulse Repetition Frequency	30 Hz (maximum) 10 Hz (nominal) 1 Hz (HD-DD DC experiments)
Wavelength Tuning Capability	Single shot
Number of Accessible Wavelengths	~ 60 ($^{12}C^{16}O_2$ isotope) ~ 50 ($^{13}C^{16}O_2$ isotope)
Pulse Type	Gain switch spike with relaxation tail
Pulse Width	~ 10 μs (non-modelocked) ~ 6 μs (modelocked)
Beam Divergence	~ 1.0 mrad (from laser) 0.285 mrad (transmitted downrange)

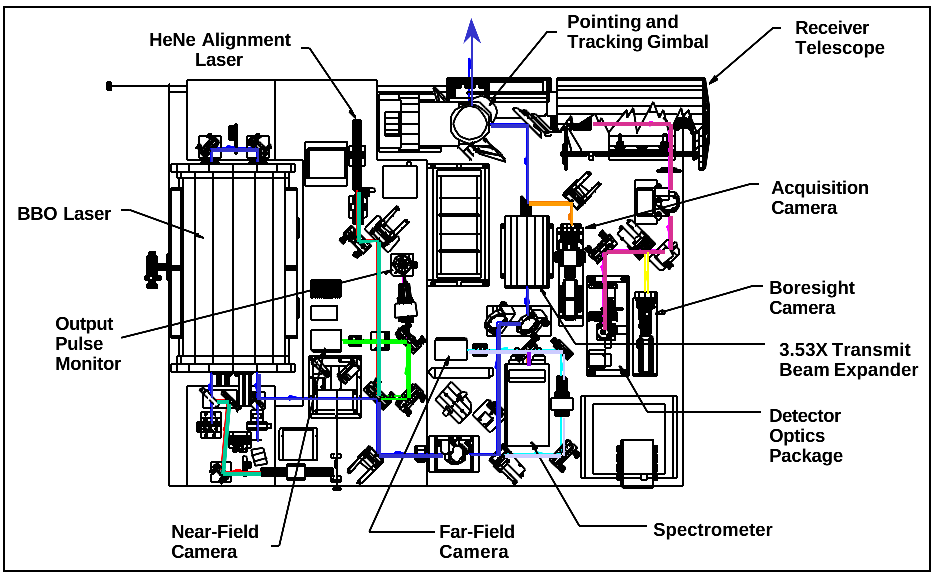

Figure 6. Plan view of laser transmitter and direct detection receiver.

D. Wavelength Agile Local Oscillator (WALO)

The Wavelength Agile Local Oscillator (WALO) was developed for stable wavelength agile operation at high PRFs (> 20 Hz). The WALO uses a cavity waveguide for the CO_2 gain medium, with acousto-optic modulators (AOMs) inside the laser cavity for wavelength tuning. Prior wavelength agile CO_2 local oscillators had used mechanical tuning of diffraction gratings, which tended to be unstable at high PRF operation (> 20 Hz), due to the mechanical settling time of the moving grating fixture. The WALO utilized paired AOMs to achieve high PRF, stable wavelength agile operation. Since the AOMs utilize acoustic waves to change the wavelength of light transmitted, the tuning time limit was determined by the propagation time of the acoustic wave in the transverse direction across the AOM, and the stabilization time of the CO_2 laser into CW operation. Tuning rates of 500 Hz were demonstrated with the WALO, which was well beyond the tuning capability of the transmitter laser used in the HD/DD DC experiments. Tuning rates of many kHz have been demonstrated by other research groups utilizing AOMs with CO_2 waveguide lasers, so the tuning rates used for the WALO are not at the limits for this type of technology. Since there are no moving parts in the design, the WALO is relatively robust, and well suited to operation in both field and airborne environments.

E. Heterodyne Receiver

The CROSS heterodyne receiver is shown in Figure 7. The receive signal and WALO beams are combined using a beam splitter, and are focused onto a 0.100 mm x 0.100 mm square HgCdTe detector with a bandwidth of 800 MHz.

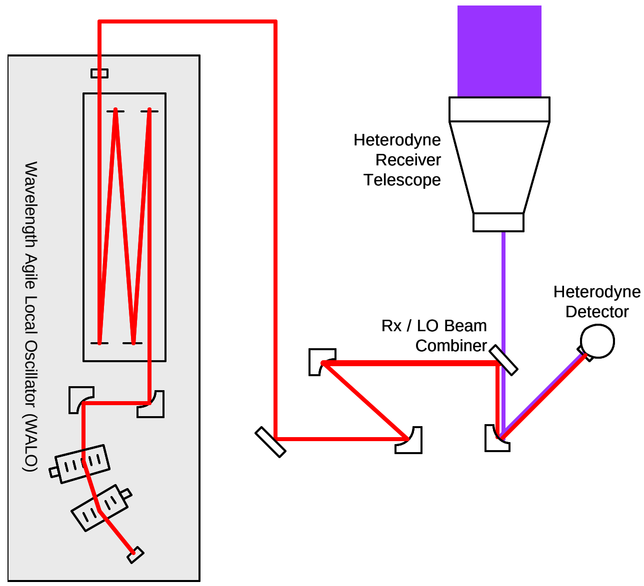

Figure 7. Layout of heterodyne receiver with Wavelength Agile Local Oscillator (WALO).

F. Gas Cell

The gas cell used in the HD/DD DC experiments (see Figure 8) is a 4’ x 4’ x 4’ aluminum cube, with IR-transmissive polyethylene windows on two sides. The gas cell was designed for both gas and liquid chemical insertion. Gas valves are incorporated into the side panels, and a funnel mechanism with heated Petry dish is mounted on the top panel to evaporate chemicals inserted in liquid form. Fans are mounted inside the cell to provide uniform mixing of the chemicals inserted. The cell has been used with gaseous sulfur hexafluoride (SF_6), gaseous ammonia (NH_3), and liquid ammonium hydroxide (NH_4OH). For the HD/DD DC experiments, only the chemicals in gaseous form (SF_6 and NH_3) were used. Insertion of gaseous chemicals was performed by filling sample cylinders with pure gas to above the ambient atmospheric pressure. The sample cylinders were connected to valves on the side of the gas cell (note sample cylinder attached to valve on right side of cell in Figure 8 photo), which were opened at the desired point in the experiment to insert the excess pressure from the sample cylinders into the cell. After a few seconds the valves were again closed, to prevent all of the gas in the sample cylinders from leaking into the cell. Although this insertion procedure is not extremely precise, it provides a relatively simple method to achieve reasonably predictable and repeatable results. From viewing the DIAL absorption plots, it appears that the internal cell fans cause complete mixing of the chemicals in the cell within 10 sec. The quick-release door panels were removed to rapidly evacuate the inserted chemicals between data sets.

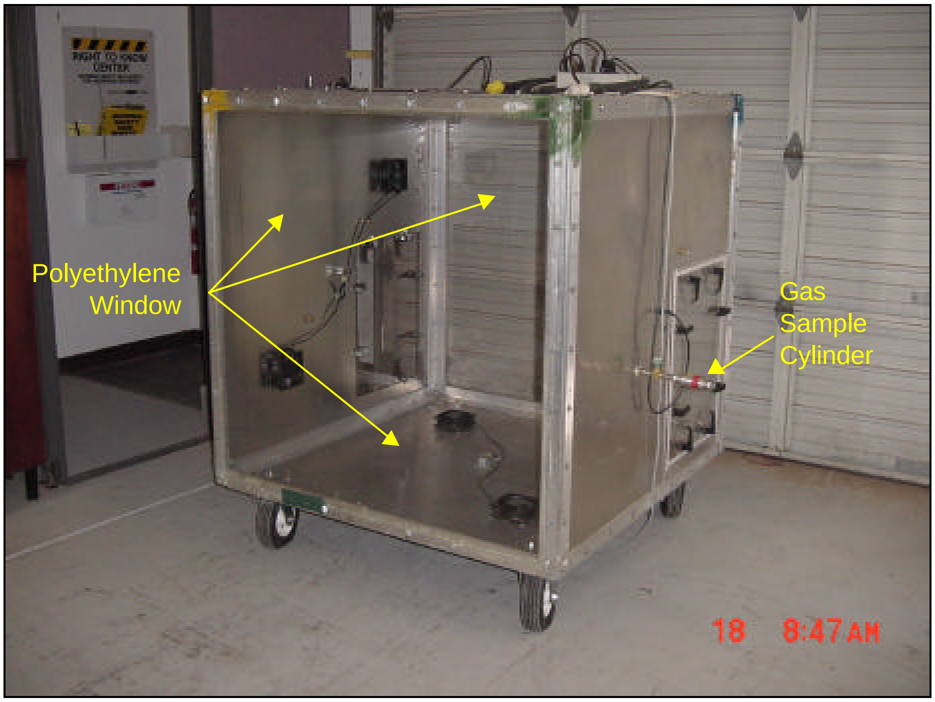

Figure 8. Photograph of 4’ x 4’ x 4’ gas cell.

G. Target Sites

Target sites at one-way ranges of 4.320 km (4KS), 7.460 km (7KS), and 14.9 / 15.3 km (15KS) were developed for use in the HD/DD DC experiments. Other target sites were also available at approximately 2 km (2KS), 5 km (5KS), and 6 km (6KS), but were not used in the HD/DD DC experiments, other than for alignment purposes. Figure 9 shows the beam paths from the transmitter location in Building 770 (B770) on Kirtland AFB, to the various target sites. The

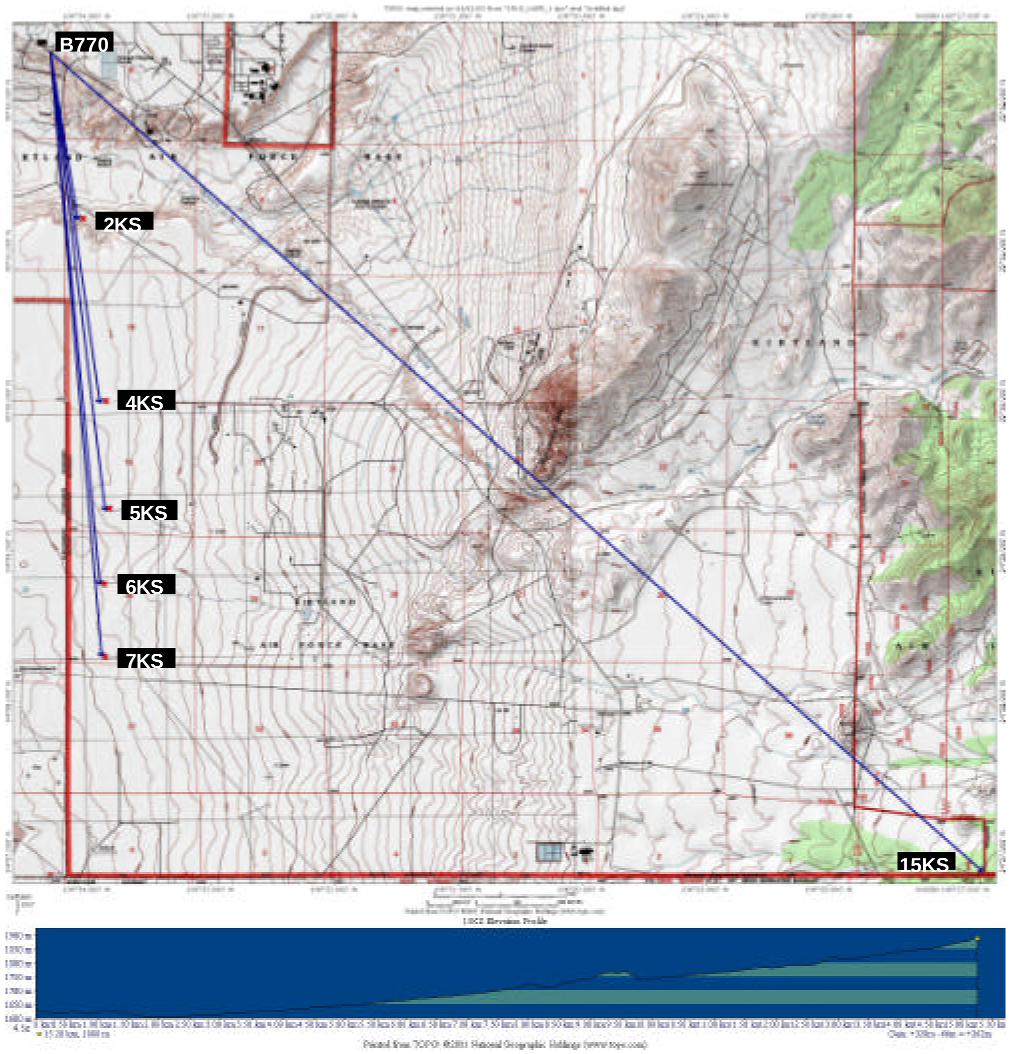

Figure 9. Topographic map with beam paths (blue arrowed lines) from B770 to 2KS, 4KS, 5KS, 6KS, 7KS, and 15KS sites. The elevation profile from B770 to the 15KS target is shown below the map.

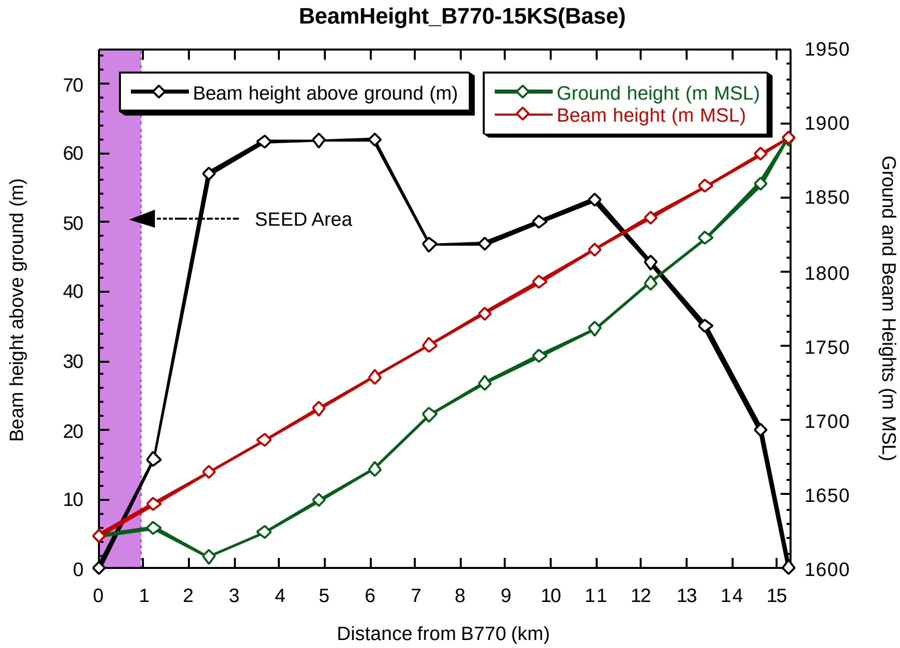

Figure 10. Beam height and elevation profile from B770 to the 15KS target.

propagation paths to all of the target sites were within 5º of horizontal, and within 100 m of the ground at all locations along the paths. The elevation profile from B770 to the 15KS target is also shown at the bottom of Figure 9, and is representative of the general elevation profile characteristics for all of the target sites. A more detailed plot showing the beam height and elevation profile from B770 to the 15KS target is given in Figure 10. A weather station was operated next to B770 to provide atmospheric pressure, temperature, and humidity measurements during the experiments. This information was input into HITRAN-PC, which was then used to calculate the expected atmospheric transmission along the propagation path.

Photographs of the target sites are shown in Figures 11-15. Figure 11 shows blueboard and flame-sprayed aluminum (FSA) targets at the 2KS site used for pointing alignment and system calibration. Figure 12 shows the blueboard and berm area targets at the 4KS site. At the time the photograph in Figure 12 was taken, only a single blueboard target was present. In early April 2003 another blueboard target using non-weathered blueboard panels was constructed and placed between the old blueboard target and berm illumination locations. Aluminum alignment targets and the berm illumination area for the 7KS site are shown in Figure 13. The 15KS blueboard target is shown in Figure 14. Two different 15KS target sites were used during the HD/DD DC experiments. The first 15KS site was located at ~ 14.9 km, and was used

until the end of 2002. The second 15KS site was located at ~ 15.3 km, and was used starting in 2003. The great majority of the experimental measurements were conducted using the second site, and all 15KS information given in this report pertains to this location, unless specifically stated otherwise. A photograph of the propagation path from B770 to the 15KS target board is shown in Figure 15.

Figure 11. Photographs of left and right sides of the 2KS site, showing the blueboard target (left, 8’ x 8’) and flame-sprayed aluminum (right, 4’ x 4’) calibration targets.

Figure 12. Photograph of 4KS target site, showing blueboard target (right of photograph) and approximate berm illumination area (yellow circle, not exactly to scale). In April 2003 a second target using non-weathered

blueboard panels was constructed and placed on the berm (yellow rectangle).

Figure 13. Photograph of 7KS target site, showing aluminum (right) and plywood (left) calibration/pointing target boards and approximate berm illumination area (yellow circle, not exactly to scale).

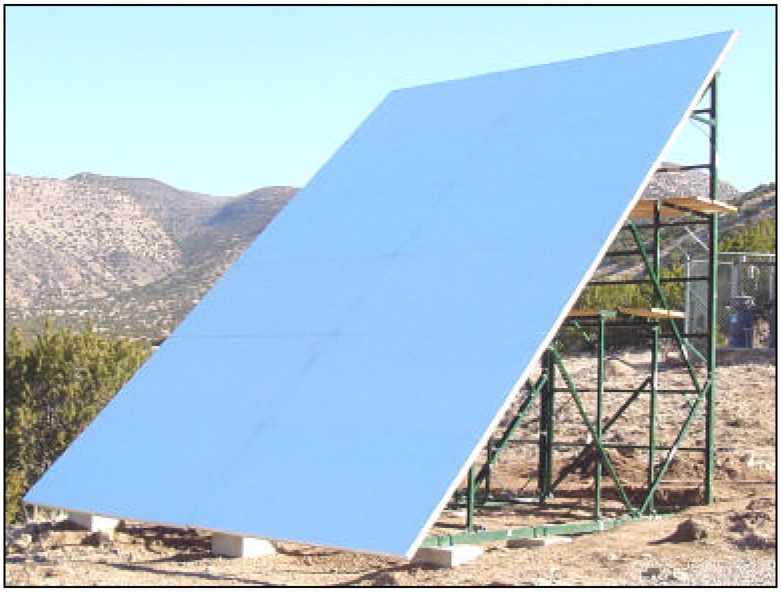

Figure 14. Photograph of 15KS blueboard target.

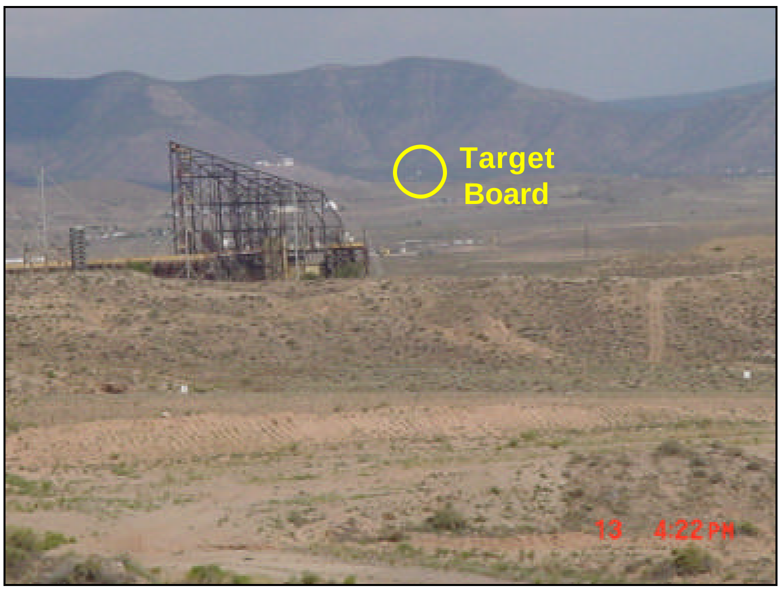

Figure 15. Photograph of propagation path from B770 to 15KS blueboard target.

Panels of blueboard insulation (8' x 4' x 2") were specially prepared for use at the target sites. The preparation method consisted of removing the external extruded surface using a 120-grit belt sander, thereby exposing the diffuse high reflectivity internal material. It was necessary to remove the external surface on all surfaces to prevent warping of the blueboard sheets. The dimensions of the blueboard target at the 4KS site were 12' long by 8' wide', and the target was placed at approximately a 60º angle of incidence, resulting in a 6' long x 8' wide target cross section. The beam diameter at the 4KS target is approximately 4' (285 μrad full-angle divergence in output space) to the second null of the transmitted beam far-field distribution, which includes ~ 85% of the total beam energy. The blueboard target at the 15KS site was 24' length x 16' width at a 45º angle of incidence, resulting in a 17' x 16' target cross section. The beam diameter at the 15KS target is approximately 9' to the second null of the far-field distribution.

Dirt berms were also used as targets at the 4KS and 7KS sites. The dirt berm reflectivity, calculated from calibrated direct detection measurements at the 4KS site, was determined to approximately match a Lambertian reflector with a total reflectivity of 3%, for angles from normal to near grazing incidence. For the approximate incidence angle of 60º for the berms, the reflectivity is therefore approximately 0.005 sr^{-1}. The blueboard and berm solid-angle reflectivities are given in Table RR1 for the various target angles used in the HD/DD DC experiments. The blueboard provides a high reflectivity for 10 μm radiation, and the reflectivity does not decrease as quickly with increasing incidence angle as would occur for a Lambertian target. It should also be noted that the blueboard reflectivities were measured in the laboratory immediately after the blueboards were prepared. The radiometric results which will be presented later in this report suggest that the blueboard reflectivity decreased significantly as the boards weathered, since they were continuously exposed to the outside elements once they were installed at the target sites. Laboratory reflectivity measurements have not been conducted on the weathered blueboards.

Table 2. Blueboard and dirt berm reflectivities

Target Material	Incidence Angle	Reflectivity (sr^{-1})
Blueboard	0º	0.094
Blueboard	45º	0.070
Blueboard	60º	0.064
Dirt berm	60º	0.005

3. Transmit and Receive Temporal and Frequency Characteristics

A detailed understanding of the temporal and frequency characteristics of the laser transmit and receive signal is required to develop accurate analysis procedures. The modelocked (spread spectrum) operation implemented to provide speckle mitigation in the heterodyne DIAL measurements differs significantly from the more commonly used single-mode heterodyne technique, and necessitates more demanding system requirements (primarily the ability to record wideband heterodyne signals, rather than narrowband signals centered on the heterodyne intermediate frequency). The signal-to-noise ratio (SNR) advantages of narrowband operation can be recovered in post-processing of the wideband signals, because of the frequency-fence structure of the laser modes. As will be shown, the laser frequency modes are narrow, and occur at spacings determined by the laser cavity length, allowing the processing bandwidth to be reduced to only those regions where the return signal occurs. Since most of the measurements reported in this paper have reasonably good heterodyne SNR values, this processing bandwidth reduction was studied, but was not implemented for the analysis results presented.

A. Modelocked Characteristics

The temporal and temporal frequency characteristics for a single outgoing modelocked laser pulse are shown in Figure 16. The outgoing (monitor) pulse characteristics were captured using direct detection of a small portion (< 1%) of the outgoing beam energy. Figure 16(a) shows the common CO_2 laser temporal pulse shape, which is composed of a gain-switch spike and a relaxation tail. An expanded view showing the modelocked pulse train is given in Figure 16(b). The temporal frequency power spectrum showing the multiple cavity longitudinal modes for the direct detection monitor pulse is shown in Figure 16(c). The modelocked characteristics are achieved by placing into the BBO laser cavity an acousto-optic modulator (AOM) with a sinusoidal variation which matches the cavity round-trip time. The AOM sinusoidal variation forces the laser cavity longitudinal modes to be in phase with each other, resulting in the modelocked temporal pulse train. Modelocking also tends to generate more longitudinal cavity modes with more stable amplitudes than allowing the laser to free-run with multiple longitudinal modes (as will be seen in Figures 19 to 21). The variations from perfect theoretical modelocking operation seen in the BBO laser pulses are believed to result mainly from the gradual degradation of the optical coatings on the intra-cavity AOM. The AOM was coated primarily for operation at 11.15 μm ($^{13}C^{16}O_2$ 10P20), but was primarily used in the HD/DD DC experiments over the wavelength range 10.25 to 10.70 μm. In addition, the AOM is an element in an open-air laser cavity, and is therefore in a high energy density region which is not completely protected from dust particles and contaminants. An increase in the visible degradation of the optical coating and in the difficulty in obtaining optimal modelocking operation was noted during the progress of the experiments, starting with the insertion of the modelocker in January 2002, and continuing until the final experiments in August 2003.

The received temporal heterodyne signal for modelocked operation is shown in Figure 17(a), with an expanded version shown in Figure 17(b). Since the transmitted modelocked laser beam contains multiple longitudinal modes, the transmit laser and local oscillator were not frequency locked, and multiple intermediate frequencies (up to 100's of MHz) are present in the heterodyne signal. The heterodyne modulation of the modelocked micropulses is especially evident in Figure 17(b).

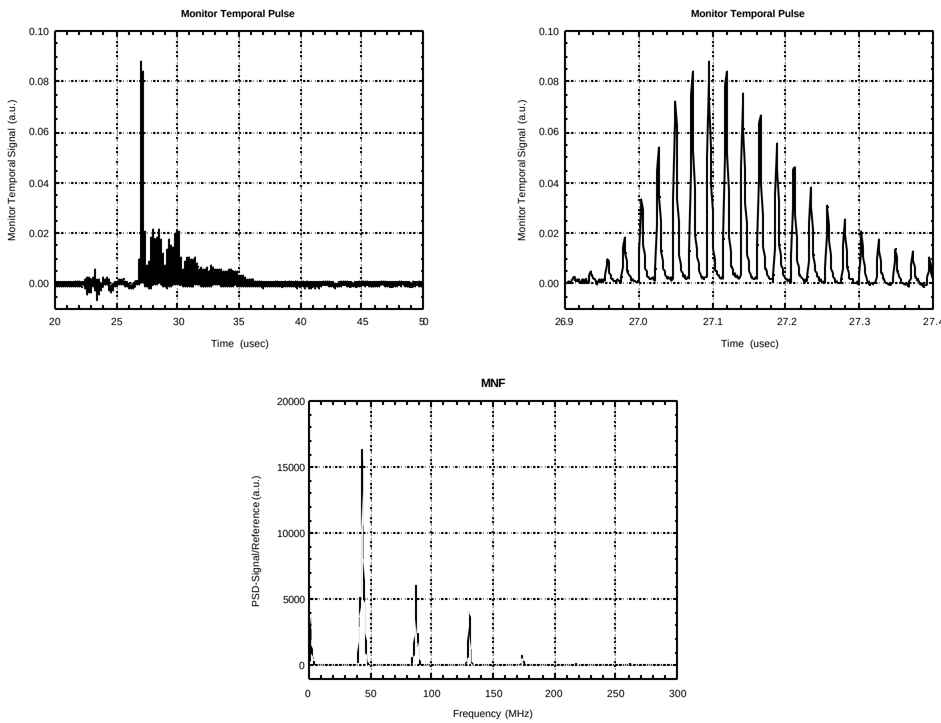

Figure 16. Modelocked laser temporal pulse (direct detection). (a) entire pulse waveform, (b) expanded time scale, (c) temporal frequency spectrum.

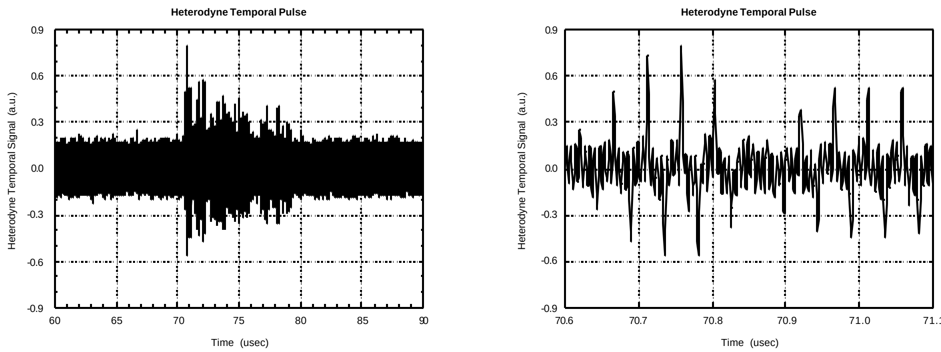

Figure 17. Heterodyne receive signal from a modelocked laser pulse. (a) entire pulse waveform, (b) expanded time scale.

Heterodyne temporal frequency spectra for modelocked operation are shown in Figure 18. The superimposed heterodyne spectra of the signal and local oscillator [calculated from 70-83 μs in Figure 17(a)] are shown in Figure 18(a). The homodyne spectra for the local oscillator [calculated from 61-66 μs in Figure 17(a)], with the DC component removed, are shown in Figure 18(b). The local oscillator output actually consists of a dominant single longitudinal cavity mode, with two smaller features, which are denoted as 'spurs'. The spurs occur at the single and double AOM frequency shifts (approximately 77 and 154 MHz). They are believed to result from slight impurities in the local oscillator dual intra-cavity AOMs, which causes some of the unshifted (in wavelength) beam to be scattered into the direction of the shifted beam. Since this can happen in both of the AOMs, the local oscillator output can consist of three frequencies, the desired frequency, a single-shifted frequency, and a double-shifted frequency. The exact frequency shifts are slightly different for each local oscillator wavelength, since the AOM frequency shift required is dependent upon the output wavelength desired.

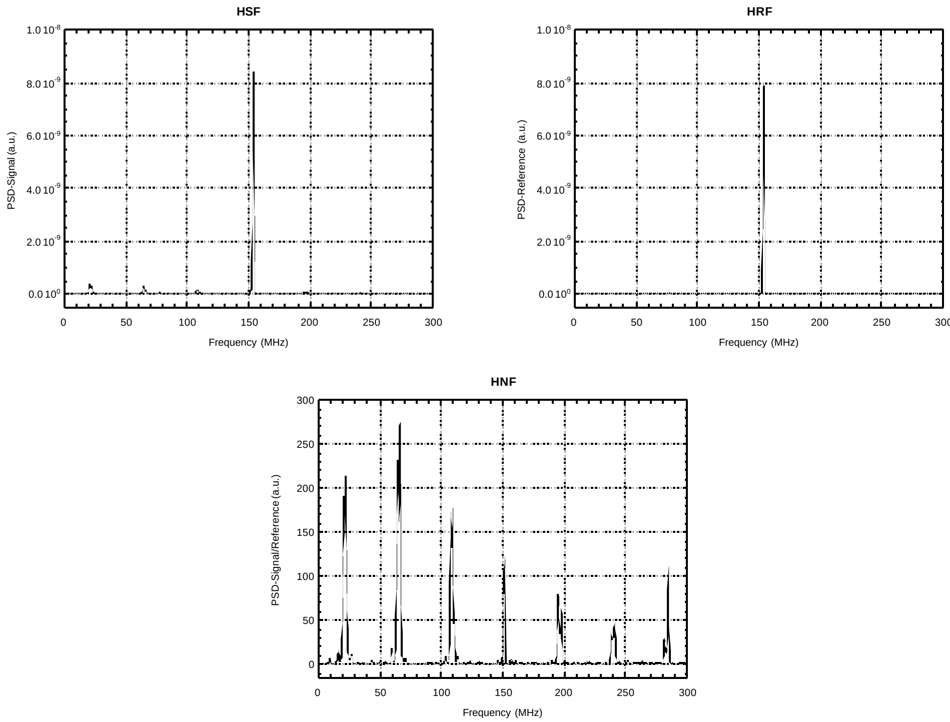

Figure 18. Heterodyne receive signal temporal spectra from a modelocked laser pulse. (a) signal + local oscillator, (b) local oscillator only, (c) normalized signal [(signal + local oscillator) / (local oscillator)].

The optical power in the spurs is more than 3 orders of magnitude less than that in the main local oscillator output, and would not be evident in most heterodyne measurements. In many laboratory or short-range heterodyne measurements, the return signal level would be much higher than that in the spurs. Also, for many heterodyne systems a single longitudinal mode transmitter is used, and the intermediate frequency and associated receiver passband would be significantly lower than the first spur frequency. In the case of the HD/DD DC measurements, however, wideband heterodyne detection is required because of the multiple longitudinal mode (MLM) nature of the transmitter, and the received signal optical power levels are of the same order of magnitude as those of the local oscillator spurs. A number of physical methods to eliminate or significantly reduce the spurs were studied, but it was determined that a simpler and less costly option was to remove the spurs in the processing algorithms. The normalization procedure used for spur removal is described in more detail in the data processing section. It should also be noted that the noise level evident in Figure 17(a) is mainly caused by the 154 MHz beating of the main LO frequency component with the second spur, and not by the local oscillator shot noise.

The heterodyne signal temporal frequency power spectrum for modelocked operation is shown in Figure 18(c), after the normalization procedure has been applied. As seen in the Figure, the local oscillator spurs at approximately 77 and 154 MHz are removed by the normalization procedure, and only the transmit laser cavity modes are present. The laser cavity modes are separated by approximately 44 MHz, which corresponds to the cavity round-trip time (~ 23 ns for a 3.4 m laser cavity length). The double peak nature of the frequency modes in Figure 18(c) is believed to result from the DC wrap-around inherent in the periodogram computation process, with the negative frequency modes happening to nearly fall back onto the positive frequency modes. Multiple-peak modes can also result from the transmit laser containing some multiple TEM output, but this is not believed to be the case in this instance.

B. Non-Modelocked Characteristics

The temporal and temporal frequency characteristics for a non-modelocked output pulse are shown in Figure 19, similar to the presentation in Figure 16 for a modelocked pulse. The gain-switch spike and relaxation tail are again evident. A small after pulse (at 39-40 μs in the plot), probably resulting from continued RF pumping during the pulse and incomplete cavity dumping, is also present for this specific pulse. The expanded scale in Figure 19(b) shows a significant difference between non-modelocked and modelocked operation. The effects of MLM operation are evident in the partial micropulse temporal structure, but the pulses are overlapped rather than distinct because the longitudinal cavity modes are not phase matched, as is the case in modelocked operation. The frequency modes are shown in Figure 19(c). Multiple modes are present, but as seen in comparison with Figure 16(c), there are fewer modes for non-modelocked operation, with a more rapid decrease in amplitude away from the main mode. This mode structure indicates that non-modelocked operation will result in some speckle mitigation, but not as much as for modelocked operation.

The heterodyne receive signal from the non-modelocked pulse is shown in Figure 20. The heterodyne modulation is evident in Figure 20(b), and follows the pulse envelope seen in Figure 19(b).

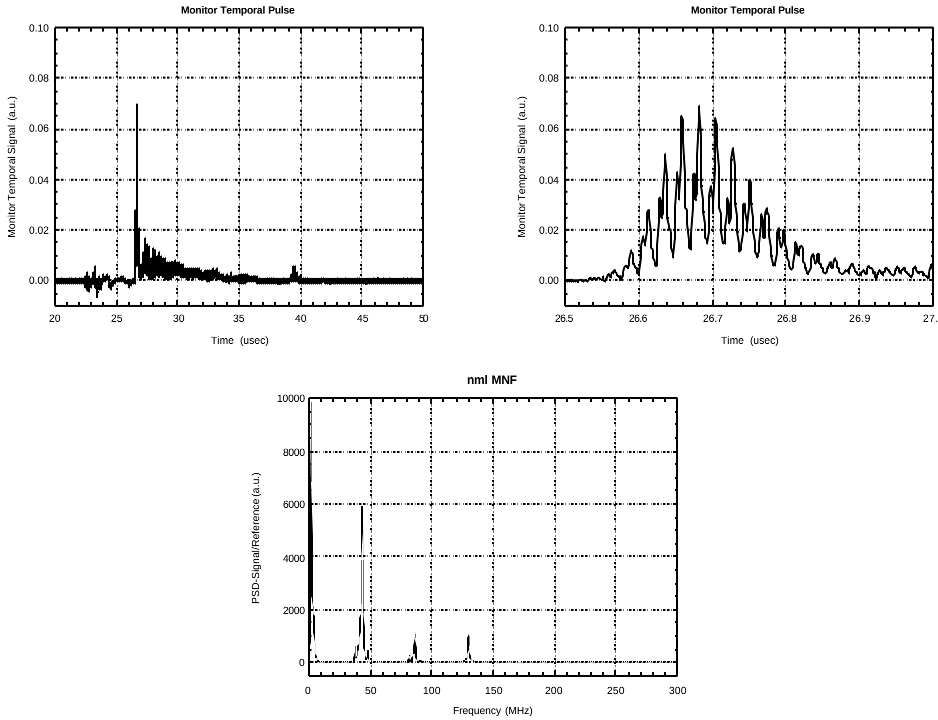

Figure 19. Non-modelocked laser temporal pulse (direct detection). (a) entire pulse waveform, (b) expanded time scale, (c) temporal frequency spectrum.

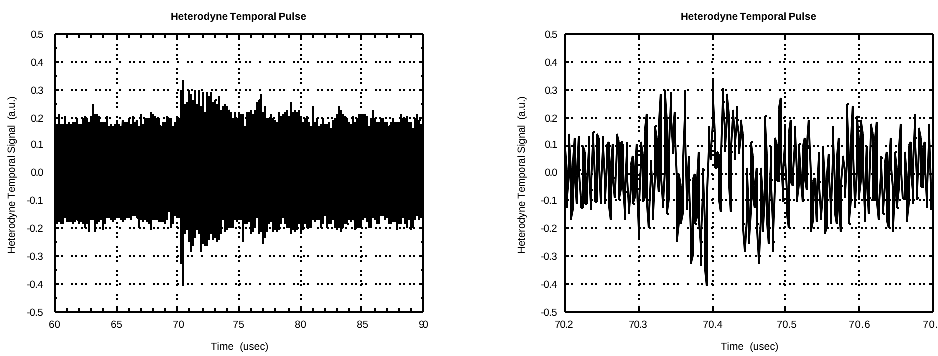

Figure 20. Heterodyne receive signal from a non-modelocked laser pulse. (a) entire pulse waveform, (b) expanded time scale.

The heterodyne signal spectra for non-modelocked operation are shown in Figure 21, in similar fashion to that for modelocked operation shown in Figure 18. In this case, the normalized spectrum shown in Figure 21(c) shows the effect of the DC wrap-around, where the set of frequency modes marked as (1) can be considered as the positive frequency modes, and those marked as (2) can be considered as the wrapped negative frequency modes. With this unwrapping, it can again be seen that the frequency mode spacing is approximately 44 MHz, as expected. Comparing Figure 21(c) and 18(c), it can be seen that the modelocked spectrum contains more modes with higher amplitudes than the non-modelocked spectrum, indicating that modelocked operation will result in a greater degree of speckle mitigation.

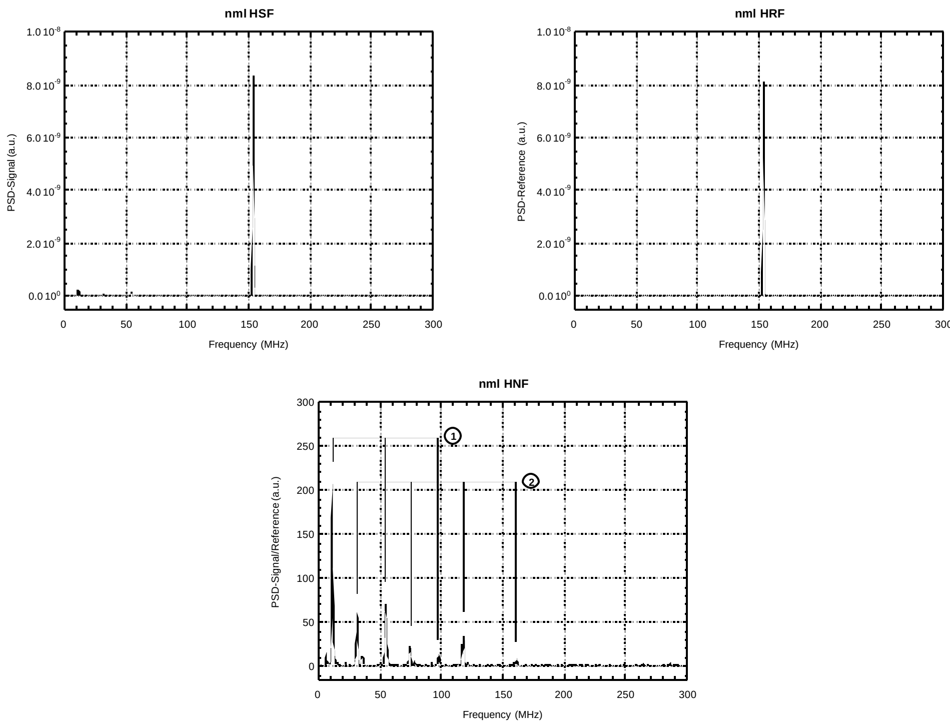

Figure 21. Heterodyne receive signal temporal spectra from a non-modelocked laser pulse. (a) signal + local oscillator, (b) local oscillator only, (c) normalized signal [(signal + local oscillator) / (local oscillator)].

4. Data Analysis and Results

A. Overview

As described previously, the development of the Coherent Remote Optical Sensing System (CROSS) began in October 1998, as the Laser Airborne Remote Sensing (LARS) program was nearing completion. Equipment development, laboratory system characterization and DIAL measurements, and preliminary open-air measurements were conducted during 1999, 2000, and 2001. Although the system continued to be upgraded and improved, the system components remained essentially the same after the HD/DD DC measurements began in February 2002. The data sets included in the radiometric, DIAL, and system characterization analyses for this report are shown in reverse chronological order in Appendix A, Table A1.

B. Radiometric Theoretical Analysis

The differential absorption lidar (DIAL) technique utilizes the variations in absorption at different interrogation wavelengths to determine a ‘spectral fingerprint’ in order to detect and quantify chemicals in the laser path. In the simplest scenario, this can be thought of as a two-wavelength system, with one wavelength tuned to an absorbing feature of a chemical, and the other wavelength used as a reference which is not absorbed. In a more general and realistic scenario, the DIAL problem can be posed in terms of using a sequence of N laser wavelengths to determine the concentrations for M chemicals. For the general case, the commonly presented 2-wavelength DIAL approach may not be usable, since the absorption of one chemical may interfere with either the on- or off-absorption wavelength of another chemical. It should be noted that conceptually there is no difference in the DIAL technique between measuring the concentrations (see Eq. 1) of the M_a atmospheric and M_m target gases, although more laser wavelengths are required to measure more gases. In the HD/DD DC experiments, the M_a contributions were determined by measuring the atmospheric pressure, temperature, and humidity, and determining the expected atmospheric transmission (τ_a) using an atmospheric model (HITRAN-PC). The DIAL equation for using N laser wavelengths to measure M (specifically M_m) target gases can be written in the following form

$$\begin{aligned} E_r(\lambda) &= E_L(\lambda)\eta_x(\lambda)\eta_{ov}\rho(\lambda)\Omega\eta_r(\lambda)\prod_{a=1}^{M_a}\exp\left(-2\int_0^R \kappa_a(\lambda)C_a(R')\,dR'\right) \\ &\quad\times\prod_{m=1}^{M_m}\exp\left(-2\int_0^R \kappa_m(\lambda)C_m(R')\,dR'\right) \\ &= E_L(\lambda)\eta_x(\lambda)\eta_{ov}\rho(\lambda)\frac{A_r}{R^2}\tau_a^2(\lambda)\eta_r(\lambda)\prod_{m=1}^{M_m}\exp\left(-2\kappa_m(\lambda)(CL)_m\right) \end{aligned} \tag{1}$$

where E_r = return energy incident on detector

E_L = laser transmit energy

η_x = system optical transmission efficiency

η_{ov} = overlap factor for transmitted beam footprint at the target, target size, and receiver field-of-view

ρ = ground reflectivity (per solid angle)

Ω = solid angle subtended by the receiver

η_r = system optical receiver efficiency

M_a = total # of absorbing atmospheric gases

κ_a = absorption coefficient of a^{th} atmospheric constituent

C_a = concentration of a^{th} atmospheric constituent

M_m = total # of absorbing target gases

κ_m = absorption coefficient of m^{th} target gas

C_m = concentration of m^{th} target gas

A_r = area of receiver

R = one-way range from transmitter to target

τ_a = one-way atmospheric transmission (includes absorption of all M_a atmospheric constituents)

$(CL)_m$ = $\int_0^R C_m(R')\,dR'$, concentration-length product for m^{th} target gas.

The above equation assumes a hard target is providing the return signal, and therefore a column-content measurement is being made. If a distributed target, such as the atmosphere or aerosols, provides the return mechanism, the received signal will be spread in time, and a range-resolved measurement will be made. The chemometric analysis is performed similarly for both column-content and range-resolved measurements, but must be done for each range window in the range-resolved case. Most long range systems utilize column-content measurements because of the significantly larger return signal level occurring from hard targets as compared to atmospheric or aerosol backscatter.

C. Direct Versus Heterodyne Detection Signal Processing Issues

The differences in the physics of the detection processes between direct and heterodyne detection requires a complete and accurate understanding of the signal processing techniques that are used. One issue that needs to be considered in the heterodyne detection case, is that the commonly derived heterodyne SNR relation

$$SNR_{HD} = \eta_{qe} \frac{\langle P_r \rangle}{h\nu} \frac{1}{2B} \tag{2}$$

for continuous wave heterodyne operation is not directly applicable to the case of a pulsed laser, where the signal will be integrated to provide a result proportional to the received energy E_r.

In the case of direct detection, the relationships between the current out of the detector I_{DD}, the instantaneous power received P_r, and the received energy E_r are given by

$$\begin{aligned} I_{DD}(t) &\propto |\varepsilon_r(t)|^2 \cong |a_r(t)\cos(\omega_r t + \varphi_r)|^2 \cong \frac{1}{2}|a_r|^2 = P_r(t) \\ U_{DD} &= \int_{\Delta T} I_{DD}(t)\,dt \propto \int_{\Delta T} P_r(t)\,dt = E_r \end{aligned} \quad . \tag{3}$$

The measured value U_{DD} is the parameter required for both radiometric and DIAL analysis. Since it is proportional to E_r, it is then also directly proportional to the total transmission of the target gases of interest. The processing is actually more complicated than the simple relation given in Eq. 3, but the key relationship between U_{DD} and E_r is retained. The details of the processing are given in Appendix C, where the code for the primary direct detection Matlab calculation program DATREDUC.m is reproduced.

Determining an equivalent heterodyne parameter U_{HD} to the direct detection parameter U_{DD} is significantly more complicated. There are many different ways to calculate a U_{HD} parameter for heterodyne detection, all of which are valid (but not necessarily optimal) as long as U_{HD} is directly proportional to the received energy E_r. In the case of heterodyne detection, the current out of the detector is given by

$$\begin{aligned} I_{HD}(t) &\propto |\varepsilon_r(t) + \varepsilon_{LO}(t)|^2 = |a_r(t)\cos(\omega_r t + \varphi_r) + a_{LO}(\cos\omega_{LO} t + \varphi_{LO})|^2 \\ &\cong |a_r(t)|^2\cos^2(\omega_r t + \varphi_r) + 2|a_r(t)a_{LO}|\cos(\omega_r t + \varphi_r)\cos(\omega_{LO} t + \varphi_{LO}) \\ &\qquad + |a_{LO}|^2\cos^2(\omega_{LO} t + \varphi_{LO}) \\ &\cong \frac{1}{2}|a_r(t)|^2 + \frac{1}{2}|a_{LO}|^2 + 2|a_r(t)a_{LO}|\cos[(\omega_r - \omega_{LO})t + (\varphi_r - \varphi_{LO})] \\ &\cong P_r(t) + P_{LO} + 2\sqrt{P_r(t)P_{LO}}\cos[(\omega_r - \omega_{LO})t + (\varphi_r - \varphi_{LO})] \\ &\cong 2\sqrt{P_r(t)P_{LO}}\cos[(\omega_r - \omega_{LO})t + (\varphi_r - \varphi_{LO})] \end{aligned} \quad . \tag{4}$$

The above derivation uses the facts that the heterodyne detector does not respond at optical frequencies, that the detector or electronics will not pass baseband (DC) signals (thereby removing the P_{LO} contribution), and that the local oscillator power P_{LO} is significantly larger than P_r (thereby removing the P_r term). The above relation has been significantly simplified, and a more complete relationship would need to include the contribution of the LO spurs, as seen previously in Figures 18(a) and 21(a). Since the optical power in the LO spurs is of the

same order of magnitude as the received instantaneous power P_r, the beat contribution between the spurs and the main LO mode is also present in the detector output, and occurs at harmonics of the AOM shift frequency (approximately 77 and 154 MHz). The presence of the LO spurs led to the construction of a customized processing technique designed to remove their effect in the calculation of U_{HD}.

The calculation of U_{HD} is primarily based upon the use of the power spectral density of I_{HD}. The power spectral density S_{S+N} of I_{HD} is computed over a temporal window where the return and local oscillator signals are present, and a separate power spectral density S_N is computed over a temporal window where the local oscillator but no signal is present. U_{HD} is then calculated from the integration over temporal frequency space of the point-by-point normalization of S_{S+N} by S_N

$$U_{HD} = \int_{\Delta F} \frac{S_{S+N}(f)}{S_N(f)} df - 1 - N_{ENF} = \int_{\Delta F} \frac{\left|\Im_{S+N}\{I_{HD}\}\right|^2}{\left|\Im_{N}\{I_{HD}\}\right|^2} df - 1 - N_{ENF} \propto E_r \quad . \tag{5}$$

Utilizing Rayleigh's energy theorem, it can be shown that U_{HD} is thereby directly proportional to E_r, as desired. The factor N_{ENF} is termed the excess noise factor, and results from the fact that point-by-point normalization is a biased processing procedure, due to the nonlinearity of the division operation. It can be shown that in the case of no signal, for the parameters used in the heterodyne processing shown in this report, the division of two random noise signals results in a value of $1+N_{ENF}$ of approximately 1.150, as compared to a value of unity for an unbiased processing procedure. N_{ENF} is strictly a function of the heterodyne SNR, with N_{ENF} approaching zero at higher SNRs. Since the N_{ENF} correction is more important at low SNRs than at higher SNRs, a constant value of $N_{ENF} = 0.150$ corresponding to the no signal case was used in the processing. The details of the heterodyne processing are also given in Appendix C, where the code for the primary heterodyne detection Matlab calculation program DATREDUC_HD_X3.m is reproduced.

D. Chemometric Theoretical Analysis

The chemometric processing is performed in exactly the same manner for both direct and heterodyne detection, since the computed parameters U_{DD} and U_{HD} are both directly proportional to E_r, and therefore to the total transmission of the target gases of interest. The most accurate and least complicated method to isolate the absorption caused by M target gases is, if possible, to perform the same measurement in the absence of the target gases as will be performed with the gases present. The initial step in the analysis procedure is to normalize the receive energy by the transmit energy. The data are then background normalized by a no-gas spectrum, leaving the spectral transmission from the target gases only. For a sequence of N laser lines and M absorbing gases, the set of equations used in the chemometric analysis can be written as

$$
\begin{aligned}
T(\lambda_1) &= \exp\left(-2\kappa(\lambda_1, g_1)\, CL(g_1)\right) \times \exp\left(-2\kappa(\lambda_1, g_2)\, CL(g_2)\right) \times \cdots \\
&\quad \times \exp\left(-2\kappa(\lambda_1, g_M)\, CL(g_M)\right) \\
T(\lambda_2) &= \exp\left(-2\kappa(\lambda_2, g_1)\, CL(g_1)\right) \times \exp\left(-2\kappa(\lambda_2, g_2)\, CL(g_2)\right) \times \cdots \\
&\quad \times \exp\left(-2\kappa(\lambda_2, g_M)\, CL(g_M)\right) \\
&\vdots \\
T(\lambda_N) &= \exp\left(-2\kappa(\lambda_N, g_1)\, CL(g_1)\right) \times \exp\left(-2\kappa(\lambda_N, g_2)\, CL(g_2)\right) \times \cdots \\
&\quad \times \exp\left(-2\kappa(\lambda_N, g_M)\, CL(g_M)\right)
\end{aligned}
\tag{6}
$$

where $T(\lambda_i)$ is the total transmission at wavelength λ_i including the contributions from all of the target gases.

A matrix equation which is linear in the unknowns $CL(g_i)$ is formed by taking the logarithm of each equation

$$
\bar{\mathbf{a}} = \frac{1}{2}\begin{bmatrix} -\ln\left(T(\lambda_1)\right) \\ -\ln\left(T(\lambda_2)\right) \\ \vdots \\ -\ln\left(T(\lambda_N)\right) \end{bmatrix} = \begin{bmatrix} \kappa(\lambda_1, g_1) & \kappa(\lambda_1, g_2) & \cdots & \kappa(\lambda_1, g_M) \\ \kappa(\lambda_2, g_1) & \kappa(\lambda_2, g_2) & \cdots & \kappa(\lambda_2, g_M) \\ \vdots & \vdots & & \vdots \\ \kappa(\lambda_N, g_1) & \kappa(\lambda_N, g_2) & \cdots & \kappa(\lambda_N, g_M) \end{bmatrix} \begin{bmatrix} CL(g_1) \\ CL(g_2) \\ \vdots \\ CL(g_M) \end{bmatrix} = \mathbf{K} \bullet \bar{\mathbf{c}} \tag{7}
$$

Applying singular-value decomposition (SVD) matrix analysis or other techniques to the above equation provides a solution $\hat{\mathbf{c}}$ for the $CL(g_i)$. Some of the advantages of the above chemometric analysis are that all chemical concentrations are solved for simultaneously, and that all of the spectral information available is used in the analysis. These characteristics provide definite improvements over the conventional 2-line DIAL analysis for handling chemicals with overlapping spectral features. Some inaccuracies have been noted for chemicals with overlapping spectral features when using the basic SVD analysis, but it is believed that applying a scheme to de-weight these wavelengths is feasible, and would improve the accuracy of the chemometric results.

E. Radiometric Results

The direct detection radiometric results, presented as the ratio of the expected return signal to the actual return signal ($F_{DD} = \tilde{U}_{DD} / \hat{U}_{DD}$) are shown in Figure 22. The results are from experiments conducted on different days using both modelocked and non-modelocked waveforms, and are separated into groups for the four different targets used. Target #1 was the earth berm located at the 4KS site, Target #2 was a highly weathered (2-year exposure) blueboard target at the 4KS site, Target #3 was a moderately weathered (2-month exposure)

blueboard target at the 4KS site, and Target #4 was the 7KS earth berm. Data points that were obvious outliers have been removed from the plot. As seen in the Figure, there is very good agreement between the measured and predicted values (within a factor of 1 – 2.5) for the 4 km and 7 km topographic targets. This agreement level is reasonable, considering that the DIAL measurements had the most emphasis, and the radiometric characterization was therefore not as extensive as had been conducted in past experiments. Previous precise radiometric measurements on the direct detection system conducted in 1998 illustrated that the level of radiometric agreement achievable with the system fully optimized was within a factor of 1 to 1.4.[4] The discrepancies seen in Figure 22 for the blueboard targets are most likely caused by inaccuracies in the assumed blueboard target reflectivity. The simulation results used reflectivity values from measurements of the blueboards immediately after they were fabricated, and before being continuously exposed to the outside elements. The blueboard reflectivity is expected to decrease as the target material weathers and blueboard dust particles build up on the surface, and is a reasonable explanation for the results from the blueboard targets. The previous measurements in 1998 were conducted immediately after the blueboard targets had been fabricated and characterized, and both blueboard and berm return signals agreed with predictions within the factor of 1 – 1.4 mentioned previously.

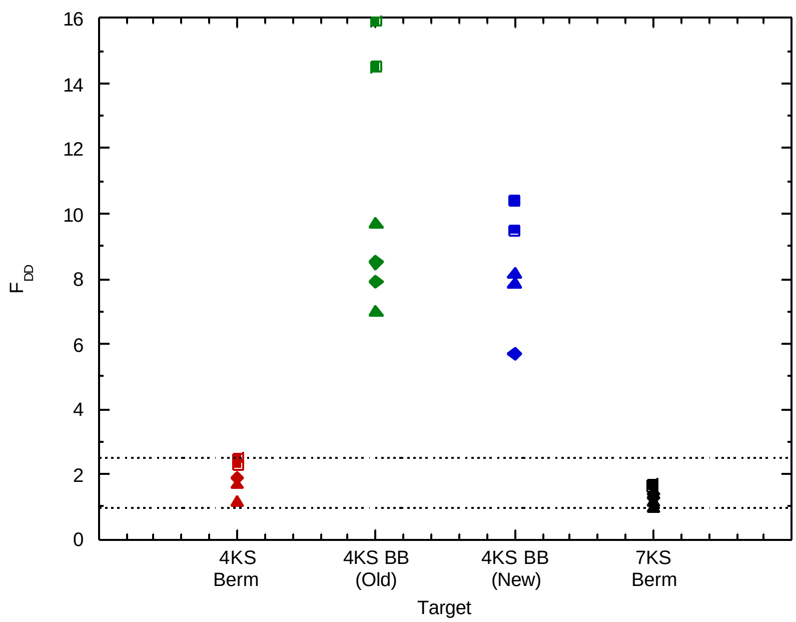

Figure 22. Direct detection radiometric results.

The heterodyne radiometric results are shown in Figure 23. Similarly to the direct detection results, the ratio of expected to measured return signal $F_{HD} = \tilde{U}_{HD} / \hat{U}_{HD}$ is computed. This ratio is further normalized by the direct detection ratio F_{DD}, in order to remove any errors caused by inaccuracies in the assumed reflectivities. Data points that were obvious outliers have been removed from the plot. As seen in the Figure, the heterodyne return signal is within a factor of approximately 6 to 20 of the expected value. The heterodyne return signal simulation includes heterodyne efficiency and signal reduction factors resulting from beam pattern mismatch between the LO (uniform) and return signal (Airy)[5,6]; distortion of the return signal phase front by atmospheric turbulence (assuming a relatively high turbulence level of $C_n^2 = 10^{-13}\ \mathrm{m}^{-2/3}$)[7]; and loss of signal caused by transmitter beam (pointing) jitter. Factors which were not able to be measured and are not included in the simulation include non-uniformity in the detector quantum efficiency (probably a negligible factor); misalignment of the transmitter footprint and receiver field-of-view (also probably a negligible factor); phase front curvature from misfocusing of the heterodyne receiver telescope (also probably negligible); and angular misalignment of the LO and receiver signal on the detector (possibly a factor of ~2 reduction). It should also be noted that the results of Frehlich and Kavaya [1991][8] suggest that the coherence loss factor caused by atmospheric turbulence may be significantly worse than that given by Clifford and Wandzura [1981][7] and used in this paper.

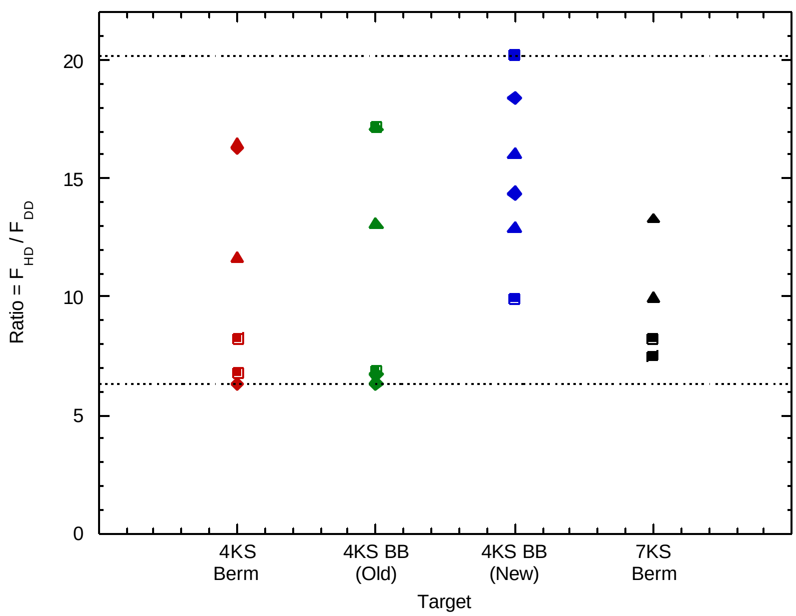

Figure 23. Normalized heterodyne radiometric results.

Overall, the difference between the expected and measured heterodyne signal levels is larger than expected, but not significantly, and could most likely be significantly reduced with a more precise system optimization. The best agreement noted to date between expected and actual return heterodyne signal levels for comparable systems is a factor of ~4[9], with most systems reporting a 5 – 10 dB (factor of 3 – 10)[10,11,12,13] reduction. With the possible loss factors not included in the analysis of the CROSS system, and the added complexity inherent in a fully wavelength-agile heterodyne system, a reduction factor of 6 – 20 compares favorably with the previous reduction factors from other researchers of 3- 10.

F. Chemometric Results (Case Studies)

The absorption spectra for SF_6 and NH_3 are shown in Figure 24. The x's indicate the absorption coefficients for the chemicals at the specific wavelengths in the 10R and 10P bands for the $^{12}C^{16}O_2$ laser isotope being used for the experiments. SF_6 has a broad absorption feature, which will affect most of the 10P laser lines. NH_3 has a much narrower absorption spectrum, and has its only significant absorption on the 10R14 laser line. For the HD/DD DC experiments, only 3-4 of the 10R lines shown on the plot (between ~ 969-982 cm^{-1}) were used in the laser sequence.

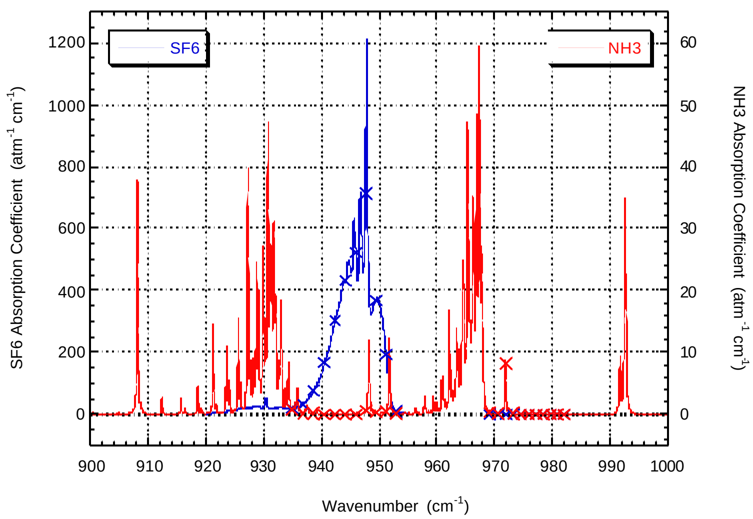

Figure 24. Absorption spectra overlap with $^{12}C^{16}O_2$ laser wavelengths for SF_6 and NH_3.

The results from the HD/DD DC tests using the spread spectrum (modelocked) transmit waveform and the diffuse blueboard target at the 4 km site are shown in Figure 25. The absorption plots for both the direct detection and heterodyne return signals are shown on the left of the Figure. The horizontal axis in these plots corresponds to time, while the vertical axis shows the laser wavelengths transmitted. From sequences 1 to 40, there was no SF_6 present

in the absorption cell. Around sequence 40, a first SF_6 insertion was made, and a second SF_6 insertion was made near sequence 70. The SF_6 absorption signature is seen clearly in both of the absorption plots, although the direct detection plot is cleaner. Rough calculations of the expected single shot SNR give a direct detection $SNR_{DD} \sim 5$, resulting from speckle spatial averaging, and a heterodyne single shot $SNR_{HD} \sim 2.5$, resulting from approximately 6 effective modes in the transmitted modelocked spectrum. After the DIAL processing techniques are applied, the SNRs shown in the absorption plots become $SNR_{DD} \sim 14$ and $SNR_{HD} \sim 7$. The graph on the bottom right of the Figure shows the computed concentration-length (CL) products as a function of time for both techniques. The table on the top right summarizes the measured CLs in each of the three reference / insertion regions. The results from the two detection techniques differ by less than 12%, which is reasonably good agreement given the number of uncontrolled variables in the experiment.

The results from the HD/DD DC tests using the spread spectrum (modelocked) transmit waveform and the topographic target at the 7.5 km site are shown in Figure 26. The SF_6 insertion timeline is essentially the same as that described for Figure 25. The SF_6 signature is again evident in both of the absorption plots. The expected single shot SNRs are the same as for the 4 km measurements ($SNR_{DD} \sim 5$ and $SNR_{HD} \sim 2.5$). After the processing techniques are applied, the SNRs become $SNR_{DD} \sim 14$ and $SNR_{HD} \sim 5$, indicating that the direct detection results are similar at both ranges, and the heterodyne results were slightly degraded at the longer range. In this case, the results from the two detection techniques differ by less than 20%, which is still reasonably good agreement.

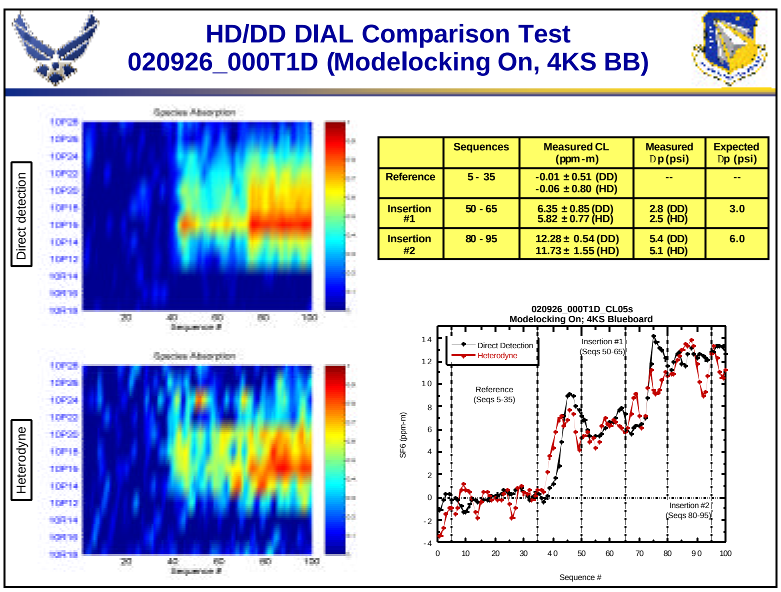

	Sequences	Measured CL (ppm-m)	Measured Δp (psi)	Expected Δp (psi)
Reference	5 - 35	-0.01 ± 0.51 (DD) -0.06 ± 0.80 (HD)	--	--
Insertion #1	50 - 65	6.35 ± 0.85 (DD) 5.82 ± 0.77 (HD)	2.8 (DD) 2.5 (HD)	3.0
Insertion #2	80 - 95	12.28 ± 0.54 (DD) 11.73 ± 1.55 (HD)	5.4 (DD) 5.1 (HD)	6.0

Figure 25. Results from the 020926 experiment using the blueboard at the 4 km site.

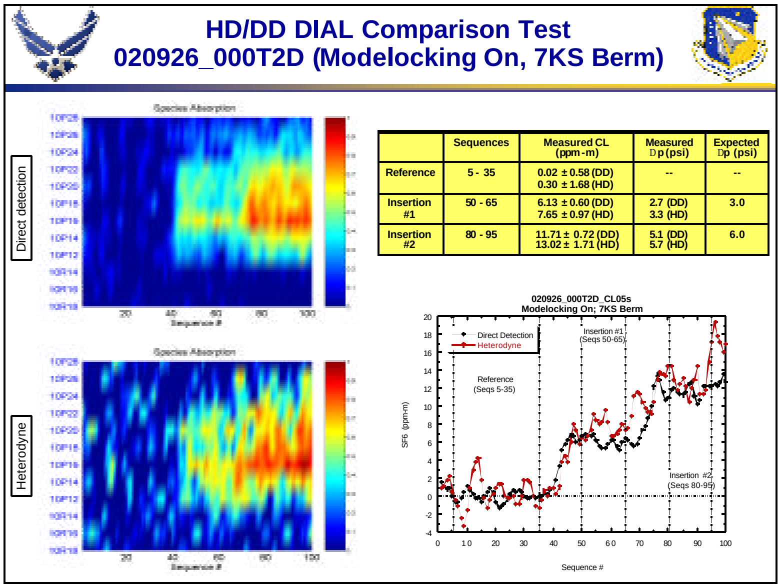

Figure 26. Results from 020926 experiment using topographic returns at the 7.5 km site.

Results from a dual insertion of SF_6 and NH_3 are shown in Figure 27. The SF_6 was inserted around sequence 40, and the NH_3 was inserted near sequence 70. As shown in Figure 24, SF_6 exhibits absorption on most of the 10P laser lines, while NH_3 has significant absorption only at the 10R14 wavelength. The CL values for SF_6 and NH_3 measured with both the direct detection and heterodyne receivers are shown on the plot.

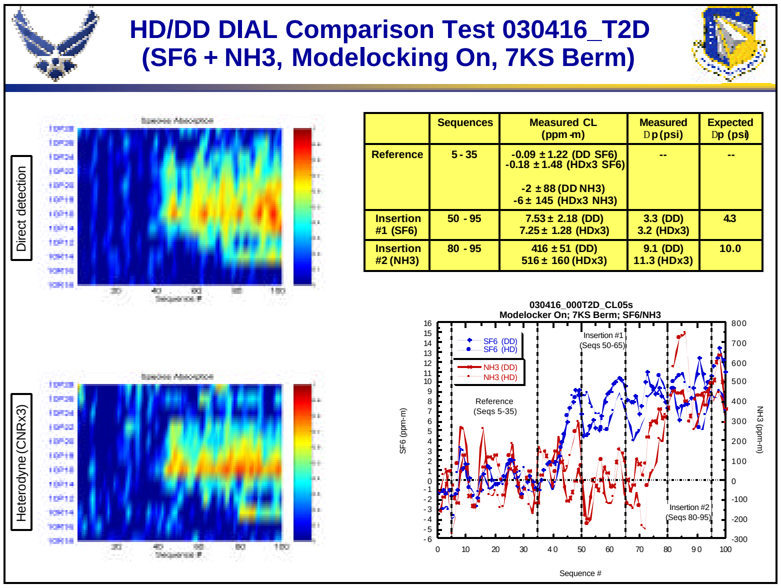

Figure 27. Results from 030416 dual SF_6 and NH_3 experiment using topographic returns at 7.5 km.

Heterodyne and direct detection DIAL results using the blueboard target at a range of 15 km are shown in Figures 28 and 29. The direct detection DIAL results are significantly noisier than at shorter ranges, which is expected since at longer horizontal ranges the direct detection system is signal-limited, and is therefore no longer in the speckle-limited regime. The direct detection signal level for the 030612 data set is extremely low, which causes significant errors in the DIAL intermediate normalization processing algorithm, and appears as the physically incorrect result of the measured absorption being saturated. The heterodyne DIAL results also show some degradation, but not to as great an extent as the direct detection results, which indicates that the heterodyne system is still operating in the speckle-limited regime, as expected.

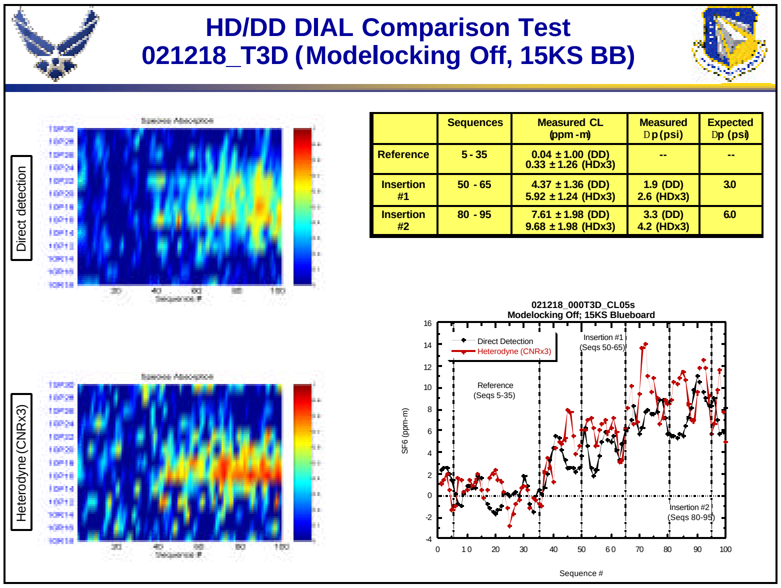

Figure 28. Results from the 021218 experiment using the blueboard at the 15 km site.

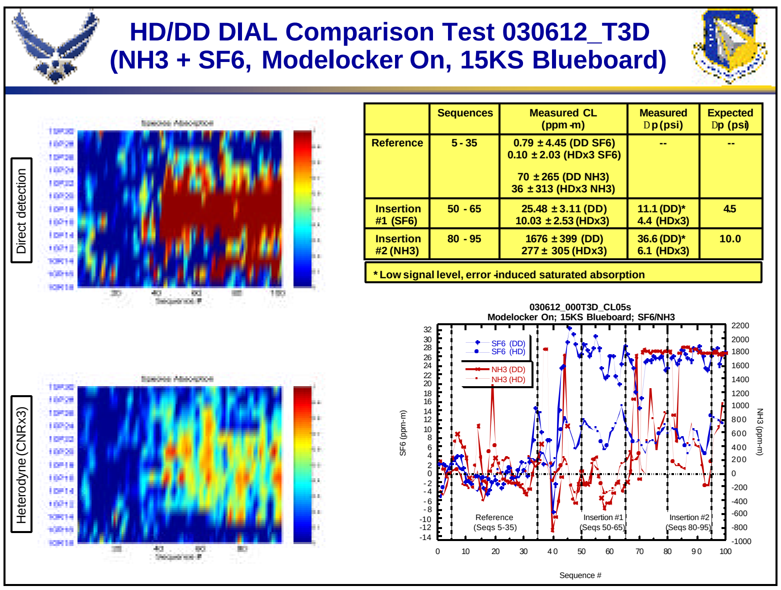

Figure 29. Results from the 030612 dual SF_6 and NH_3 experiment using the blueboard at 15 km.

G. Chemometric Results (Compilation and Comparisons)

This section will provide a summary of the DIAL chemometric results for the HD/DD DC experiments. Detailed results for all of the primary HD/DD DC experiments are shown in Appendix B. The expected and measured concentration-length (CL) products from all of the HD/DD DC data sets used in this report are shown in Figure 30. Prior to March 2004 (~ Day #60), the common experiment technique was to begin data collection with no gas in the cell, then add SF_6 approximately 1/3 of the way through the data set, and then add more SF_6 approximately 2/3 of the way through the data set. The initial SF_6 insertion CL measurements are shown in blue in the Figure, with the second SF_6 CL measurements shown in green. After March 2004, the experiment technique was changed to normally have the first insertion with SF_6 (shown in blue), and the second insertion with NH_3 (shown in red). The dashed lines on the plots have no significance, but are shown to more clearly indicate the different gas insertions. To reduce clutter from overlap of the symbols on the plot, measurements from the 4KS blueboards (4KS BB) were shifted left by ½ day, and measurements from the 7KS berm were shifted right by ½ day.

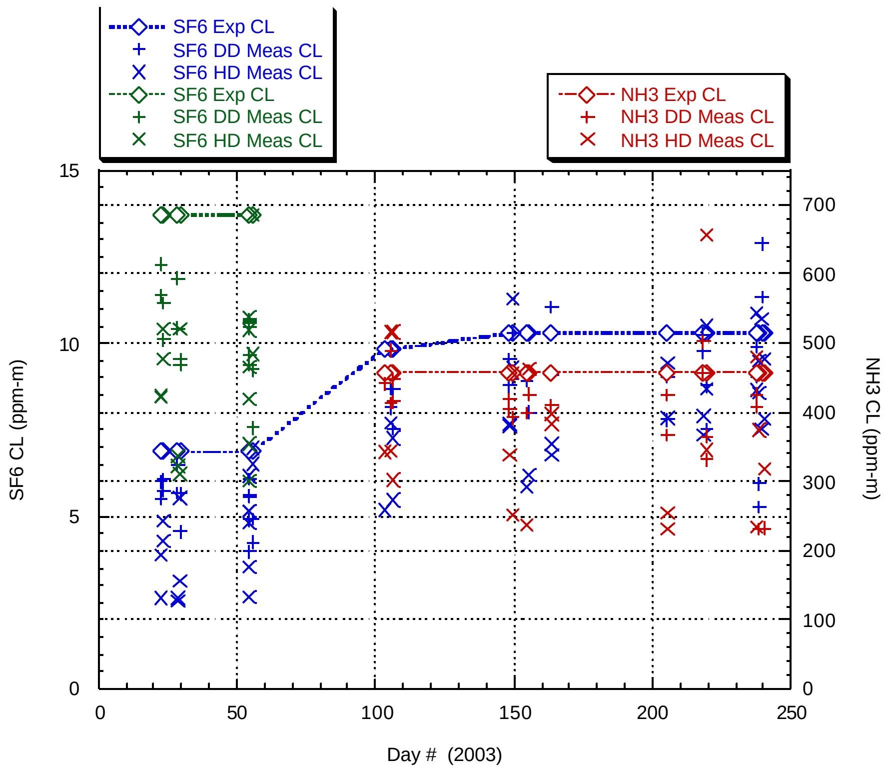

Figure 30. Expected and measured CL values from HD/DD DC experiments.

Although there is a significant amount of scatter in the results shown in Figure 30, a few general conclusions can be drawn. During the time period of these measurements, both the heterodyne and direct detection DIAL systems were being continually improved, both with respect to the equipment, and to the alignment and experimental procedures. This is evidenced by noting that prior to March 2004, the measured CL results were significantly lower than the expected values, and the measured CLs never significantly exceeded the expected values. After March 2004, the measured CLs still tended to be lower than the expected values, but were closer to the expected value, and sometimes exceeded it. This improvement continued until the final measurements made in August of 2004.

It is believed that the measured CL's being consistently lower than expected probably results from a systematic error, possibly from inaccuracies in the gas insertion procedure or from errors in the compensation of the spectral absorption coefficients for the experiment atmospheric pressure and temperature. Since the primary purpose of the HD/DD DC experiment series was to compare heterodyne and direct detection DIAL, relative results were emphasized, and extraordinary efforts were not made to calibrate the system for absolute accuracy. Previous measurements of SF_6, NH_3, and Freon R-134A made during ground tests in 1998[4] with only the LARS direct detection DIAL system showed slightly more accurate DIAL results than achieved with the HD/DD DC direct detection measurements. The more accurate results in 1998 were possible primarily because only a single system and single target were being used, allowing more meticulous alignment and system calibration. The more complex nature of the HD/DD DC experiment reduced the capability to optimize all of the system components simultaneously, and would be expected to result in reduced DIAL measurement accuracy. Even with the slightly reduced accuracy, the comparisons between the heterodyne and direct detection DIAL results are still valid and provide the key information required to analyze and compare the capabilities of the techniques.

To better study the effects of the various system parameters on the DIAL accuracy, the measurements were separated into groups by the experiment and system parameters. A summary of the DIAL results for these related measurements is given in Table 3. The Table separates the measurements by the detection technique used, the target gas, the modelocking configuration, the time period when the measurements were made, the number of individual measurements included in the group, and the average and standard deviation of the measured to expected concentration-length (CL) ratio. It should be noted that even though there were more than 158 individual DIAL measurements made, the compiled grouping results may still not be statistically significant, since there are many parameters which may affect the DIAL measurements, resulting in a small number of similar measurements for each grouping. The DIAL results have a significant amount of scatter, and an empirical decision was made to consider any individual values which fell below 50% or above 150% of the expected CL to be outliers, and to remove these values from the analysis.

Table 3. Summary of DIAL Results

Target	Detection Technique	Target Gas	Mode-locking	Time Segment	Number of Measurements	Measured / Expected CL Ratio
4KS BB	DD	SF6	On	Post–Mar 04	5	0.99 ± 0.15
4KS BB	DD	SF6	Off	Post–Mar 04	6	0.93 ± 0.10
4KS BB	HD	SF6	On	Post–Mar 04	6	0.77 ± 0.17
4KS BB	HD	SF6	Off	Post–Mar 04	5	0.78 ± 0.18
7KS Berm	DD	SF6	On	Post–Mar 04	7	0.68 ± 0.24
7KS Berm	DD	SF6	Off	Post–Mar 04	8	0.78 ± 0.28
7KS Berm	HD	SF6	On	Post–Mar 04	7	0.87 ± 0.16
7KS Berm	HD	SF6	Off	Post–Mar 04	8	0.76 ± 0.14
4KS BB	DD	NH3	On	Post–Mar 04	5	0.98 ± 0.06
4KS BB	DD	NH3	Off	Post–Mar 04	5	0.93 ± 0.10
4KS BB	HD	NH3	On	Post–Mar 04	4	0.78 ± 0.26
4KS BB	HD	NH3	Off	Post–Mar 04	3	0.59 ± 0.14
7KS Berm	DD	NH3	On	Post–Mar 04	5	0.79 ± 0.18
7KS Berm	DD	NH3	Off	Post–Mar 04	7	0.82 ± 0.16
7KS Berm	HD	NH3	On	Post–Mar 04	7	0.83 ± 0.20
7KS Berm	HD	NH3	Off	Post–Mar 04	6	0.84 ± 0.34
4KS BB	DD	SF6 (Low)	On	Pre–Mar 04	5	0.82 ± 0.08
4KS BB	DD	SF6 (Low)	Off	Pre–Mar 04	5	0.80 ± 0.12
4KS BB	HD	SF6 (Low)	On	Pre–Mar 04	5	0.55 ± 0.24
4KS BB	HD	SF6 (Low)	Off	Pre–Mar 04	5	0.59 ± 0.16

4KS BB	DD	SF6 (High)	On	Pre–Mar 04	5	0.80 ± 0.09
4KS BB	DD	SF6 (High)	Off	Pre–Mar 04	5	0.77 ± 0.04
4KS BB	HD	SF6 (High)	On	Pre–Mar 04	5	0.59 ± 0.14
4KS BB	HD	SF6 (High)	Off	Pre–Mar 04	5	0.61 ± 0.11
7KS Berm	DD	SF6 (Low)	On	Pre–Mar 04	3	0.81 ± 0.08
7KS Berm	DD	SF6 (Low)	Off	Pre–Mar 04	3	0.71 ± 0.12
7KS Berm	HD	SF6 (Low)	On	Pre–Mar 04	3	0.84 ± 0.15
7KS Berm	HD	SF6 (Low)	Off	Pre–Mar 04	3	0.67 ± 0.25
7KS Berm	DD	SF6 (High)	On	Pre–Mar 04	3	0.70 ± 0.04
7KS Berm	DD	SF6 (High)	Off	Pre–Mar 04	3	0.68 ± 0.13
7KS Berm	HD	SF6 (High)	On	Pre–Mar 04	3	0.82 ± 0.16
7KS Berm	HD	SF6 (High)	Off	Pre–Mar 04	3	0.64 ± 0.17

The average measured-to-expected CL ratios are shown in Figure 31 for the different data groupings, and the standard deviation of the ratios are shown in Figure 32. The data points are again slightly offset on the x-axis for the different groupings to reduce clutter from overlap of the symbols. As noted previously, definitive conclusions probably should not be drawn from this data because the statistical significance is questionable because of the small number of data points included in each grouping, but some probable conclusions can still be made:

1) **The pre-March measured CL values are generally lower than those from post-March.** As stated previously, this is believed to result from improvements in the system hardware and the experimental alignment and procedures. Because of this effect, it is generally better to rely more on the post-March data to draw conclusions about the effects of the different parameters on the DIAL accuracy.

2) The direct detection measurements from the 4KS BB appear to give the most accurate DIAL results, with the closest match to the expected CL value, and the least variability. Referring to Figure 1, this is expected since in the HD/DD DC experiments the direct detection system is expected to outperform the heterodyne system in the speckle-limited regime. This is a result of direct detection spatial averaging providing more speckle mitigation than is achievable with the heterodyne spread spectrum operation in the system configurations used for the HD/DD DC experiments. It should be noted that the amount of speckle mitigation for the heterodyne system could be significantly and easily increased by designing the laser transmitter to include more frequency modes than was possible with the specific BBO laser configuration used in these experiments.

3) The direct detection system tends to be in the transition region between speckle- and signal-limited operation at 7 km, while the heterodyne system is still in the speckle-limited region. The DIAL measurement accuracies and variabilities are generally similar for direct detection operation at 7 km, and heterodyne operation at both 4 km and 7 km. This is seen for

both SF_6 and NH_3, in the post-March data. A possible explanation for this behavior is that the heterodyne system is operating in the speckle-limited regime at both 4 km and 7 km, while the direct detection system is in the speckle-limited regime at 4 km, but is entering the transition region between speckle- and signal-limited operation at 7 km (see Figure 1).

4) **Modelocking improves heterodyne DIAL accuracy.** This is most easily seen by noting that the modelocked heterodyne results from 7 km are closer to the expected CL value, and have lower variability than the non-modelocked results. The same results are expected from the 4 km measurements, but the 4 km data does not conclusively support or contradict the expected result.

5) **Direct detection results are better with modelocking off.** Since spatial averaging is the primary speckle mitigation technique for direct detection, it is expected that the increased laser power available with non-modelocked operation will provide the best results. The results shown in Figures 31 and 32 generally support this conclusion. A possible reason that not all of the data points demonstrate this result, is that it appears that the system transmit pointing jitter is reduced when using the modelocked pulse train, which improves the DIAL results.

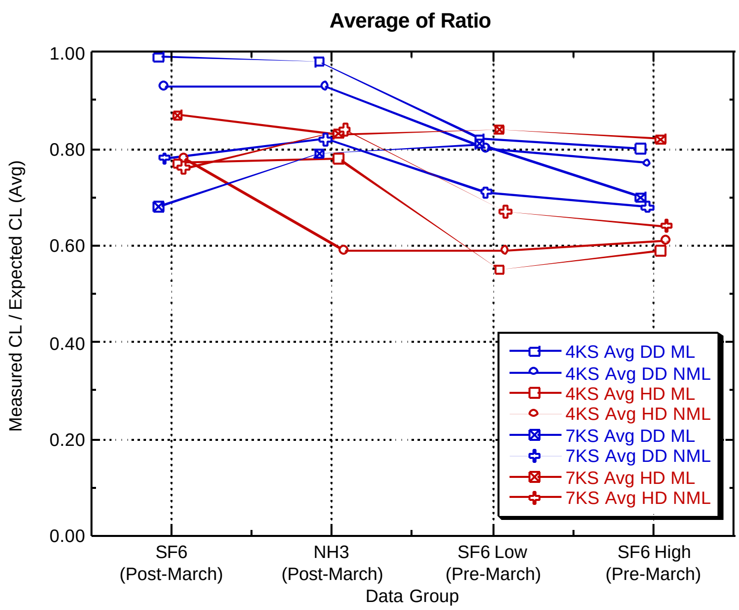

Figure 31. Average measured CL / expected CL ratio.

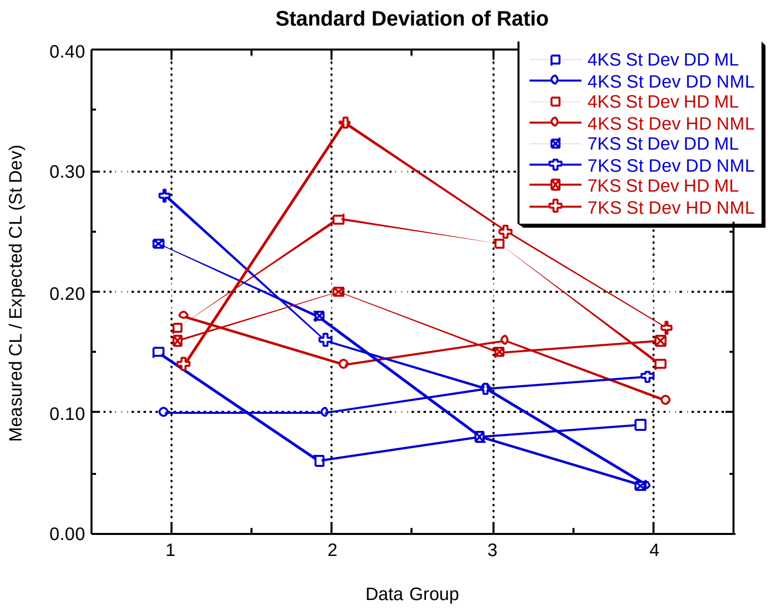

Figure 32. Standard deviation of measured CL / expected CL ratio.

5. Summary and Conclusions

The HD/DD DC experiments were designed to provide a direct, simultaneous comparison of the radiometric and chemical detection sensitivities of the heterodyne and direct detection receiver techniques. Many parameters affect radiometric and DIAL accuracy, and it is often not clear why measurements differ from the expected results. Numerous unresolved issues exist about the capabilities and characterizations of DIAL systems, especially with respect to systems utilizing heterodyne detection. In order to address some of the major issues, and to provide an empirical comparison of performance when the effects of all individual factors can not be determined, an experiment technique was developed that provided the first direct simultaneous comparisons of heterodyne and direct detection DIAL measurements.

The radiometric results showed that the direct detection return signal was within a factor of 1 to 2.5 of the expected value, while the heterodyne return signal was within a factor of 6 to 20. Previous specialized direct detection radiometric efforts at AFRL/DE had resulted in agreement factors of approximately 1 to 1.4. The premier heterodyne radiometric efforts by other research groups have demonstrated agreement factors of 3 to 10. The level of radiometric agreement achieved in the HD/DD DC experiments is reasonable in comparison with these previous efforts, considering that the primary focus of the experiments was on multiple wavelength DIAL measurements, which significantly increases the system complexity with respect to single wavelength measurements.

A primary issue concerning the accuracy of heterodyne DIAL measurements is the sensitivity of the heterodyne detection process to speckle, which directly affects chemical detection capability. For the HD/DD DC measurements a speckle mitigation technique utilizing a spread spectrum (modelocked) transmit waveform was employed and studied. The heterodyne DIAL results showed slightly higher variability (within a factor of 2, as determined from the minimum detectable absorption level) than the direct detection results, but were much better than the results that would be expected from a heterodyne system not employing a speckle mitigation concept.

The measurements also indicate that the relative DIAL performance of heterodyne detection improves with increasing range in comparison with direct detection, as would be expected. The ability of heterodyne systems to maintain speckle limited performance at ranges where direct detection systems become signal limited allows smaller systems to be used for the same range requirements, and allows a longer standoff range to be achieved with similar size systems.

The primary conclusion of the HD/DD DC experiment series is that heterodyne DIAL is a feasible and demonstrated technique, and has definite utility, especially for long standoff range operation.

References

[1] Killinger, D.K., N. Menyuk, and W.E. DeFeo, "Experimental comparison of heterodyne and direct detection for pulsed differential absorption CO_2 lidar," *Appl. Opt., 22,* 682-689, (1983).

[2] Higdon, N.S., D.C. Senft, M.J. Fox, C.M. Hamilton, B.T. Kelly, J.A. Dowling, D.F. Pierrottet, D.R. Dean, D.A. Richter, and R.R. Bousek, "Development and testing of a long-range airborne CO_2 DIAL chemical detection system," *Propagation and Imaging Through the Atmosphere, SPIE Vol. 3433,* 181-189, (1998).

[3] Pierrottet, D.F. and D.C. Senft, "CO_2 Coherent Differential Absorption LIDAR," *Chemical and Biological Sensing, SPIE Vol. 4036,* 17-23, (2000).

[4] Senft, D.C., M.J. Fox, C.M. Hamilton, D.A. Richter, N.S. Higdon, and B.T. Kelly, "Performance characterization and ground testing of an airborne CO_2 differential absorption lidar system (Phase II)," *Laser Radar Technology and Applications, SPIE Vol. 3707,* 165-176, (1999).

[5] Cohen, S.C., "Heterodyne detection: phase front alignment, beam spot size, and detector uniformity," *Appl. Opt., 14,* 1953-1959, (1975).

[6] Fowler, S., G.W. Kamerman, and G. Lawson, "Analysis of heterodyne efficiency for coherent laser radars," *Appl. Laser Radar Technology, SPIE Vol. 1936,* 137-146, (1993).

[7] Clifford, S.F. and S. Wandzura, "Monostatic heterodyne lidar performance: the effect of the turbulent atmosphere," *Appl. Opt., 20,* 514-516, (1981).

[8] Frehlich, R.G. and M.J. Kavaya, "Coherent laser radar performance for general atmospheric refractive turbulence," *Appl. Opt., 30,* 5325-5352, (1991).

[9] Brandewie, R.A. and W.C. Davis, "," *Appl. Opt., 11,* 1526-xxx, (1972).

[10] Foord, R., R. Jones, J.M. Vaughan, and D.V. Willets, "Precise comparison of experimental and theoretical SNRs in CO_2 laser heterodyne systems," *Appl. Opt, 22,* 3787-3795, (1983).

[11] Schwiesow, R.L. and R.E. Cupp, "Calibration of a cw infrared Doppler lidar," *Appl. Opt., 19,* 3168-3172, (1980).

[12] Post, M.J., R.A. Richter, R.M. Hardesty, T.R. Lawrence, and F.F. Hall, "National Oceanic and Atmospheric Administration's (NOAA) pulsed, coherent, infrared Doppler lidar – characteristics and data," *Proc. Soc. Photo-Opt. Instrum. Eng., 300,* 60-65, (1981).

[13] Shapiro, J.H., "Precise comparison of experimental and theoretical SNRs in CO_2 laser heterodyne systems: comments," *Appl. Opt., 24,* 1245-1247, (1985).

Appendix A. HD/DD DC Datasets

Table A1. HD/DD DC Datasets

Date (yymmdd)	Used in Figure	Filename	Target	Modelocked	Gas / System Configuration
030828		Test	15KS BB	No	No gas cell
030828		Test1a	4KS BB (old)	No	No gas cell
030828		Test1b	4KS BB (old)	Yes	No gas cell
030828		Test1c	4KS berm	No	No gas cell
030828		Test1d	4KS berm	Yes	No gas cell
030828		Test2a	4KS BB (new)	No	No gas cell
030828		Test2b	4KS BB (new)	No	Empty cell / SF6 / NH3
030828		Test2c	4KS BB (new)	Yes	No gas cell
030828		Test2d	4KS BB (new)	Yes	Empty cell / SF6 / NH3
030828		Test3a	7KS berm	No	No gas cell
030828		Test3b	7KS berm	No	Empty cell / SF6 / NH3
030828		Test3c	7KS berm	Yes	No gas cell
030828		Test3d	7KS berm	Yes	Empty cell / SF6 / NH3
030828		Test4a	None	No	System characterization test
030826		Test1a	4KS BB (old)	No	No gas cell
030826		Test1b	4KS BB (old)	Yes	No gas cell
030826		Test1c	4KS berm	No	No gas cell
030826		Test1d	4KS berm	Yes	No gas cell
030826		Test1e	4KS berm	No	No gas cell
030826		Test2a	4KS BB (new)	No	No gas cell
030826		Test2b	4KS BB (new)	No	Empty cell / SF6 / NH3
030826		Test2c	4KS BB (new)	Yes	No gas cell
030826		Test2d	4KS BB (new)	Yes	Empty cell / SF6 / NH3
030826		Test3a	7KS berm	No	No gas cell
030826		Test3b	7KS berm	No	Empty cell / SF6 / NH3
030826		Test3c	7KS berm	Yes	No gas cell
030826		Test3d	7KS berm	Yes	Empty cell / SF6 / NH3
030820		Test1a	4KS BB (old)	No	No gas cell
030820		Test1b	4KS BB (old)	Yes	No gas cell
030820		Test1c	4KS berm	No	No gas cell
030820		Test1d	4KS berm	Yes	No gas cell
030820		Test5a	None	No	System characterization test

030807		Test1a	4KS BB (old)	No	No gas cell
030807		Test1b	4KS BB (old)	Yes	No gas cell
030807		Test1c	4KS berm	No	No gas cell
030807		Test1d	4KS berm	Yes	No gas cell
030807		Test2a	4KS BB (new)	No	No gas cell
030807		Test2b	4KS BB (new)	No	Empty cell / SF6 / NH3
030807		Test2c	4KS BB (new)	Yes	No gas cell
030807		Test2d	4KS BB (new)	Yes	Empty cell / SF6 / NH3
030807		Test3a	7KS berm	No	No gas cell
030807		Test3b	7KS berm	No	Empty cell / SF6 / NH3
030807		Test3c	7KS berm	Yes	No gas cell
030807		Test3d	7KS berm	Yes	Empty cell / SF6 / NH3
030724		Test1a	4KS BB (old)	No	No gas cell
030724		Test1b	4KS BB (old)	Yes	No gas cell
030724		Test1c	4KS berm	No	No gas cell
030724		Test1d	4KS berm	Yes	No gas cell
030724		Test1e	4KS BB (new)	No	No gas cell
030724		Test1f	4KS BB (new)	Yes	No gas cell
030724		Test2a	7KS berm	No	No gas cell
030724		Test2b	7KS berm	No	Empty cell / SF6 / NH3
030724		Test2c	7KS berm	Yes	No gas cell
030724		Test2d	7KS berm	Yes	Empty cell / SF6 / NH3
030612		Test1a	4KS BB (old)	No	No gas cell
030612		Test1b	4KS BB (old)	Yes	No gas cell
030612		Test1c	4KS berm	No	No gas cell
030612		Test1d	4KS berm	Yes	No gas cell
030612		Test1e	4KS BB (new)	No	No gas cell
030612		Test1f	4KS BB (new)	Yes	No gas cell
030612		Test2a	7KS berm	No	No gas cell
030612		Test2b	7KS berm	No	Empty cell / SF6 / NH3
030612		Test2c	7KS berm	Yes	No gas cell
030612		Test2d	7KS berm	Yes	Empty cell / SF6 / NH3
030612		Test3a	15KS BB	No	No gas cell
030612		Test3b	15KS BB	No	Empty cell / SF6 / NH3
030612		Test3c	15KS BB	Yes	No gas cell
030612	29	Test3d	15KS BB	Yes	Empty cell / SF6 / NH3
030604		Test1a	4KS BB (old)	Out	No gas cell
030604		Test1b	4KS berm	Out	No gas cell
030604		Test1c	4KS BB (new)	Out	No gas cell

030604		Test1d	4KS BB (new)	Out	Empty cell / SF6 / NH3
030604		Test2a	7KS berm	Out	No gas cell
030604		Test2b	7KS berm	Out	Empty cell / SF6 / NH3
030529		Test1a	4KS BB (old)	No	No gas cell
030529		Test1b	4KS BB (old)	Yes	No gas cell
030529		Test2a	4KS berm	No	No gas cell
030529		Test2b	4KS berm	Yes	No gas cell
030529		Test3a	4KS BB (new)	No	No gas cell
030529		Test3b	4KS BB (new)	No	Empty cell / SF6 / NH3
030529		Test3c	4KS BB (new)	Yes	No gas cell
030529		Test3d	4KS BB (new)	Yes	Empty cell / SF6 / NH3
030529		Test4a	7KS berm	No	No gas cell
030529		Test4b	7KS berm	No	Empty cell / SF6 / NH3
030529		Test4c	7KS berm	Yes	No gas cell
030529		Test4d	7KS berm	Yes	Empty cell / SF6 / NH3
030527		Test1a	None	N/A	System char. (HD bias current)
030527		Test1b	None	N/A	System char. (HD bias current)
030527		Test1c	None	N/A	System char. (HD bias current)
030527		Test1d	None	N/A	System char. (HD bias current)
030522		Test1a	4KS BB (new)	No	System characterization
030522		Test1b	4KS BB (new)	Yes	System characterization
030502		Test1a	4KS BB (new)	No	System characterization
030502		Test1b	4KS BB (new)	Yes	System characterization
030416		Test1a	4KS BB (new)	No	No gas cell
030416		Test1b	4KS BB (new)	No	Empty cell / SF6 / NH3
030416		Test1c	4KS BB (new)	Yes	No gas cell
030416		Test1aa	4KS BB (new)	No	No gas cell
030416		Test1d	4KS BB (new)	Yes	Empty cell / SF6 / NH3
030416		Test2a	7KS berm	No	No gas cell
030416		Test2b	7KS berm	No	Empty cell / SF6 / NH3
030416		Test2c	7KS berm	Yes	No gas cell
030416	27	Test2d	7KS berm	Yes	Empty cell / SF6 / NH3
030415		Test1a	4KS BB (old)	No	No gas cell
030415		Test1b	4KS BB (old)	Yes	No gas cell
030415		Test1c	4KS BB (new)	Yes	No gas cell

030415		Test1d	4KS BB (new)	Yes	Empty cell / SF6 / NH3
030415		Test1e	4KS BB (new)	No	No gas cell
030415		Test1f	4KS BB (new)	No	Empty cell / SF6 / NH3
030401		Test1a	4KS BB (old)	No	No gas cell
030401		Test1b	4KS BB (old)	No	Empty cell / SF6 / SF6
030401		Test1c	4KS BB (old)	Yes	No gas cell
030401		Test1d	4KS BB (old)	Yes	Empty cell / SF6 / SF6
030401		Test1e	4KS berm	No	No gas cell
030401		Test1f	4KS berm	Yes	No gas cell
030401		Test2a	7KS berm	No	No gas cell
030401		Test2b	7KS berm	No	Empty cell / SF6 / SF6
030401		Test2c	7KS berm	Yes	No gas cell
030401		Test2d	7KS berm	Yes	Empty cell / SF6 / SF6
030401		Test3a	6KS CC	No	No gas cell
030401		Test3b	6KS CC	No	Empty cell / SF6 / SF6
030401		Test3c	6KS CC	Yes	No gas cell
030401		Test3d	6KS CC	Yes	Empty cell / SF6 / SF6
030321		Test1a	6KS CC	No	No gas cell
030321		Test1b	6KS CC	Yes	No gas cell
030321		Test1c	6KS CC	Yes	No gas cell
030321		Test2a	4KS BB (old)	No	No gas cell
030224		Test1a	4KS BB (old)	No	No gas cell
030224		Test1b	4KS BB (old)	No	Empty cell / SF6 / SF6
030224		Test1c	4KS BB (old)	Yes	No gas cell
030224		Test1d	4KS BB (old)	Yes	Empty cell / SF6 / SF6
030224		Test2a	4KS BB (old)	No	No gas cell
030224		Test2b	4KS BB (old)	No	Empty cell / SF6 / SF6
030224		Test2c	4KS BB (old)	Yes	No gas cell
030224		Test2d	4KS BB (old)	Yes	Empty cell / SF6 / SF6
030224		Test3a	4KS BB (old)	No	No gas cell
030224		Test3b	4KS BB (old)	No	Empty cell / SF6 / SF6
030224		Test3c	4KS BB (old)	Yes	No gas cell
030224		Test3d	4KS BB (old)	Yes	Empty cell / SF6 / SF6
030224		Test4a	7KS berm	No	No gas cell
030224		Test4b	7KS berm	No	Empty cell / SF6 / SF6
030224		Test4c	7KS berm	Yes	No gas cell
030224		Test4d	7KS berm	Yes	Empty cell / SF6 / SF6
030204		Test1a	4KS BB (old)	No	Empty cell / SF6 / SF6
030204		Test1b	4KS BB (old)	Yes	Empty cell / SF6 / SF6

030204		Test1c	4KS BB (old)	No	Empty cell / SF6 / SF6
030204		Test1d	4KS BB (old)	Yes	Empty cell / SF6 / SF6
030204		Test1e	4KS BB (old)	No	No gas cell
030204		Test1f	4KS BB (old)	Yes	No gas cell
030204		Test2a	7KS berm	No	No gas cell
030204		Test2b	7KS berm	No	Empty cell / SF6 / SF6
030204		Test2c	7KS berm	Yes	Empty cell / SF6 / SF6
030204		Test2d	7KS berm	Yes	No gas cell
030129		Test1a	4KS BB (old)	No	No gas cell
030129		Test1b	4KS BB (old)	No	Empty cell / SF6 / SF6
030129		Test1c	4KS BB (old)	Yes	No gas cell
030129		Test1d	4KS BB (old)	Yes	Empty cell / SF6 / SF6
030129		Test2a	7KS berm	No	No gas cell
030129		Test2b	7KS berm	No	Empty cell / SF6 / SF6
030129		Test2c	7KS berm	Yes	No gas cell
030129		Test2d	7KS berm	Yes	Empty cell / SF6 / SF6
030123		Test1a	4KS BB (old)	No	No gas cell
030123		Test1b	4KS BB (old)	No	Empty cell / SF6 / SF6
030123		Test1c	4KS BB (old)	Yes	No gas cell
030123		Test1d	4KS BB (old)	Yes	Empty cell / SF6 / SF6
030123		Test2a	7KS berm	No	No gas cell
030123		Test2b	7KS berm	No	Empty cell / SF6 / SF6
030123		Test2c	7KS berm	Yes	No gas cell
030123		Test2d	7KS berm	Yes	Empty cell / SF6 / SF6
021218		Test1a	4KS BB (old)	No	No gas cell
021218		Test1b	4KS BB (old)	No	Empty cell / SF6 / SF6
021218		Test1c	4KS BB (old)	Yes	No gas cell
021218		Test1d	4KS BB (old)	Yes	Empty cell / SF6 / SF6
021218		Test2a	7KS berm	No	No gas cell
021218		Test2b	7KS berm	No	Empty cell / SF6 / SF6
021218		Test2c	7KS berm	Yes	No gas cell
021218		Test2d	7KS berm	Yes	Empty cell / SF6 / SF6
021218		Test3a	15KS BB	No	No gas cell
021218		Test3b	15KS BB	No	Empty cell / SF6 / SF6
021218		Test3c	15KS BB	No	No gas cell
021218	28	Test3d	15KS BB	No	Empty cell / SF6 / SF6
021218		Test3e	15KS BB	Yes	No gas cell
021218		Test3f	15KS BB	Yes	Empty cell / SF6 / SF6
021217		Test1a	15KS BB	No	No gas cell

021217		Test2a	4KS BB (old)	No	No gas cell
021217		Test2b	4KS BB (old)	No	Empty cell / SF6 / SF6
021217		Test2c	4KS BB (old)	Yes	No gas cell
021217		Test2d	4KS BB (old)	Yes	Empty cell / SF6 / SF6
020926		Test1a	4KS BB (old)	No	Empty cell / SF6 / SF6
020926		Test1b	4KS BB (old)	No	No gas cell
020926		Test1c	4KS BB (old)	Yes	No gas cell
020926	25	Test1d	4KS BB (old)	Yes	Empty cell / SF6 / SF6
020926		Test1e	4KS BB (old)	Yes	No gas cell
020926		Test1f	4KS BB (old)	Yes	Empty cell / SF6 / SF6
020926		Test2a	7KS berm	Yes	No gas cell
020926		Test2b	7KS berm	Yes	Empty cell / SF6 / SF6
020926		Test2c	7KS berm	Yes	No gas cell
020926	26	Test2d	7KS berm	Yes	Empty cell / SF6 / SF6
020926		Test2e	7KS berm	No	No gas cell
020926		Test2f	7KS berm	No	Empty cell / SF6 / SF6
020916		Test1a	4KS BB (old)	No	Empty cell / SF6 / SF6
020916		Test1b	4KS BB (old)	No	No gas cell
020916		Test1c	4KS BB (old)	Yes	No gas cell
020916		Test1d	4KS BB (old)	Yes	Empty cell / SF6 / SF6
020916		Test2a	7KS berm	No	No gas cell
020916		Test2b	7KS berm	No	Empty cell / SF6 / SF6
020916		Test2c	7KS berm	Yes	No gas cell
020916		Test2d	7KS berm	Yes	Empty cell / SF6 / SF6
020821		Test1a	4KS BB (old)	Yes	Empty cell / SF6 / SF6
020821		Test1b	4KS BB (old)	Yes	No gas cell
020821		Test1c	4KS BB (old)	No	No gas cell
020821		Test1d	4KS BB (old)	No	Empty cell / SF6 / SF6
020821		Test2a	7KS berm	Yes	No gas cell
020821		Test2b	7KS berm	Yes	Empty cell / SF6 / SF6
020821		Test2c	7KS berm	No	No gas cell
020821		Test2d	7KS berm	No	Empty cell / SF6 / SF6
020806		Test1a	4KS BB (old)	Yes	No gas cell
020806		Test1b	4KS BB (old)	Yes	Empty cell / SF6 / SF6
020806		Test1c	4KS BB (old)	No	No gas cell
020806		Test1d	4KS BB (old)	No	Empty cell / SF6 / SF6
020717		Test1a	4KS BB (old)	No	No gas cell, 10P20 only
020717		Test1c	4KS BB (old)	No	No gas cell, 10P20 only
020717		Test1d	4KS BB (old)	Yes	No gas cell, 10P20 only

020717		Test2a	4KS BB (old)	No	Empty cell / SF6 / SF6
020717		Test2b	4KS BB (old)	No	No gas cell
020717		Test2c	4KS BB (old)	Yes	No gas cell
020717		Test2d	4KS BB (old)	Yes	Empty cell / SF6 / SF6
020717		Test3a	7KS berm	No	No gas cell, 10P20 only
020717		Test3b	7KS berm	Yes	No gas cell, 10P20 only
020717		Test4a	7KS berm	No	No gas cell
020717		Test4b	7KS berm	Yes	No gas cell
020711		Test1a	4KS BB (old)	No	No gas cell, 10P20 only
020711		Test1b	4KS BB (old)	Yes	No gas cell, 10P20 only
020711		Test2a	4KS BB (old)	No	Empty cell / SF6 / SF6
020711		Test2b	4KS BB (old)	No	No gas cell
020711		Test2c	4KS BB (old)	Yes	No gas cell
020711		Test2d	4KS BB (old)	Yes	Empty cell / SF6 / SF6
020711		Test3a	None	No	System characterization test
020711		Test3b	None	Yes	System characterization test
020710		Test1a	4KS BB (old)	No	No gas cell, 10P20 only
020710		Test2a	4KS BB (old)	Yes	No gas cell, 10P20 only
020710		Test3a	4KS BB (old)	No	Empty cell / SF6 / SF6
020710		Test3b	4KS BB (old)	Yes	Empty cell / SF6 / SF6
020710		Test3c	4KS BB (old)	No	No gas cell
020710		Test3d	4KS BB (old)	Yes	No gas cell
020710		Test4a	7KS berm	No	No gas cell
020710		Test4b	7KS berm	Yes	No gas cell
020710		Test4c	7KS berm	No	Empty cell / SF6 / SF6
020710		Test4d	7KS berm	Yes	Empty cell / SF6 / SF6
020703		Test1a	4KS BB (old)	No	No gas cell, 10P20 only
020703		Test1b	4KS BB (old)	Yes	No gas cell, 10P20 only
020703		Test2a	4KS BB (old)	No	Empty cell / SF6 / SF6
020703		Test2b	4KS BB (old)	No	Empty cell / SF6 / SF6
020703		Test2c	4KS BB (old)	No	No gas cell
020703		Test2d	4KS BB (old)	Yes	Empty cell / SF6 / SF6
020703		Test3a	7KS berm	No	No gas cell
020703		Test3b	7KS berm	Yes	No gas cell
020703		Test3c	7KS berm	No	Empty cell / SF6 / SF6
020703		Test3d	7KS berm	Yes	Empty cell / SF6 / SF6
020703		Test4a	7KS berm	No	No gas cell
020703		Test4b	7KS berm	Yes	No gas cell
020529		Test1a	4KS berm	Yes	Empty cell / SF6 / SF6

020529		Test1b	4KS berm	Yes	Empty cell / SF6 / SF6
020513		Test1	4KS berm	Yes	Empty cell / SF6 / SF6
020513		Test2	7KS berm	Yes	Empty cell / SF6 / SF6
020513		Test3	7KS berm	Yes	Empty cell / SF6 / SF6
020507		Test1	4KS BB (old)	Yes	Empty cell / SF6 / SF6
020507		Test2	7KS berm	Yes	Empty cell / SF6 / SF6
020506		Test1	4KS BB (old)	Yes	No gas cell
020506		Test2	4KS BB (old)	Yes	Empty cell / SF6 / SF6
020506		Test3	7KS berm	Yes	SF6 (steady state)
020506		Test4	4KS BB (old)	Yes	SF6 (steady state)
020506		Test5	4KS BB (old)	Yes	No gas cell
020506		Test7	4KS BB (old)	Yes	No gas cell

Appendix B. HD/DD DC DIAL Results

HD/DD DIAL Comparison Test 030828_T3D (SF6 + NH3, ML On, 7KS Berm, 12” HD Rx)

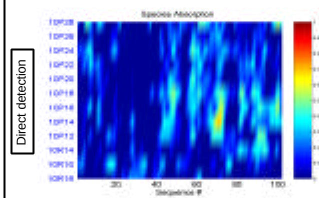

	Sequences	Measured CL (ppm-m)	Measured Dp (psi)	Expected Dp (psi)
Reference	5 - 35	-0.79 ± 1.82 (DD SF6) 0.22 ± 2.15 (HDx3 SF6) -20 ± 96 (DD NH3) 6 ± 140 (HDx3 NH3)	--	--
Insertion #1 (SF6)	50 - 65	2.00 ± 1.64 (DD) 7.82 ± 2.53 (HDx3)	0.9 (DD) 3.4 (HDx3)	4.5
Insertion #2 (NH3)	80 - 95	232 ± 82 (DD) 319 ± 254 (HDx3)	5.1 (DD) 7.0 (HDx3)	10.0

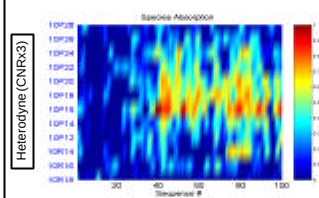

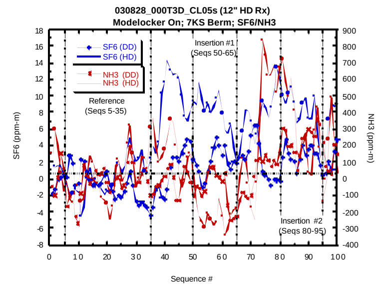

HD/DD DIAL Comparison Test 030828_T3B (SF6 + NH3, ML Off, 7KS Berm, 12” HD Rx)

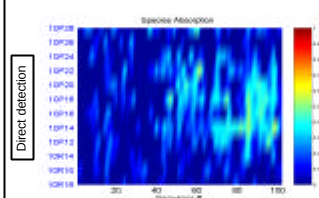

	Sequences	Measured CL (ppm-m)	Measured Dp (psi)	Expected Dp (psi)
Reference	5 - 35	-0.19 ± 1.25 (DD SF6) 0.25 ± 3.36 (HDx3 SF6) -11 ± 101 (DD NH3) 26 ± 233 (HDx3 NH3)	--	--
Insertion #1 (SF6)	50 - 65	2.38 ± 0.95 (DD) 9.55 ± 1.48 (HDx3)	1.0 (DD) 4.2 (HDx3)	4.5
Insertion #2 (NH3)	80 - 95	81 ± 108 (DD) 178 ± 244 (HDx3)	1.8 (DD) 3.9 (HDx3)	10.0

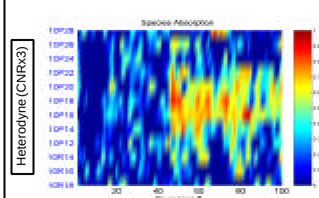

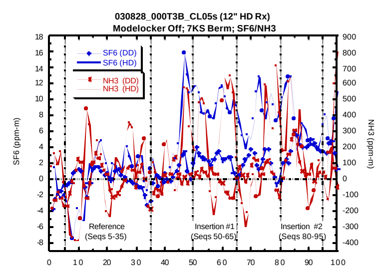

HD/DD DIAL Comparison Test 030828_T2D (SF6 + NH3, ML On, 4KS New BB, 12” HD Rx)

Direct detection

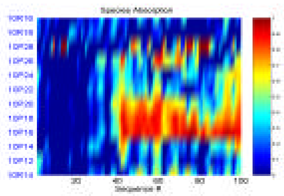

Heterodyne (CNRx3)

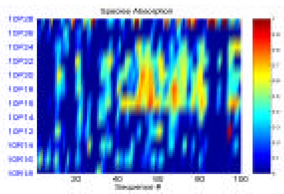

	Sequences	Measured CL (ppm-m)	Measured Dp (psi)	Expected Dp (psi)
Reference	5 - 35	-1.74 ± 3.67 (DD SF6) -0.28 ± 3.67 (HDx3 SF6) -82 ± 185 (DD NH3) 9 ± 257 (HDx3 NH3)	--	--
Insertion #1 (SF6)	50 - 65	12.89 ± 3.29 (DD) 7.53 ± 2.41 (HDx3)	5.6 (DD) 3.3 (HDx3)	4.5
Insertion #2 (NH3)	80 - 95	211 ± 205 (DD) *** ± *** (HDx3)	4.6 (DD) *** (HDx3)	10.0

*** Signal drop-out on heterodyne

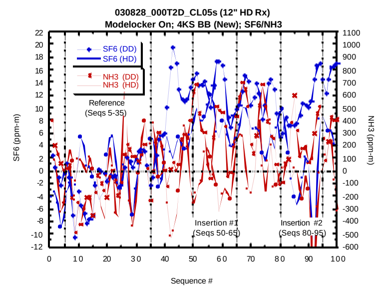

HD/DD DIAL Comparison Test 030828_T2B (SF6 + NH3, ML Off, 4KS New BB, 12” HD Rx)

Direct detection

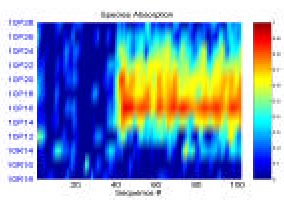

Heterodyne (CNRx3)

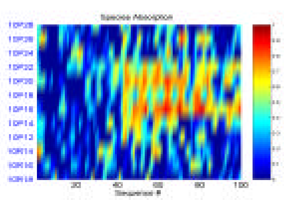

	Sequences	Measured CL (ppm-m)	Measured Dp (psi)	Expected Dp (psi)
Reference	5 - 35	-0.14 ± 1.16 (DD SF6) 0.31 ± 2.16 (HDx3 SF6) 7 ± 179 (DD NH3) 19 ± 269 (HDx3 NH3)	--	--
Insertion #1 (SF6)	50 - 65	11.33 ± 1.20 (DD) 10.70 ± 2.92 (HDx3)	5.0 (DD) 4.7 (HDx3)	4.5
Insertion #2 (NH3)	80 - 95	188 ± 54 (DD) 84 ± 187 (HDx3)	4.1 (DD) 1.8 (HDx3)	10.0

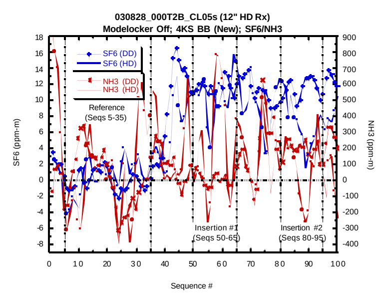

HD/DD DIAL Comparison Test 030826_T3D (SF6 + NH3, ML On, 7KS Berm, 12” HD Rx)

Direct detection

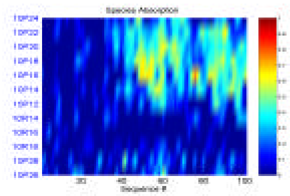

Heterodyne (CNRx3)

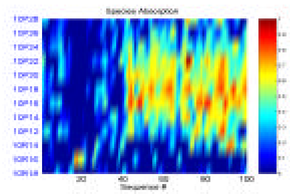

	Sequences	Measured CL (ppm-m)	Measured Δp (psi)	Expected Δp (psi)
Reference	5 - 35	-0.15 ± 0.94 (DD SF6) -0.01 ± 2.65 (HDx3 SF6) -7 ± 106 (DD NH3) 13 ± 160 (HDx3 NH3)	--	--
Insertion #1 (SF6)	50 - 65	5.95 ± 1.52 (DD) 9.49 ± 1.27 (HDx3)	2.6 (DD) 4.2 (HDx3)	4.5
Insertion #2 (NH3)	80 - 95	4 ± 83 (DD) 375 ± 295 (HDx3)	0.1 (DD) 8.2 (HDx3)	10.0

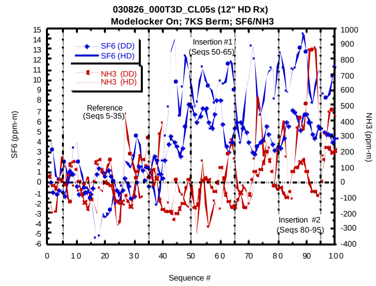

HD/DD DIAL Comparison Test 030826_T3B (SF6 + NH3, ML Off, 7KS Berm, 12” HD Rx)

Direct detection

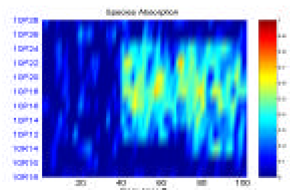

Heterodyne (CNRx3)

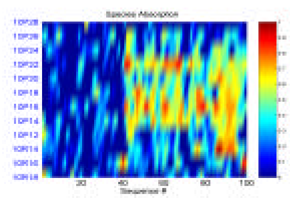

	Sequences	Measured CL (ppm-m)	Measured Δp (psi)	Expected Δp (psi)
Reference	5 - 35	0.00 ± 0.79 (DD SF6) 0.53 ± 1.44 (HDx3 SF6) 6 ± 81 (DD NH3) 17 ± 150 (HDx3 NH3)	--	--
Insertion #1 (SF6)	50 - 65	5.26 ± 0.96 (DD) 8.56 ± 2.10 (HDx3)	2.3 (DD) 3.7 (HDx3)	4.5
Insertion #2 (NH3)	80 - 95	231 ± 114 (DD) 788 ± 517 (HDx3)	5.0 (DD) 17.2 (HDx3)	10.0

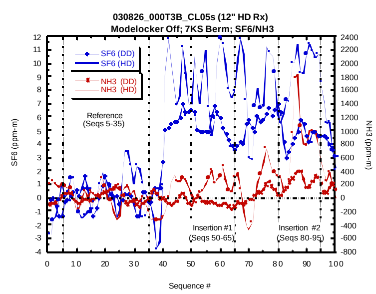

HD/DD DIAL Comparison Test 030826_T2D (SF6 + NH3, ML On, 4KS New BB, 12” HD Rx)

Direct detection

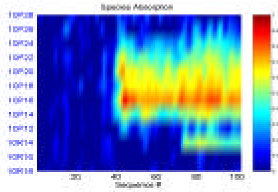

Heterodyne (CNRx3)

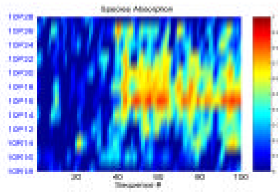

	Sequences	Measured CL (ppm-m)	Measured Δp (psi)	Expected Δp (psi)
Reference	5 - 35	-0.11 ± 0.82 (DD SF6) -0.05 ± 1.92 (HDx3 SF6) -4 ± 50 (DD NH3) 26 ± 224 (HDx3 NH3)	--	--
Insertion #1 (SF6)	50 - 65	9.04 ± 0.57 (DD) 10.88 ± 1.15 (HDx3)	4.0 (DD) 4.8 (HDx3)	4.5
Insertion #2 (NH3)	80 - 95	426 ± 69 (DD) 234 ± 247 (HDx3)	9.3 (DD) 5.1 (HDx3)	10.0

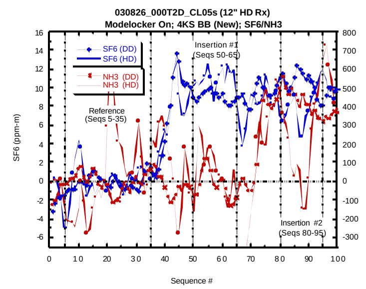

HD/DD DIAL Comparison Test 030826_T2B (SF6 + NH3, ML Off, 4KS New BB, 12” HD Rx)

Direct detection

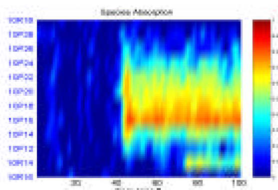

Heterodyne (CNRx3)

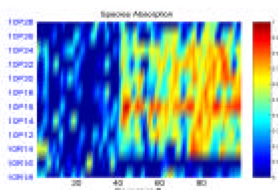

	Sequences	Measured CL (ppm-m)	Measured Δp (psi)	Expected Δp (psi)
Reference	5 - 35	0.01 ± 0.87 (DD SF6) 0.31 ± 1.91 (HDx3 SF6) -1 ± 51 (DD NH3) 26 ± 197 (HDx3 NH3)	--	--
Insertion #1 (SF6)	50 - 65	9.92 ± 0.79 (DD) 8.65 ± 2.54 (HDx3)	4.3 (DD) 3.8 (HDx3)	4.5
Insertion #2 (NH3)	80 - 95	409 ± 75 (DD) 480 ± 169 (HDx3)	8.9 (DD) 10.5 (HDx3)	10.0

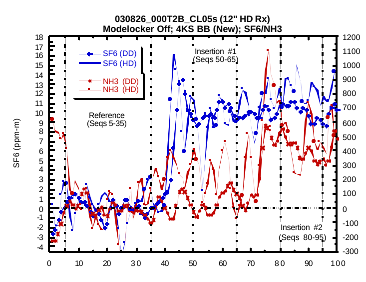

HD/DD DIAL Comparison Test 030807_T3D (SF6 + NH3, Modelocking Off, 7KS Berm)

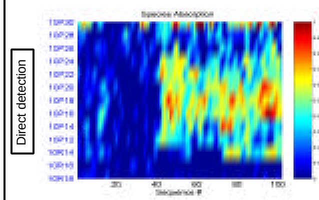

	Sequences	Measured CL (ppm-m)	Measured Dp (psi)	Expected Dp (psi)
Reference	5 - 35	-0.04 ± 1.67 (DD SF6) -0.07 ± 1.69 (HDx3 SF6) -6 ± 129 (DD NH3) 9 ± 105 (HDx3 NH3)	--	--
Insertion #1 (SF6)	50 - 65	7.50 ± 1.27 (DD) 10.50 ± 1.17 (HDx3)	3.3 (DD) 4.6 (HDx3)	4.5
Insertion #2 (NH3)	80 - 95	332 ± 138 (DD) 346 ± 153 (HDx3)	7.3 (DD) 7.6 (HDx3)	10.0

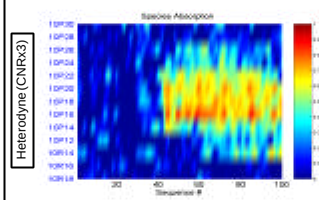

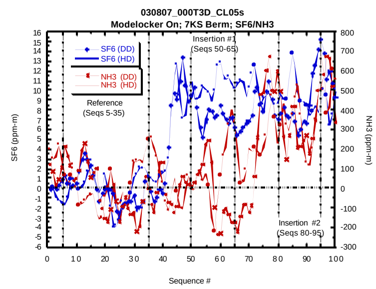

HD/DD DIAL Comparison Test 030807_T3B (SF6 + NH3, Modelocking Off, 7KS Berm)

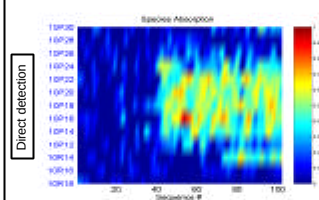

	Sequences	Measured CL (ppm-m)	Measured Dp (psi)	Expected Dp (psi)
Reference	5 - 35	0.05 ± 0.87 (DD SF6) 0.08 ± 2.09 (HDx3 SF6) 4 ± 66 (DD NH3) 5 ± 160 (HDx3 NH3)	--	--
Insertion #1 (SF6)	50 - 65	8.77 ± 1.77 (DD) 8.66 ± 1.39 (HDx3)	3.8 (DD) 3.8 (HDx3)	4.5
Insertion #2 (NH3)	80 - 95	366 ± 133 (DD) 657 ± 313 (HDx3)	8.0 (DD) 14.4 (HDx3)	10.0

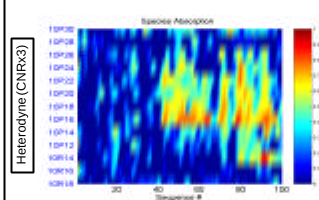

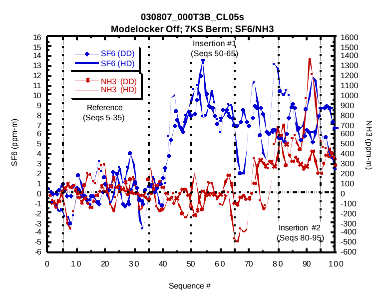

HD/DD DIAL Comparison Test 030807_T2D (SF6 + NH3, Modelocking On, 4KS New BB)

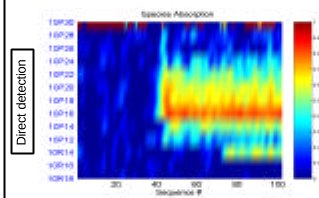

	Sequences	Measured CL (ppm-m)	Measured Dp (psi)	Expected Dp (psi)
Reference	5 - 35	-0.11 ± 0.80 (DD SF6) 0.07 ± 1.49 (HDx3 SF6) -4 ± 58 (DD NH3) 4 ± 152 (HDx3 NH3)	--	--
Insertion #1 (SF6)	50 - 65	10.27 ± 0.53 (DD) 7.90 ± 1.63 (HDx3)	4.5 (DD) 3.5 (HDx3)	4.5
Insertion #2 (NH3)	80 - 95	457 ± 75 (DD) 219 ± 91 (HDx3)	10.0 (DD) 4.8 (HDx3)	10.0

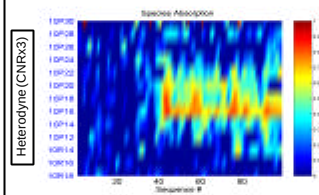

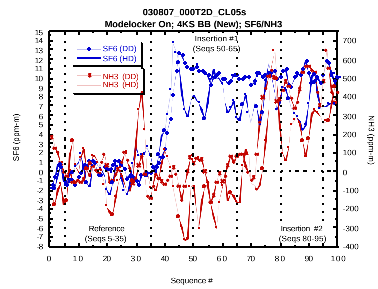

HD/DD DIAL Comparison Test 030807_T2B (SF6 + NH3, Modelocking Off, 4KS New BB)

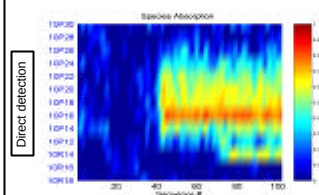

	Sequences	Measured CL (ppm-m)	Measured Dp (psi)	Expected Dp (psi)
Reference	5 - 35	0.05 ± 1.08 (DD SF6) 0.02 ± 1.55 (HDx3 SF6) -1 ± 66 (DD NH3) 18 ± 169 (HDx3 NH3)	--	--
Insertion #1 (SF6)	50 - 65	9.75 ± 0.68 (DD) 7.34 ± 1.79 (HDx3)	4.3 (DD) 3.2 (HDx3)	4.5
Insertion #2 (NH3)	80 - 95	503 ± 64 (DD) 105 ± 130 (HDx3)	11.0 (DD) 2.3 (HDx3)	10.0

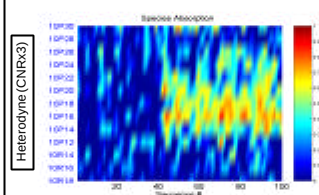

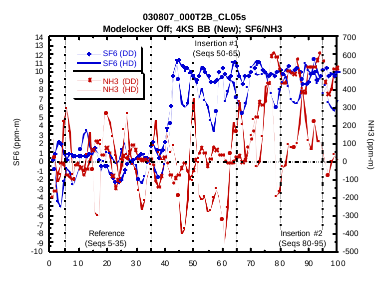

HD/DD DIAL Comparison Test 030724_T2D (SF6 + NH3, Modelocking On, 7KS Berm)

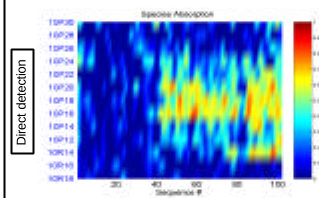

	Sequences	Measured CL (ppm-m)	Measured Δp (psi)	Expected Δp (psi)
Reference	5 - 35	0.17 ± 1.02 (DD SF6) 0.07 ± 1.67 (HDx3 SF6) 5 ± 52 (DD NH3) 10 ± 119 (HDx3 NH3)	--	--
Insertion #1 (SF6)	50 - 65	7.79 ± 1.38 (DD) 9.42 ± 1.48 (HDx3)	3.4 (DD) 4.1 (HDx3)	4.5
Insertion #2 (NH3)	80 - 95	425 ± 182 (DD) 231 ± 210 (HDx3)	9.3 (DD) 5.0 (HDx3)	10.0

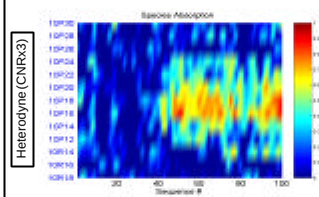

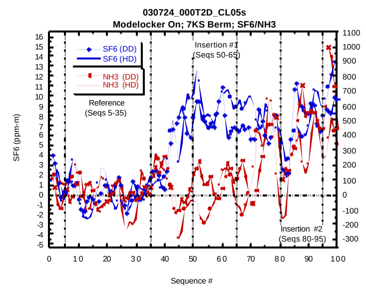

HD/DD DIAL Comparison Test 030724_T2B (SF6 + NH3, Modelocking Off, 7KS Berm)

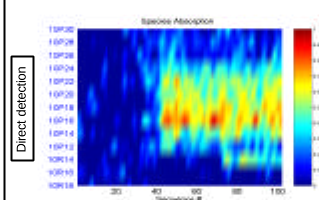

	Sequences	Measured CL (ppm-m)	Measured Δp (psi)	Expected Δp (psi)
Reference	5 - 35	0.01 ± 0.79 (DD SF6) 0.08 ± 1.59 (HDx3 SF6) -1 ± 62 (DD NH3) -8 ± 148 (HDx3 NH3)	--	--
Insertion #1 (SF6)	50 - 65	9.02 ± 1.31 (DD) 7.84 ± 1.37 (HDx3)	3.9 (DD) 3.4 (HDx3)	4.5
Insertion #2 (NH3)	80 - 95	367 ± 91 (DD) 255 ± 234 (HDx3)	8.0 (DD) 5.6 (HDx3)	10.0

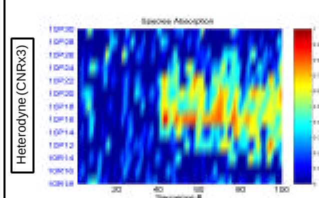

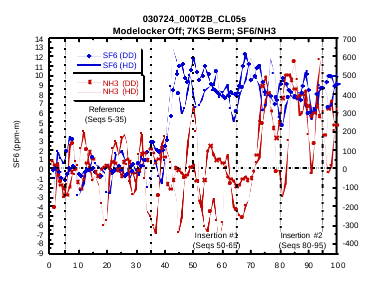

HD/DD DIAL Comparison Test 030612_T3D (NH3 + SF6, Modelocker On, 15KS Blueboard)

Direct detection

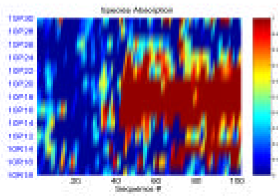

Heterodyne (CNRx3)

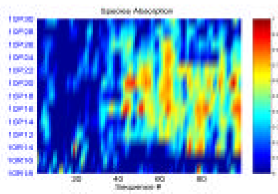

	Sequences	Measured CL (ppm-m)	Measured Dp (psi)	Expected Dp (psi)
Reference	5 - 35	0.79 ± 4.45 (DD SF6) 0.10 ± 2.03 (HDx3 SF6) 70 ± 265 (DD NH3) 36 ± 313 (HDx3 NH3)	--	--
Insertion #1 (SF6)	50 - 65	25.48 ± 3.11 (DD) 10.03 ± 2.53 (HDx3)	11.1 (DD)* 4.4 (HDx3)	4.5
Insertion #2 (NH3)	80 - 95	1676 ± 399 (DD) 277 ± 305 (HDx3)	36.6 (DD)* 6.1 (HDx3)	10.0

* Low signal level, error-induced saturated absorption

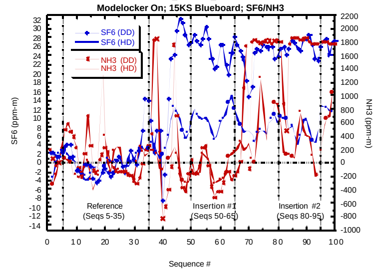

HD/DD DIAL Comparison Test 030612_T3B (NH3 + SF6, Modelocker Off, 15KS Blueboard)

Direct detection

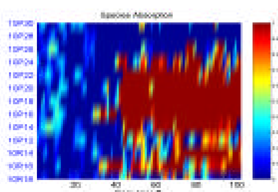

Heterodyne (CNRx3)

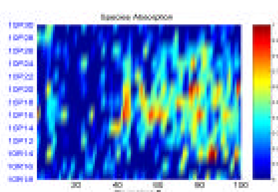

	Sequences	Measured CL (ppm-m)	Measured Dp (psi)	Expected Dp (psi)
Reference	5 - 35	1.01 ± 2.33 (DD SF6) 0.22 ± 2.21 (HDx3 SF6) 28 ± 129 (DD NH3) 6 ± 205 (HDx3 NH3)	--	--
Insertion #1 (SF6)	50 - 65	26.73 ± 3.53 (DD) 6.47 ± 1.62 (HDx3)	11.7 (DD)* 2.8 (HDx3)	4.5
Insertion #2 (NH3)	80 - 95	1801 ± 28 (DD) 631 ± 581 (HDx3)	39.4 (DD)* 13.8 (HDx3)	10.0

* Low signal level, error-induced saturated absorption

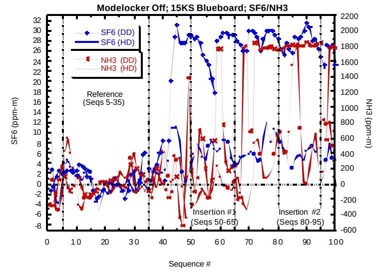

HD/DD DIAL Comparison Test 030612_T2D (SF6 + NH3, Modelocking On, 7KS Berm)

Direct detection

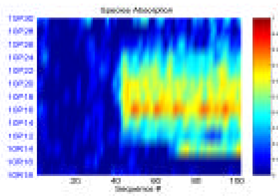

Heterodyne (CNRx3)

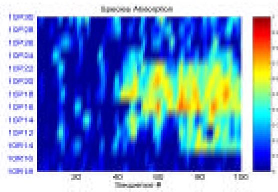

	Sequences	Measured CL (ppm-m)	Measured Dp (psi)	Expected Dp (psi)
Reference	5 - 35	0.05 ± 0.68 (DD SF6) 0.01 ± 1.24 (HDx3 SF6) 1 ± 60 (DD NH3) -3 ± 132 (HDx3 NH3)	--	--
Insertion #1 (SF6)	50 - 65	9.10 ± 0.61 (DD) 6.77 ± 1.72 (HDx3)	4.0 (DD) 3.0 (HDx3)	4.5
Insertion #2 (NH3)	80 - 95	410 ± 45 (DD) 397 ± 90 (HDx3)	9.0 (DD) 8.7 (HDx3)	10.0

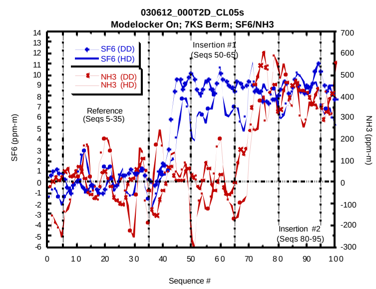

HD/DD DIAL Comparison Test 030612_T2B (SF6 + NH3, Modelocking Off, 7KS Berm)

Direct detection

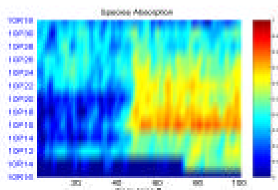

Heterodyne (CNRx3)

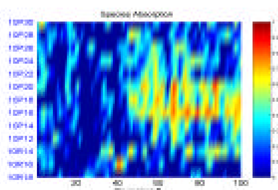

	Sequences	Measured CL (ppm-m)	Measured Dp (psi)	Expected Dp (psi)
Reference	5 - 35	2.58 ± 0.54 (DD SF6) 0.29 ± 1.82 (HDx3 SF6) 23 ± 56 (DD NH3) 12 ± 186 (HDx3 NH3)	--	--
Insertion #1 (SF6)	50 - 65	11.05 ± 0.66 (DD) 7.08 ± 1.91 (HDx3)	4.8 (DD) 3.1 (HDx3)	4.5
Insertion #2 (NH3)	80 - 95	410 ± 46 (DD) 383 ± 125 (HDx3)	9.0 (DD) 8.4 (HDx3)	10.0

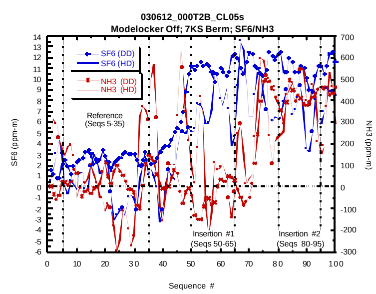

HD/DD DIAL Comparison Test 030604_T2B (NH3 + SF6, Modelocker Out, 7KS Berm)

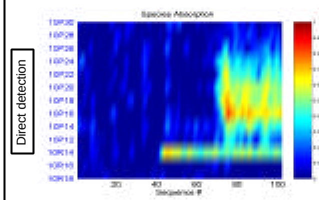

	Sequences	Measured CL (ppm-m)	Measured Dp (psi)	Expected Dp (psi)
Reference	5 - 35	0.03 ± 0.60 (DD SF6) 0.16 ± 2.01 (HDx3 SF6) -1 ± 55 (DD NH3) 2 ± 155 (HDx3 NH3)	--	--
Insertion #1 (NH3)	50 - 65	426 ± 67 (DD) 462 ± 149 (HDx3)	9.3 (DD) 10.1 (HDx3)	10.0
Insertion #2 (SF6)	80 - 95	8.00 ± 0.86 (DD) 6.19 ± 4.13 (HDx3)	3.5 (DD) 2.7 (HDx3)	4.5

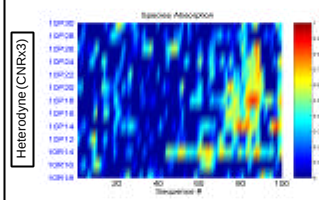

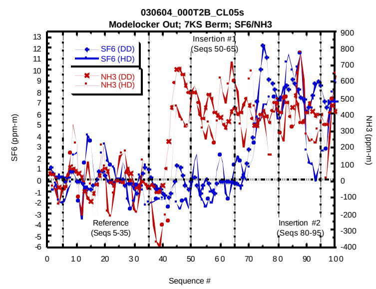

HD/DD DIAL Comparison Test 030604_T1D (SF6 + NH3, Modelocker Out, 4KS New BB)

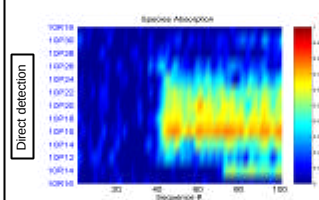

	Sequences	Measured CL (ppm-m)	Measured Dp (psi)	Expected Dp (psi)
Reference	5 - 35	0.02 ± 0.68 (DD SF6) 0.15 ± 1.69 (HDx3 SF6) -1 ± 38 (DD NH3) 25 ± 249 (HDx3 NH3)	--	--
Insertion #1 (SF6)	50 - 65	8.92 ± 1.08 (DD) 5.86 ± 1.79 (HDx3)	3.9 (DD) 2.6 (HDx3)	4.5
Insertion #2 (NH3)	80 - 95	399 ± 44 (DD) 237 ± 221 (HDx3)	8.7 (DD) 5.2 (HDx3)	10.0

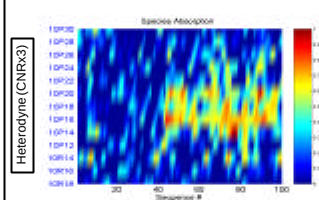

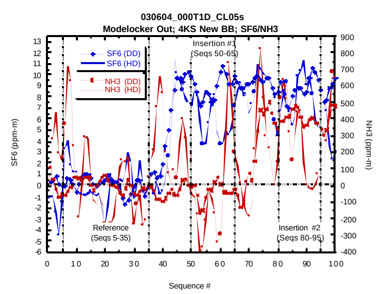

HD/DD DIAL Comparison Test 030529_T4D (SF6 + NH3, Modelocking On, 7KS Berm)

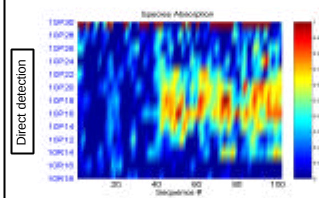

	Sequences	Measured CL (ppm-m)	Measured Dp (psi)	Expected Dp (psi)
Reference	5 - 35	0.05 ± 1.72 (DD SF6) -0.16 ± 2.01 (HDx3 SF6) 0 ± 125 (DD NH3) 9 ± 148 (HDx3 NH3)	--	--
Insertion #1 (SF6)	50 - 65	8.96 ± 2.70 (DD) 11.28 ± 0.96 (HDx3)	3.9 (DD) 4.9 (HDx3)	4.5
Insertion #2 (NH3)	80 - 95	203 ± 95 (DD) 457 ± 119 (HDx3)	4.4 (DD) 10.0 (HDx3)	10.0

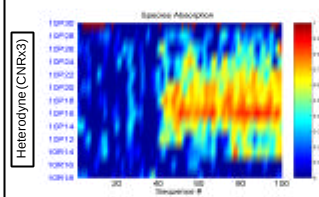

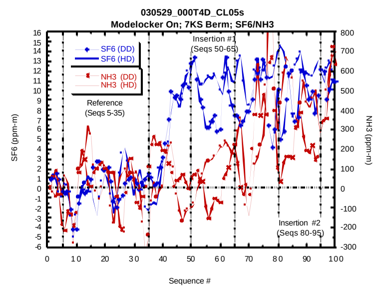

HD/DD DIAL Comparison Test 030529_T4B (SF6 + NH3, Modelocking Off, 7KS Berm)

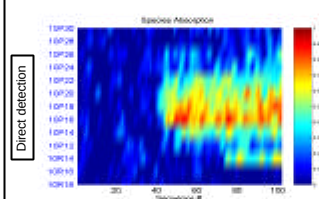

	Sequences	Measured CL (ppm-m)	Measured Dp (psi)	Expected Dp (psi)
Reference	5 - 35	0.05 ± 0.76 (DD SF6) 0.07 ± 2.36 (HDx3 SF6) 5 ± 88 (DD NH3) -2 ± 238 (HDx3 NH3)	--	--
Insertion #1 (SF6)	50 - 65	10.31 ± 0.97 (DD) 9.32 ± 1.84 (HDx3)	4.5 (DD) 4.1 (HDx3)	4.5
Insertion #2 (NH3)	80 - 95	392 ± 120 (DD) 251 ± 257 (HDx3)	8.6 (DD) 5.5 (HDx3)	10.0

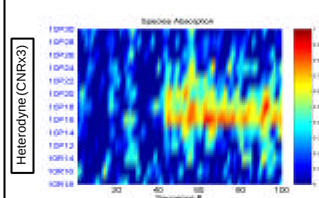

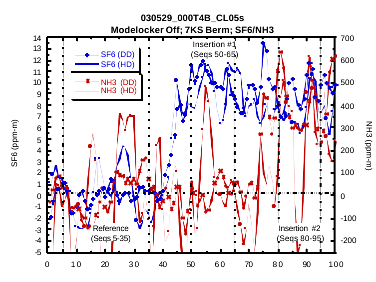

HD/DD DIAL Comparison Test 030529_T3D (SF6 + NH3, Modelocking On, 4KS New BB)

Direct detection

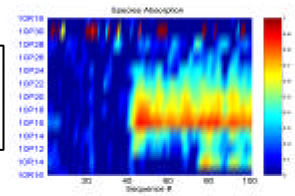

Heterodyne (CNRx3)

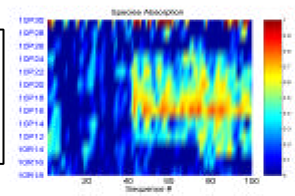

	Sequences	Measured CL (ppm-m)	Measured Δp (psi)	Expected Δp (psi)
Reference	5 - 35	-0.12 ± 0.78 (DD SF6) 0.03 ± 1.69 (HDx3 SF6) -7 ± 78 (DD NH3) 13 ± 219 (HDx3 NH3)	--	--
Insertion #1 (SF6)	50 - 65	9.56 ± 1.03 (DD) 7.66 ± 1.43 (HDx3)	4.2 (DD) 3.3 (HDx3)	4.5
Insertion #2 (NH3)	80 - 95	418 ± 128 (DD) 339 ± 196 (HDx3)	9.1 (DD) 7.4 (HDx3)	10.0

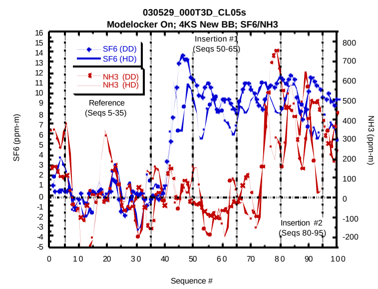

HD/DD DIAL Comparison Test 030529_T3B (SF6 + NH3, Modelocking Off, 4KS New BB)

Direct detection

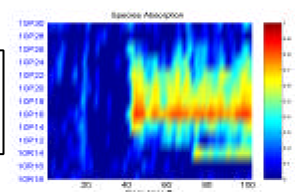

Heterodyne (CNRx3)

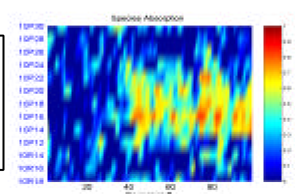

	Sequences	Measured CL (ppm-m)	Measured Δp (psi)	Expected Δp (psi)
Reference	5 - 35	0.00 ± 1.11 (DD SF6) 0.18 ± 1.65 (HDx3 SF6) -5 ± 80 (DD NH3) 18 ± 201 (HDx3 NH3)	--	--
Insertion #1 (SF6)	50 - 65	8.78 ± 1.35 (DD) 7.59 ± 1.01 (HDx3)	3.8 (DD) 3.3 (HDx3)	4.5
Insertion #2 (NH3)	80 - 95	404 ± 60 (DD) 209 ± 194 (HDx3)	8.8 (DD) 4.6 (HDx3)	10.0

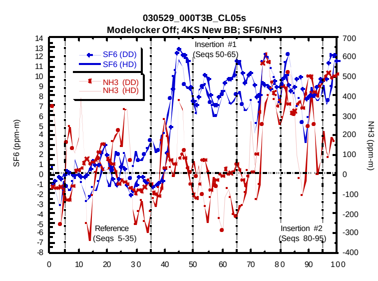

HD/DD DIAL Comparison Test 030416_T2Dm (SF6 + NH3, Modelocking On, 7KS Berm)

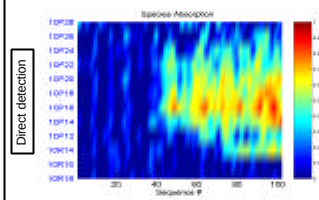

	Sequences	Measured CL (ppm-m)	Measured Δp (psi)	Expected Δp (psi)
Reference	5 - 35	-0.09 ± 1.22 (DD SF6) -0.18 ± 1.48 (HDx3 SF6) -2 ± 88 (DD NH3) -6 ± 145 (HDx3 NH3)	--	--
Insertion #1 (SF6)	50 - 95	7.53 ± 2.18 (DD) 7.25 ± 1.28 (HDx3)	3.3 (DD) 3.2 (HDx3)	4.3
Insertion #2 (NH3)	80 - 95	416 ± 51 (DD) 516 ± 160 (HDx3)	9.1 (DD) 11.3 (HDx3)	10.0

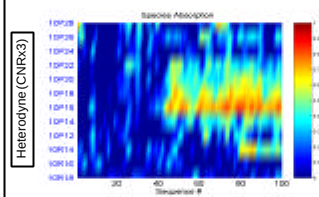

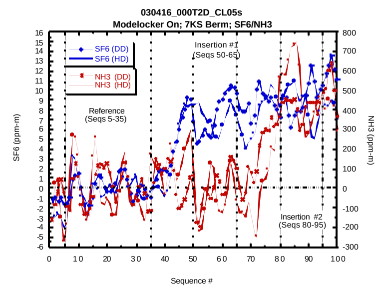

HD/DD DIAL Comparison Test 030416_T2B (SF6 + NH3, Modelocking Off, 7KS Berm)

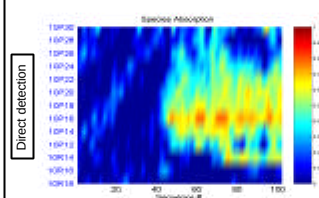

	Sequences	Measured CL (ppm-m)	Measured Δp (psi)	Expected Δp (psi)
Reference	5 - 35	0.05 ± 0.97 (DD SF6) 0.39 ± 4.33 (HDx3 SF6) -1 ± 58 (DD NH3) 4 ± 216 (HDx3 NH3)	--	--
Insertion #1 (SF6)	50 - 95	8.66 ± 1.03 (DD) 5.47 ± 3.74 (HDx3)	3.8 (DD) 2.4 (HDx3)	4.3
Insertion #2 (NH3)	80 - 95	447 ± 91 (DD) 302 ± 243 (HDx3)	9.8 (DD) 6.6 (HDx3)	10.0

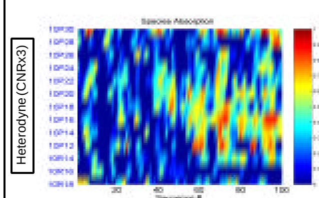

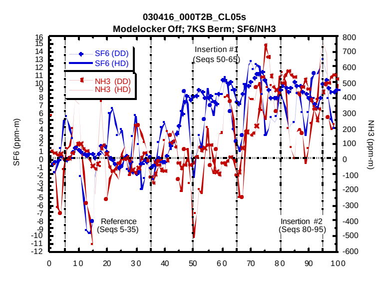

HD/DD DIAL Comparison Test 030416_T1D (SF6 + NH3, Modelocking On, 4KS New BB)

Direct detection

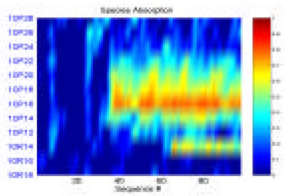

Heterodyne (CNRx3)

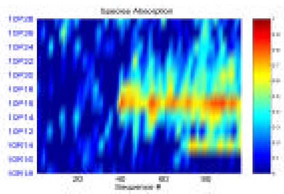

	Sequences	Measured CL (ppm-m)	Measured Dp (psi)	Expected Dp (psi)
Reference	5 - 35	-0.14 ± 1.41 (DD SF6) 0.02 ± 1.19 (HDx3 SF6) -0.14 ± 1.41 (DD NH3) 0.02 ± 1.19 (HDx3 NH3)	--	--
Insertion #1 (SF6)	50 - 95	8.68 ± 1.11 (DD) 7.69 ± 1.33 (HDx3)	3.8 (DD) 3.4 (HDx3)	4.3
Insertion #2 (NH3)	80 - 95	490 ± 68 (DD) 517 ± 93 (HDx3)	10.7 (DD) 11.3 (HDx3)	10.0

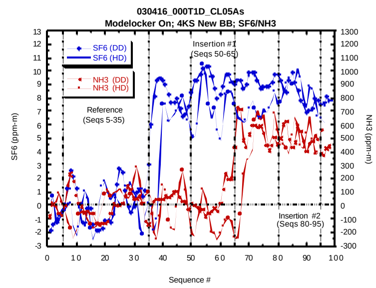

HD/DD DIAL Comparison Test 030416_T1B (SF6 + NH3, Modelocking Off, 4KS New BB)

Direct detection

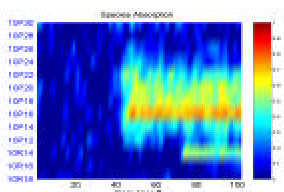

Heterodyne (CNRx3)

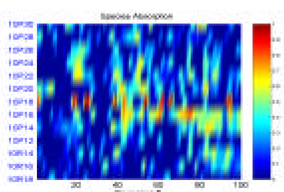

	Sequences	Measured CL (ppm-m)	Measured Dp (psi)	Expected Dp (psi)
Reference	5 - 35	0.01 ± 0.60 (DD SF6) 0.23 ± 2.64 (HDx3 SF6) 0 ± 54 (DD NH3) 3 ± 157 (HDx3 NH3)	--	--
Insertion #1 (SF6)	50 - 95	8.13 ± 0.58 (DD) 3.73 ± 3.00 (HDx3)	3.6 (DD) 1.6 (HDx3)	4.3
Insertion #2 (NH3)	80 - 95	414 ± 34 (DD) 344 ± 149 (HDx3)	9.0 (DD) 7.5 (HDx3)	10.0

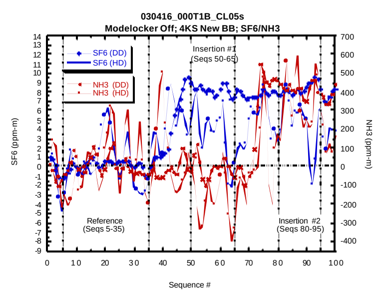

HD/DD DIAL Comparison Test 030415_T1F (SF6 + NH3, Modelocking Off, 4KS New BB)

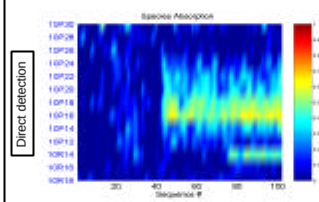

	Sequences	Measured CL (ppm-m)	Measured Dp (psi)	Expected Dp (psi)
Reference	5 - 35	0.13 ± 0.92 (DD SF6) 0.86 ± 2.29 (HDx3 SF6) 11 ± 79 (DD NH3) 57 ± 258 (HDx3 NH3)	--	--
Insertion #1 (SF6)	50 - 95	4.84 ± 0.52 (DD) 5.11 ± 3.08 (HDx3)	2.1 (DD) 2.2 (HDx3)	4.3
Insertion #2 (NH3)	80 - 95	353 ± 73 (DD) -82 ± 176 (HDx3)	7.7 (DD) -1.8 (HDx3)	10.0

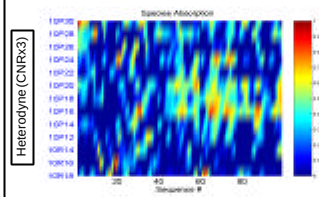

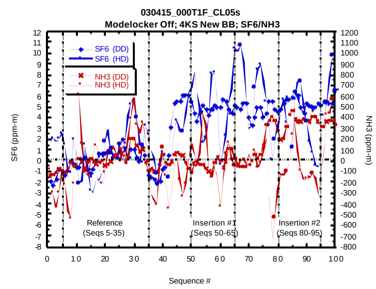

HD/DD DIAL Comparison Test 030415_T1D (SF6 + NH3, Modelocking On, 4KS New BB)

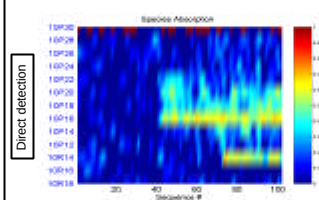

	Sequences	Measured CL (ppm-m)	Measured Dp (psi)	Expected Dp (psi)
Reference	5 - 35	-0.06 ± 0.59 (DD SF6) 0.13 ± 1.13 (HDx3 SF6) 2 ± 91 (DD NH3) 0 ± 77 (HDx3 NH3)	--	--
Insertion #1 (SF6)	50 - 95	4.38 ± 0.53 (DD) 5.18 ± 1.67 (HDx3)	1.9 (DD) 2.3 (HDx3)	4.3
Insertion #2 (NH3)	80 - 95	442 ± 96 (DD) 342 ± 138 (HDx3)	9.7 (DD) 7.5 (HDx3)	10.0

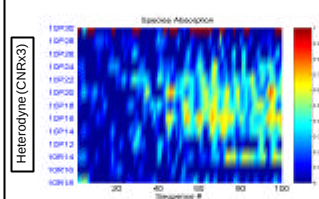

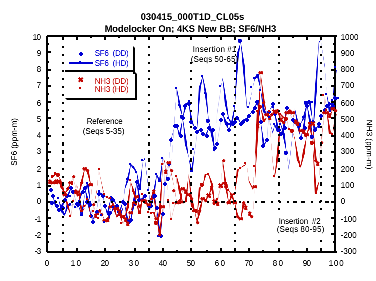

HD/DD DIAL Comparison Test 030224_T4D (Modelocking On, 7KS Berm, 0ND/5X)

Direct detection

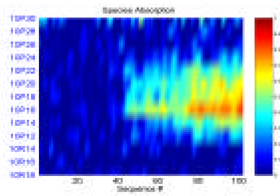

Heterodyne (CNRx3)

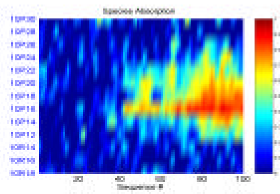

	Sequences	Measured CL (ppm-m)	Measured Dp (psi)	Expected Dp (psi)
Reference	5 - 35	0.03 ± 0.49 (DD) 0.15 ± 0.98 (HDx3)	--	--
Insertion #1	50 - 65	4.92 ± 1.00 (DD) 6.96 ± 1.40 (HDx3)	2.2 (DD) 3.0 (HDx3)	3.0
Insertion #2	80 - 95	9.23 ± 0.76 (DD) 13.71 ± 1.23 (HDx3)	4.0 (DD) 6.0 (HDx3)	6.0

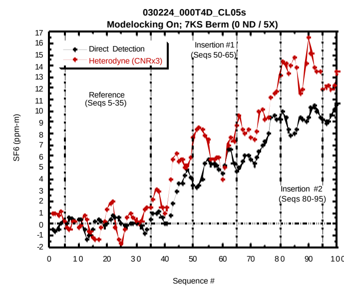

HD/DD DIAL Comparison Test 030224_T4B (Modelocking Off, 7KS Berm, 0ND/5X)

Direct detection

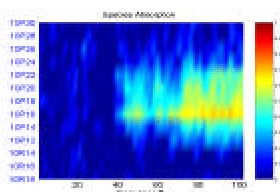

Heterodyne (CNRx3)

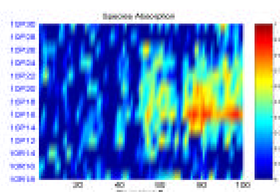

	Sequences	Measured CL (ppm-m)	Measured Dp (psi)	Expected Dp (psi)
Reference	5 - 35	-0.01 ± 0.66 (DD) 0.24 ± 1.54 (HDx3)	--	--
Insertion #1	50 - 65	4.24 ± 0.73 (DD) 6.50 ± 1.18 (HDx3)	1.9 (DD) 2.8 (HDx3)	3.0
Insertion #2	80 - 95	7.56 ± 0.50 (DD) 9.69 ± 1.83 (HDx3)	3.3 (DD) 4.2 (HDx3)	6.0

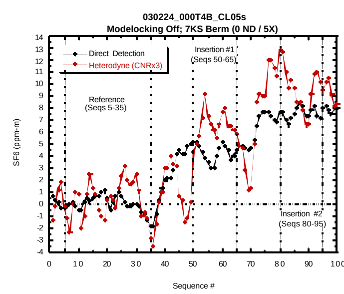

HD/DD DIAL Comparison Test
030224_T3D (Modelocking On, 4KS BB, 1ND/5X)

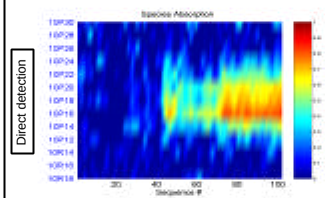

	Sequences	Measured CL (ppm-m)	Measured Δp (psi)	Expected Δp (psi)
Reference	5 - 35	0.03 ± 1.10 (DD) 0.08 ± 0.89 (HDx3)	--	--
Insertion #1	50 - 65	4.89 ± 0.69 (DD) 6.15 ± 1.37 (HDx3)	2.1 (DD) 2.7 (HDx3)	3.0
Insertion #2	80 - 95	10.45 ± 0.61 (DD) 10.78 ± 1.75 (HDx3)	4.6 (DD) 4.7 (HDx3)	6.0

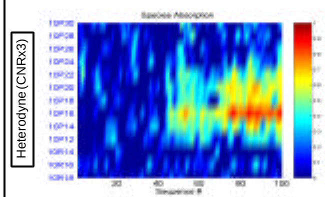

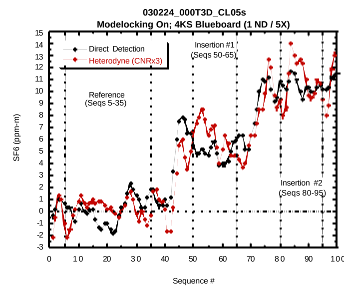

HD/DD DIAL Comparison Test
030224_T3B (Modelocking Off, 4KS BB, 1ND/5X)

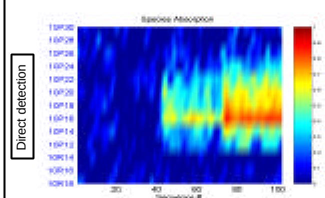

	Sequences	Measured CL (ppm-m)	Measured Δp (psi)	Expected Δp (psi)
Reference	5 - 35	-0.02 ± 0.73 (DD) 0.34 ± 1.50 (HDx3)	--	--
Insertion #1	50 - 65	5.57 ± 0.70 (DD) 3.52 ± 2.29 (HDx3)	2.4 (DD) 1.5 (HDx3)	3.0
Insertion #2	80 - 95	10.71 ± 0.70 (DD) 7.09 ± 1.86 (HDx3)	4.7 (DD) 3.1 (HDx3)	6.0

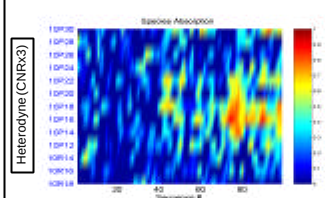

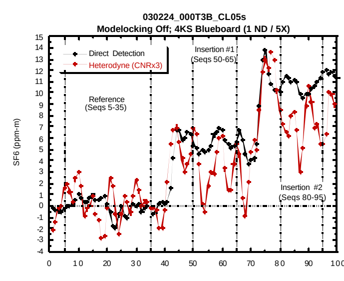

HD/DD DIAL Comparison Test 030224_T2D (Modelocking On, 4KS BB, 1ND/10X)

Direct detection

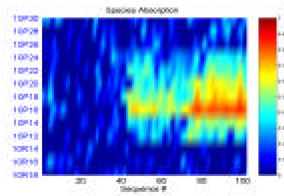

Heterodyne (CNRx3)

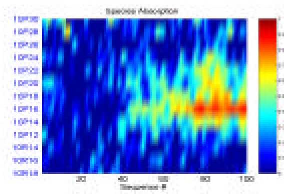

	Sequences	Measured CL (ppm-m)	Measured Δp (psi)	Expected Δp (psi)
Reference	5 - 35	0.14 ± 1.23 (DD) 0.10 ± 1.09 (HDx3)	--	--
Insertion #1	50 - 65	6.09 ± 0.72 (DD) 5.13 ± 0.91 (HDx3)	2.7 (DD) 2.2 (HDx3)	3.0
Insertion #2	80 - 95	10.63 ± 0.96 (DD) 10.38 ± 1.59 (HDx3)	4.7 (DD) 4.5 (HDx3)	6.0

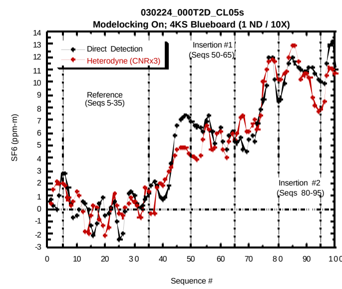

HD/DD DIAL Comparison Test 030224_T2B (Modelocking Off, 4KS BB, 1ND/10X)

Direct detection

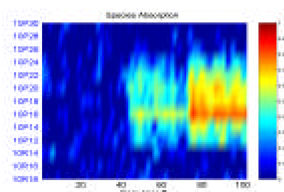

Heterodyne (CNRx3)

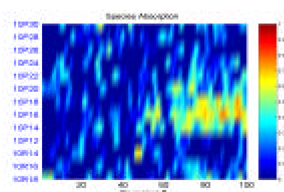

	Sequences	Measured CL (ppm-m)	Measured Δp (psi)	Expected Δp (psi)
Reference	5 - 35	0.00 ± 0.62 (DD) 0.02 ± 1.64 (HDx3)	--	--
Insertion #1	50 - 65	5.60 ± 0.60 (DD) 2.65 ± 1.96 (HDx3)	2.5 (DD) 1.2 (HDx3)	3.0
Insertion #2	80 - 95	10.60 ± 1.07 (DD) 6.03 ± 1.13 (HDx3)	4.6 (DD) 2.6 (HDx3)	6.0

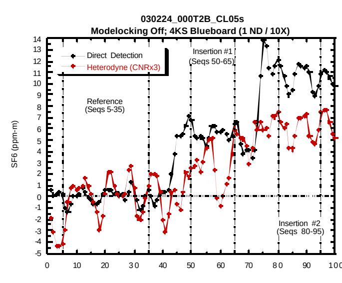

HD/DD DIAL Comparison Test
030224_T1D (Modelocking On, 4KS BB, 3ND/10X)

Direct detection

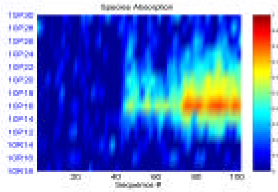

Heterodyne (CNRx3)

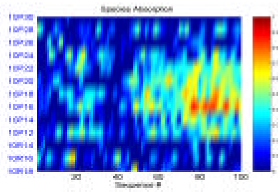

	Sequences	Measured CL (ppm-m)	Measured Dp (psi)	Expected Dp (psi)
Reference	5 - 35	0.03 ± 0.53 (DD) 2.02 ± 1.46 (HDx3)	--	--
Insertion #1	50 - 65	3.98 ± 0.69 (DD) 5.15 ± 1.19 (HDx3)	1.7 (DD) 2.3 (HDx3)	3.0
Insertion #2	80 - 95	9.68 ± 0.89 (DD) 9.31 ± 1.55 (HDx3)	4.2 (DD) 4.1 (HDx3)	6.0

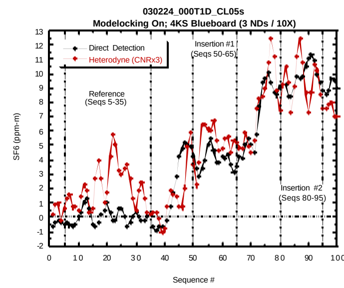

HD/DD DIAL Comparison Test
030224_T1B (Modelocking Off, 4KS BB, 3ND/10X)

Direct detection

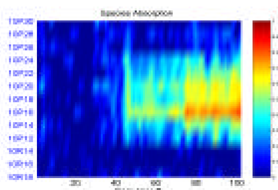

Heterodyne (CNRx3)

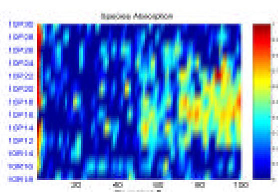

	Sequences	Measured CL (ppm-m)	Measured Dp (psi)	Expected Dp (psi)
Reference	5 - 35	0.08 ± 0.81 (DD) 0.11 ± 1.43 (HDx3)	--	--
Insertion #1	50 - 65	5.58 ± 0.53 (DD) 4.78 ± 1.56 (HDx3)	2.4 (DD) 2.1 (HDx3)	3.0
Insertion #2	80 - 95	9.38 ± 0.90 (DD) 8.39 ± 1.77 (HDx3)	4.1 (DD) 3.7 (HDx3)	6.0

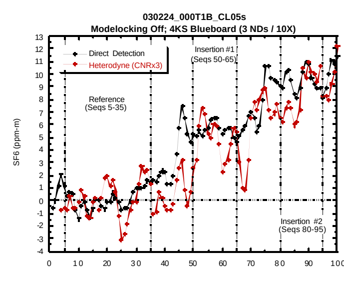

HD/DD DIAL Comparison Test
030129_T2D (Modelocking On, 7KS Berm)

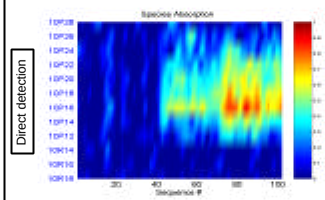

	Sequences	Measured CL (ppm-m)	Measured Dp (psi)	Expected Dp (psi)
Reference	5 - 35	-0.03 ± 1.28 (DD) -0.06 ± 1.01 (HDx3)	--	--
Insertion #1	50 - 65	5.64 ± 0.51 (DD) 5.52 ± 1.05 (HDx3)	2.5 (DD) 2.4 (HDx3)	3.0
Insertion #2	80 - 95	9.52 ± 1.84 (DD) 10.41 ± 1.36 (HDx3)	4.2 (DD) 4.6 (HDx3)	6.0

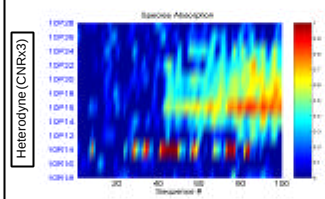

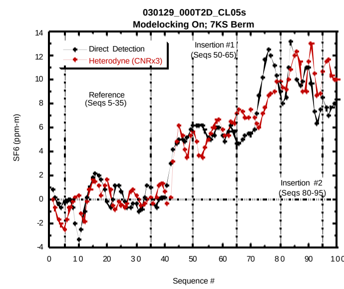

HD/DD DIAL Comparison Test
030129_T2B (Modelocking Off, 7KS Berm)

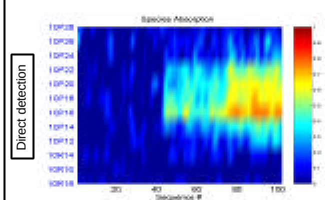

	Sequences	Measured CL (ppm-m)	Measured Dp (psi)	Expected Dp (psi)
Reference	5 - 35	0.01 ± 0.49 (DD) 0.01 ± 1.81 (HDx3)	--	--
Insertion #1	50 - 65	4.56 ± 0.70 (DD) 3.12 ± 1.16 (HDx3)	2.0 (DD) 1.4 (HDx3)	3.0
Insertion #2	80 - 95	9.39 ± 0.82 (DD) 6.21 ± 1.20 (HDx3)	4.1 (DD) 2.7 (HDx3)	6.0

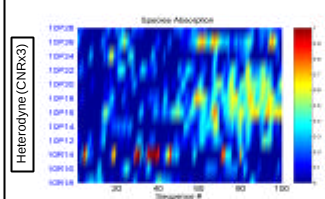

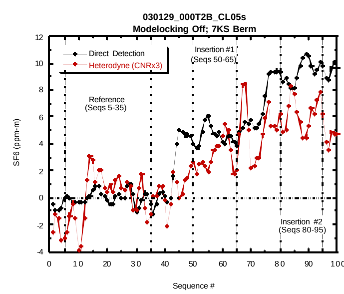

HD/DD DIAL Comparison Test
030129_T1D (Modelocking On, 4KS BB)

	Sequences	Measured CL (ppm-m)	Measured Dp (psi)	Expected Dp (psi)
Reference	5 - 35	0.03 ± 0.75 (DD) -0.10 ± 1.25 (HDx3)	--	--
Insertion #1	50 - 65	6.48 ± 0.61 (DD) 2.55 ± 1.17 (HDx3)	2.8 (DD) 1.1 (HDx3)	3.0
Insertion #2	80 - 95	11.88 ± 0.81 (DD) 6.45 ± 0.71 (HDx3)	5.2 (DD) 2.8 (HDx3)	6.0

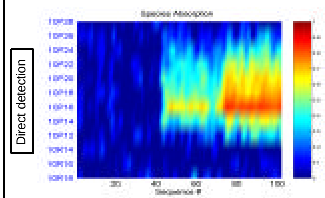

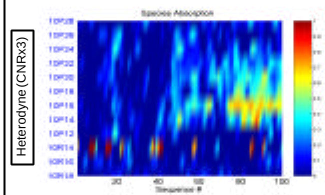

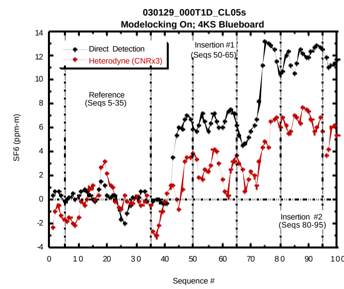

HD/DD DIAL Comparison Test
030129_T1B (Modelocking Off, 4KS BB)

	Sequences	Measured CL (ppm-m)	Measured Dp (psi)	Expected Dp (psi)
Reference	5 - 35	-0.01 ± 0.66 (DD) 0.05 ± 2.18 (HDx3)	--	--
Insertion #1	50 - 65	5.68 ± 0.63 (DD) 2.64 ± 2.72 (HDx3)	2.5 (DD) 1.2 (HDx3)	3.0
Insertion #2	80 - 95	10.43 ± 0.49 (DD) 6.75 ± 1.79 (HDx3)	4.6 (DD) 3.0 (HDx3)	6.0

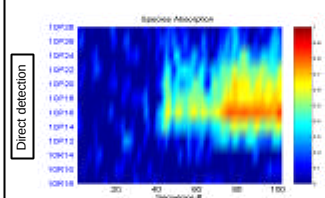

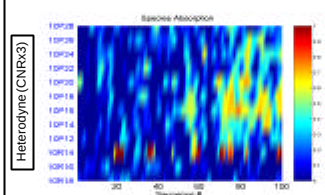

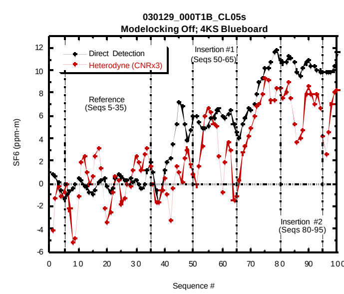

HD/DD DIAL Comparison Test
030123_T2D (Modelocking On, 7KS Berm)

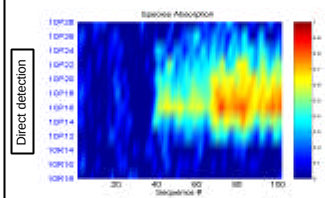

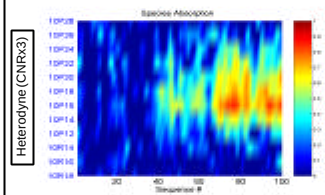

	Sequences	Measured CL (ppm-m)	Measured Dp (psi)	Expected Dp (psi)
Reference	5 - 35	0.01 ± 0.84 (DD) -0.06 ± 1.42 (HDx3)	--	--
Insertion #1	50 - 65	6.07 ± 0.50 (DD) 4.84 ± 1.25 (HDx3)	2.7 (DD) 2.1 (HDx3)	3.0
Insertion #2	80 - 95	10.11 ± 1.44 (DD) 9.54 ± 1.97 (HDx3)	4.4 (DD) 4.2 (HDx3)	6.0

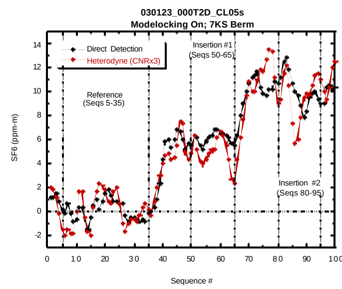

HD/DD DIAL Comparison Test
030123_T2B (Modelocking Off, 7KS Berm)

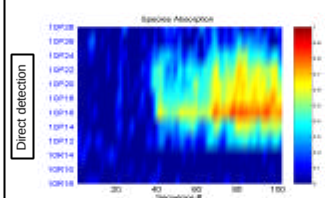

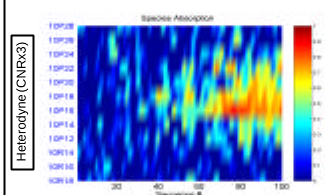

	Sequences	Measured CL (ppm-m)	Measured Dp (psi)	Expected Dp (psi)
Reference	5 - 35	0.00 ± 0.71 (DD) 0.09 ± 1.93 (HDx3)	--	--
Insertion #1	50 - 65	5.75 ± 0.53 (DD) 4.28 ± 2.18 (HDx3)	2.5 (DD) 1.9 (HDx3)	3.0
Insertion #2	80 - 95	11.17 ± 0.75 (DD) 10.41 ± 0.96 (HDx3)	4.9 (DD) 4.6 (HDx3)	6.0

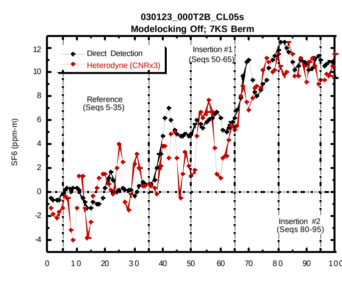

HD/DD DIAL Comparison Test
030123_T1D (Modelocking On, 4KS BB)

Direct detection

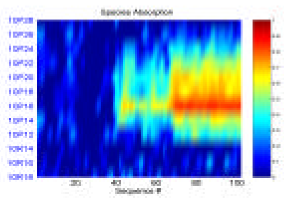

Heterodyne (CNRx3)

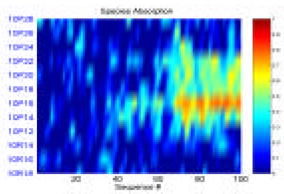

	Sequences	Measured CL (ppm-m)	Measured Dp (psi)	Expected Dp (psi)
Reference	5 - 35	0.07 ± 0.92 (DD) 0.03 ± 1.12 (HDx3)	--	--
Insertion #1	50 - 65	5.52 ± 0.80 (DD) 2.64 ± 1.15 (HDx3)	2.4 (DD) 1.2 (HDx3)	3.0
Insertion #2	80 - 95	12.29 ± 0.53 (DD) 8.46 ± 0.83 (HDx3)	5.4 (DD) 3.7 (HDx3)	6.0

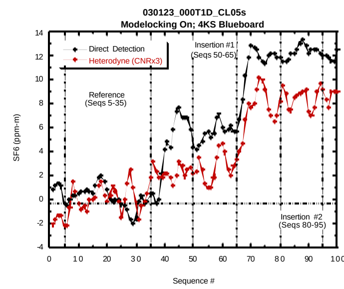

HD/DD DIAL Comparison Test
030123_T1B (Modelocking Off, 4KS BB)

Direct detection

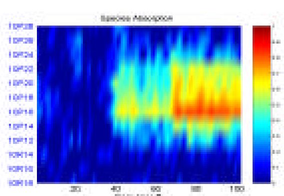

Heterodyne (CNRx3)

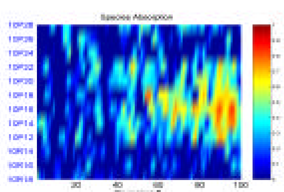

	Sequences	Measured CL (ppm-m)	Measured Dp (psi)	Expected Dp (psi)
Reference	5 - 35	0.05 ± 0.72 (DD) 0.22 ± 2.24 (HDx3)	--	--
Insertion #1	50 - 65	5.99 ± 0.55 (DD) 3.85 ± 2.67 (HDx3)	2.6 (DD) 1.7 (HDx3)	3.0
Insertion #2	80 - 95	11.37 ± 0.74 (DD) 8.48 ± 2.50 (HDx3)	5.0 (DD) 3.7 (HDx3)	6.0

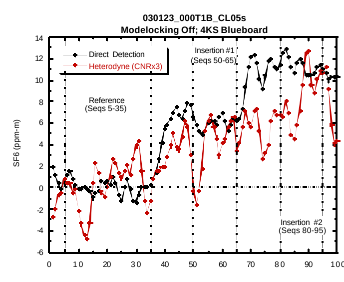

HD/DD DIAL Comparison Test
021218_T3F (Modelocking On, 15KS BB)

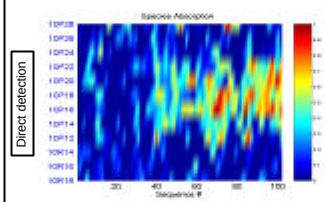

	Sequences	Measured CL (ppm-m)	Measured Dp (psi)	Expected Dp (psi)
Reference	5 - 35	0.08 ± 1.78 (DD) 0.18 ± 1.82 (HDx3)	--	--
Insertion #1	50 - 65	4.69 ± 1.12 (DD) 3.53 ± 1.51 (HDx3)	2.1 (DD) 1.5 (HDx3)	3.0
Insertion #2	80 - 95	7.40 ± 3.02 (DD) 7.99 ± 1.93 (HDx3)	3.2 (DD) 3.5 (HDx3)	6.0

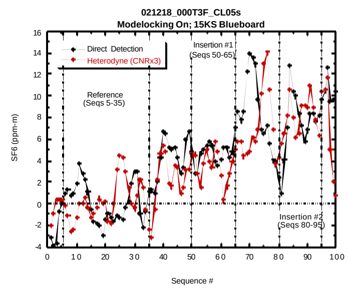

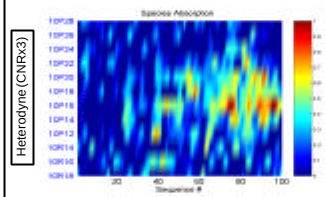

HD/DD DIAL Comparison Test
021218_T3D (Modelocking Off, 15KS BB)

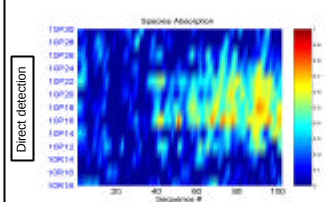

	Sequences	Measured CL (ppm-m)	Measured Dp (psi)	Expected Dp (psi)
Reference	5 - 35	0.04 ± 1.00 (DD) 0.33 ± 1.26 (HDx3)	--	--
Insertion #1	50 - 65	4.37 ± 1.36 (DD) 5.92 ± 1.24 (HDx3)	1.9 (DD) 2.6 (HDx3)	3.0
Insertion #2	80 - 95	7.61 ± 1.98 (DD) 9.68 ± 1.98 (HDx3)	3.3 (DD) 4.2 (HDx3)	6.0

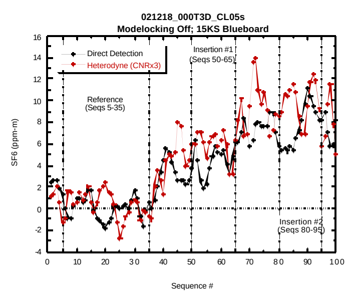

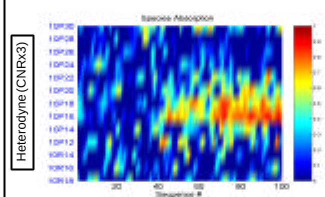

HD/DD DIAL Comparison Test
020926_000T2F (Modelocking Off, 7KS Berm)

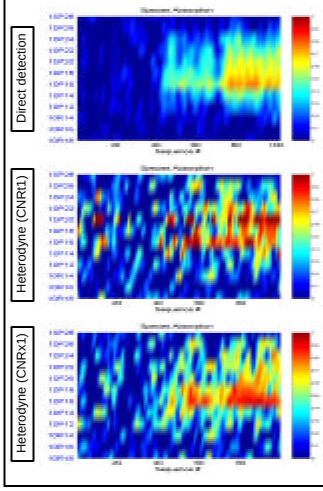

	Sequences	Measured CL (ppm-m)	Measured Dp (psi)	Expected Dp (psi)
Reference	5 - 35	0.03 ± 0.56 (DD) 1.41 ± 3.65 (HDt1) 0.34 ± 2.11 (HDx1)	--	–
Insertion #1	50 - 65	4.75 ± 0.47 (DD) 9.14 ± 4.65 (HDt1) 9.02 ± 2.50 (HDx1)	2.1 (DD) 4.0 (HDt1) 3.9 (HDx1)	3.0
Insertion #2	80 - 95	9.28 ± 0.92 (DD) 14.57 ± 2.22 (HDt1) 13.02 ± 2.11 (HDx1)	4.1 (DD) 6.4 (HDt1) 5.7 (HDx1)	6.0

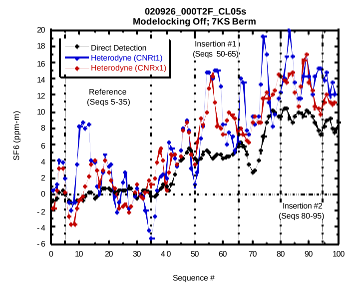

HD/DD DIAL Comparison Test
020926_000T2D (Modelocking On, 7KS Berm)

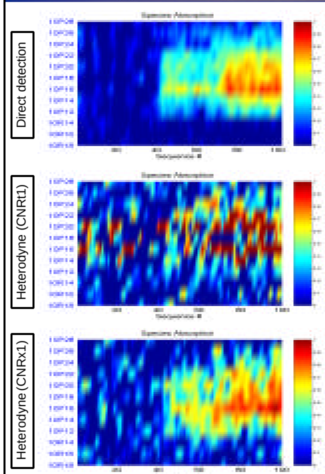

	Sequences	Measured CL (ppm-m)	Measured Dp (psi)	Expected Dp (psi)
Reference	5 - 35	0.02 ± 0.58 (DD) 3.48 ± 4.66 (HDt1) 0.30 ± 1.68 (HDx1)	--	--
Insertion #1	50 - 65	6.13 ± 0.60 (DD) 6.96 ± 2.89 (HDt1) 7.65 ± 0.97 (HDx1)	2.7 (DD) 3.0 (HDt1) 3.3 (HDx1)	3.0
Insertion #2	80 - 95	11.71 ± 0.72 (DD) 16.41 ± 3.80 (HDt1) 13.02 ± 1.71 (HDx1)	5.1 (DD) 7.2 (HDt1) 5.7 (HDx1)	6.0

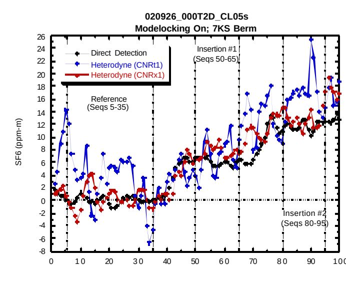

HD/DD DIAL Comparison Test
020926_000T1D (Modelocking On, 4KS BB)

Direct detection

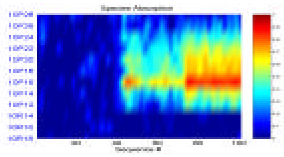

Heterodyne (CNRt1)

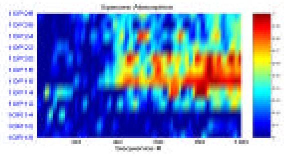

Heterodyne (CNRx1)

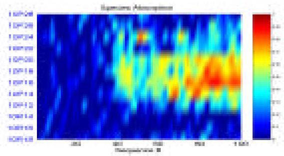

	Sequences	Measured CL (ppm-m)	Measured Δp (psi)	Expected Δp (psi)
Reference	5 - 35	-0.01 ± 0.51 (DD) 0.13 ± 1.19 (HDt1) -0.06 ± 0.80 (HDx1)	--	--
Insertion #1	50 - 65	6.35 ± 0.85 (DD) 8.99 ± 2.02 (HDt1) 5.82 ± 0.77 (HDx1)	2.8 (DD) 3.9 (HDt1) 2.5 (HDx1)	3.0
Insertion #2	80 - 95	12.28 ± 0.54 (DD) 17.18 ± 2.88 (HDt1) 11.73 ± 1.55 (HDx1)	5.4 (DD) 7.5 (HDt1) 5.1 (HDx1)	6.0

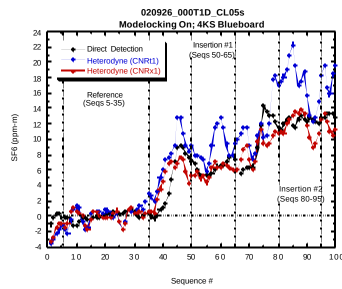

HD/DD DIAL Comparison Test
020926_000T1A (Modelocking Off, 4KS BB)

Direct detection

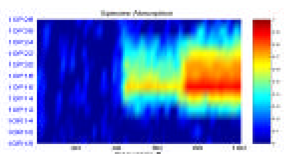

Heterodyne (CNRt1)

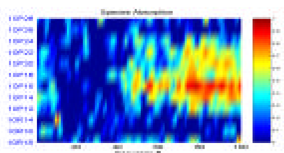

Heterodyne (CNRx1)

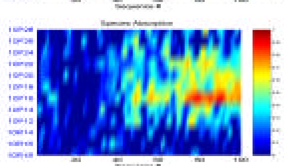

	Sequences	Measured CL (ppm-m)	Measured Δp (psi)	Expected Δp (psi)
Reference	5 - 35	0.04 ± 0.59 (DD) 0.02 ± 1.69 (HDt1) 0.01 ± 1.88 (HDx1)	--	--
Insertion #1	50 - 65	7.18 ± 0.38 (DD) 7.23 ± 1.92 (HDt1) 5.74 ± 1.60 (HDx1)	3.1 (DD) 3.2 (HDt1) 2.5 (HDx1)	3.0
Insertion #2	80 - 95	14.27 ± 0.26 (DD) 12.29 ± 0.77 (HDt1) 10.04 ± 1.00 (HDx1)	6.2 (DD) 5.4 (HDt1) 4.4 (HDx1)	6.0

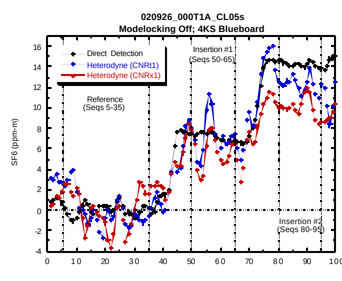

HD/DD DIAL Comparison Test
020916_000T2D (Modelocking On, 7KS Berm)

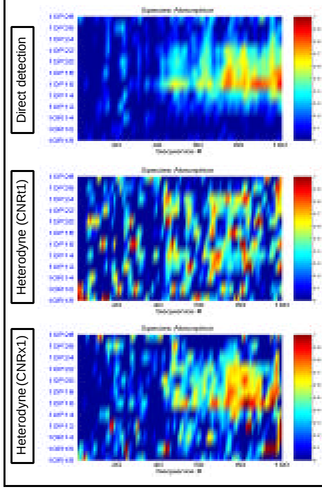

	Sequences	Measured CL (ppm-m)	Measured Dp (psi)	Expected Dp (psi)
Reference	5 - 35	0.00 ± 1.15 (DD) 1.17 ± 3.44 (HDt1) -0.09 ± 1.99 (HDx1)	--	--
Insertion #1	50 - 65	4.79 ± 1.32 (DD) 2.37 ± 2.53 (HDt1) 5.03 ± 1.22 (HDx1)	2.1 (DD) 1.0 (HDt1) 2.2 (HDx1)	3.0
Insertion #2	80 - 95	8.59 ± 0.91 (DD) 6.30 ± 4.90 (HDt1) 9.96 ± 4.13 (HDx1)	3.6 (DD) 2.8 (HDt1) 4.3 (HDx1)	6.0

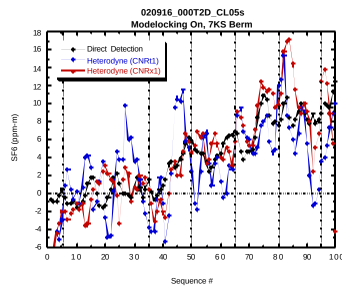

HD/DD DIAL Comparison Test
020916_000T2B (Modelocking Off, 7KS Berm)

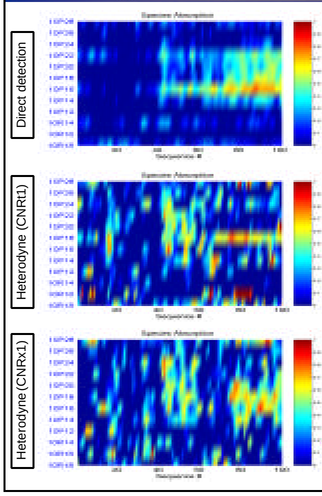

	Sequences	Measured CL (ppm-m)	Measured Dp (psi)	Expected Dp (psi)
Reference	5 - 35	-1.98 ± 0.62 (DD) 0.22 ± 2.79 (HDt1) 0.43 ± 2.20 (HDx1)	--	--
Insertion #1	50 - 65	2.73 ± 1.23 (DD) 3.84 ± 2.26 (HDt1) 3.11 ± 3.12 (HDx1)	1.2 (DD) 1.7 (HDt1) 1.4 (HDx1)	3.0
Insertion #2	80 - 95	7.28 ± 1.20 (DD) 1.65 ± 2.90 (HDt1) 5.72 ± 1.98 (HDx1)	3.2 (DD) 0.7 (HDt1) 2.5 (HDx1)	6.0

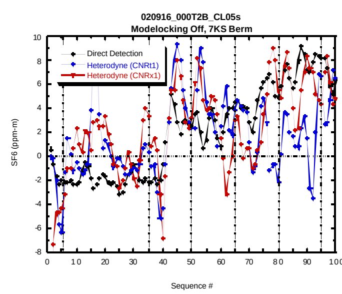

HD/DD DIAL Comparison Test
020916_000T1D (Modelocking On, 4KS BB)

Direct detection

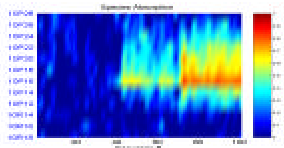

Heterodyne (CNRt1)

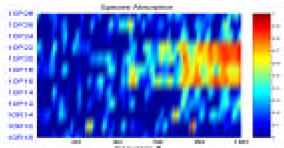

Heterodyne (CNRx1)

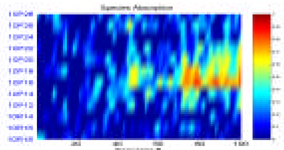

	Sequences	Measured CL (ppm-m)	Measured Δp (psi)	Expected Δp (psi)
Reference	5 - 35	-0.03 ± 0.94 (DD) 0.09 ± 1.35 (HDt1) 0.00 ± 1.43 (HDx1)	--	--
Insertion #1	50 - 65	5.16 ± 0.68 (DD) 2.94 ± 1.48 (HDt1) 2.72 ± 0.82 (HDx1)	2.3 (DD) 1.3 (HDt1) 1.2 (HDx1)	3.0
Insertion #2	80 - 95	10.10 ± 0.92 (DD) 10.40 ± 2.15 (HDt1) 7.47 ± 1.59 (HDx1)	4.4 (DD) 4.6 (HDt1) 3.3 (HDx1)	6.0

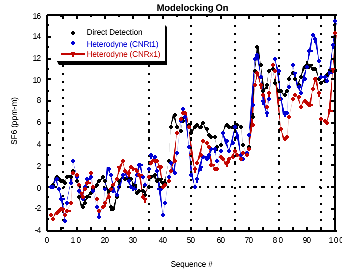

HD/DD DIAL Comparison Test
020916_000T1A (Modelocking Off, 4KS BB)

Direct detection

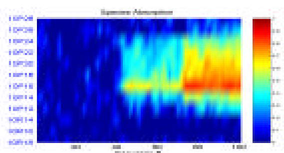

Heterodyne (CNRt1)

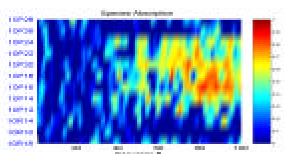

Heterodyne (CNRx1)

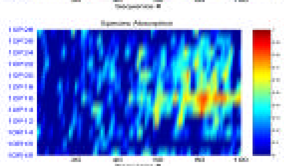

	Sequences	Measured CL (ppm-m)	Measured Δp (psi)	Expected Δp (psi)
Reference	5 - 35	0.00 ± 0.61 (DD) 0.24 ± 1.26 (HDt1) 0.08 ± 1.57 (HDx1)	--	--
Insertion #1	50 - 65	5.80 ± 0.50 (DD) 5.86 ± 2.15 (HDt1) 3.82 ± 1.48 (HDx1)	2.5 (DD) 2.6 (HDt1) 1.7 (HDx1)	3.0
Insertion #2	80 - 95	12.16 ± 0.36 (DD) 11.84 ± 1.48 (HDt1) 7.80 ± 1.72 (HDx1)	5.3 (DD) 5.2 (HDt1) 3.4 (HDx1)	6.0

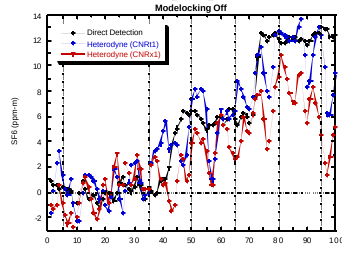

HD/DD DIAL Comparison Test
020806_000T1D (Non-Modelocked, 4KS BB)

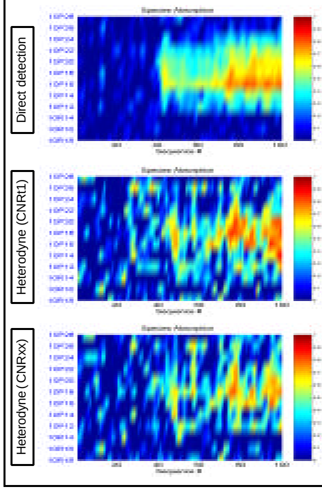

	Sequences	Measured CL (ppm-m)	Measured Δp (psi)	Expected Δp (psi)
Reference	5 - 35	0.03 ± 0.77 (DD) 0.33 ± 2.52 (HDt1) 0.22 ± 1.36 (HDxx)	--	--
Insertion #1	50 - 65	5.80 ± 0.39 (DD) 4.36 ± 1.86 (HDt1) 3.43 ± 1.97 (HDxx)	2.5 (DD) 1.9 (HDt1) 1.5 (HDxx)	3.0
Insertion #2	80 - 95	10.56 ± 0.89 (DD) 8.67 ± 2.54 (HDt1) 6.65 ± 2.36 (HDxx)	4.6 (DD) 3.8 (HDt1) 2.9 (HDxx)	6.0

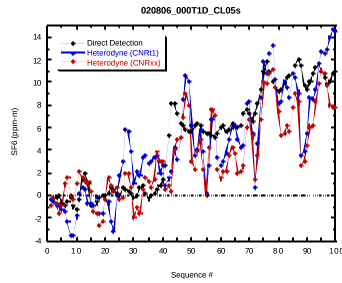

HD/DD DIAL Comparison Test
020806_000T1B (Modelocked, 4KS BB)

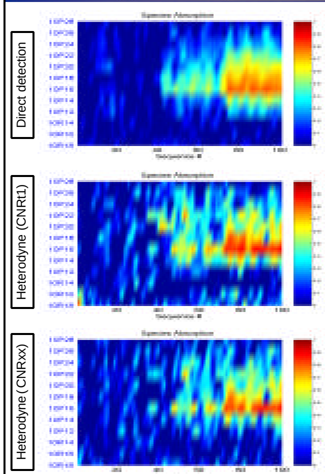

	Sequences	Measured CL (ppm-m)	Measured Δp (psi)	Expected Δp (psi)
Reference	5 - 35	-0.05 ± 0.85 (DD) -0.03 ± 1.92 (HDt1) -0.04 ± 1.62 (HDxx)	--	--
Insertion #1	50 - 65	4.73 ± 0.55 (DD) 6.21 ± 1.65 (HDt1) 5.00 ± 1.42 (HDxx)	2.1 (DD) 2.7 (HDt1) 2.2 (HDxx)	3.0
Insertion #2	80 - 95	10.85 ± 0.41 (DD) 10.81 ± 1.68 (HDt1) 9.15 ± 0.92 (HDxx)	4.7 (DD) 4.7 (HDt1) 4.0 (HDxx)	6.0

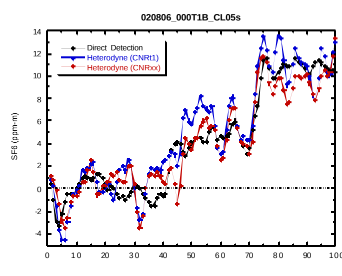

HD/DD DIAL Comparison Test
020717_000T2D (Modelocked, 4KS BB)

Direct detection

Heterodyne (CNRt1)

Heterodyne (CNRxx)

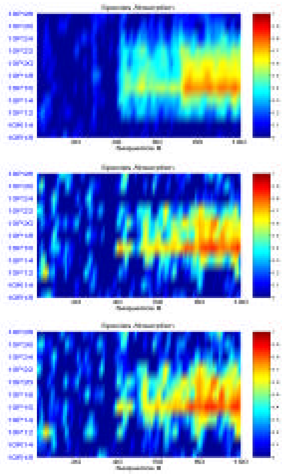

	Sequences	Measured CL (ppm-m)	Measured Δp (psi)	Expected Δp (psi)
Reference	5 - 35	0.08 ± 0.71 (DD) 0.11 ± 1.82 (HDt1) 0.04 ± 1.37 (HDxx)	--	--
Insertion #1	50 - 65	5.77 ± 0.55 (DD) 5.62 ± 1.67 (HDt1) 6.08 ± 1.71 (HDxx)	2.5 (DD) 2.5 (HDt1) 2.7 (HDxx)	3.0
Insertion #2	80 - 95	9.92 ± 0.59 (DD) 10.40 ± 1.10 (HDt1) 10.90 ± 1.32 (HDxx)	4.3 (DD) 4.6 (HDt1) 4.8 (HDxx)	6.0

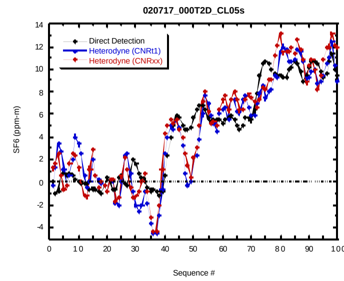

HD/DD DIAL Comparison Test
020717_000T2A (Non-Modelocked, 4KS BB)

Direct detection

Heterodyne (CNRt1)

Heterodyne (CNRxx)

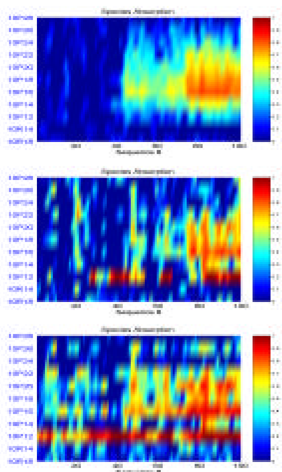

	Sequences	Measured CL (ppm-m)	Measured Δp (psi)	Expected Δp (psi)
Reference	5 - 35	0.00 ± 0.69 (DD) 0.11 ± 2.83 (HDt1) 3.76 ± 1.57 (HDxx)	0.0 0.0 1.6	--
Insertion #1	50 - 65	5.98 ± 0.64 (DD) 3.21 ± 2.77 (HDt1) 7.52 ± 2.66 (HDxx)	2.6 (DD) 1.4 (HDt1) 3.3 (HDxx)	3.0
Insertion #2	80 - 95	12.21 ± 0.77 (DD) 11.10 ± 2.13 (HDt1) 14.27 ± 2.70 (HDxx)	5.3 (DD) 4.8 (HDt1) 6.2 (HDxx)	6.0

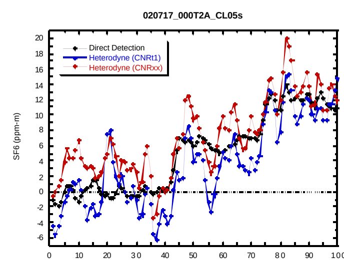

HD/DD DIAL Comparison Test 020529_000001 (HD Tx-Normalized, 4KS BB)

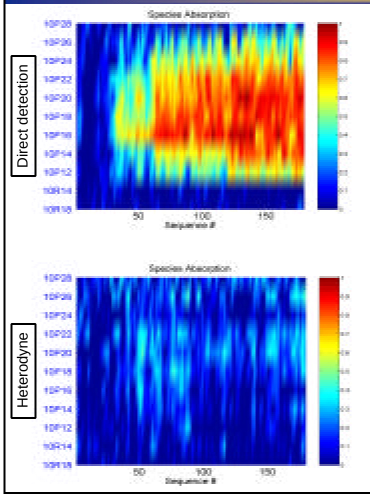

	Sequences [Time (hh:mm:ss)]	Measured CL (ppm-m)	Measured Dp (psi)	Expected Dp (psi)
Reference	10 – 25 [1:00:13 – 1:00:32]	0.26 ± 0.98 (DD) -0.34 ± 1.13 (HD)	–	–
Insertion #1	40 – 55 [1:00:52 – 1:01:11]	7.95 ± 1.24 (DD) 2.25 ± 1.42 (HD)	3.5 (DD) 1.0 (HD)	3.0
Insertion #2	70 – 85 [1:01:31 – 1:01:50]	15.46 ± 1.47 (DD) 2.54 ± 0.81 (HD)	6.8 (DD) 1.1 (HD)	6.0
Steady State	100 – 115 [1:07:10 – 1:08:29]	16.91 ± 1.41 (DD) 0.97 ± 0.89 (HD)	7.4 (DD) 0.4 (HD)	6.0
Insertion #3 (*sat)	130 – 145 [1:07:49 – 1:08:08]	20.14 ± 2.53 (DD) 0.53 ± 1.16 (HD)	8.8 (DD) 0.2 (HD)	9.0
Insertion #4 (*sat)	160 – 175 [1:08:28 – 1:08:47]	17.43 ± 2.74 (DD) 1.35 ± 0.99 (HD)	7.6 (DD) 0.6 (HD)	12.0

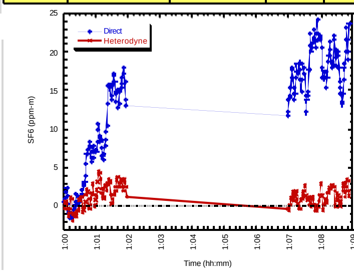

HD/DD DIAL Comparison Test 020529_000001 (HD Not Tx-Normalized, 4KS BB)

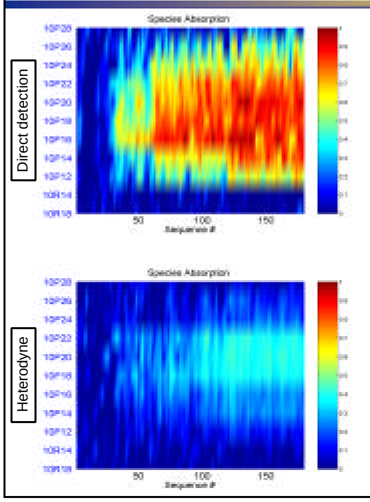

	Sequences [Time (hh:mm:ss)]	Measured CL (ppm-m)	Measured Dp (psi)	Expected Dp (psi)
Reference	10 – 25 [1:00:13 – 1:00:32]	0.26 ± 0.98 (DD) -0.01 ± 0.55 (HD)	–	–
Insertion #1	40 – 55 [1:00:52 – 1:01:11]	7.95 ± 1.24 (DD) 2.28 ± 0.70 (HD)	3.5 (DD) 1.0 (HD)	3.0
Insertion #2	70 – 85 [1:01:31 – 1:01:50]	15.46 ± 1.47 (DD) 2.98 ± 0.46 (HD)	6.8 (DD) 1.3 (HD)	6.0
Steady State	100 – 115 [1:07:10 – 1:08:29]	16.91 ± 1.41 (DD) 3.62 ± 0.48 (HD)	7.4 (DD) 1.6 (HD)	6.0
Insertion #3 (*sat)	130 – 145 [1:07:49 – 1:08:08]	20.14 ± 2.53 (DD) 3.98 ± 0.26 (HD)	8.8 (DD) 1.7 (HD)	9.0
Insertion #4 (*sat)	160 – 175 [1:08:28 – 1:08:47]	17.43 ± 2.74 (DD) 4.14 ± 0.28 (HD)	7.6 (DD) 1.8 (HD)	12.0

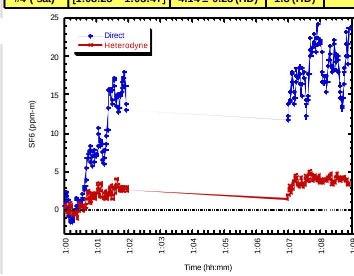

HD/DD DIAL Comparison Test 020513_000003 (4KS BB)

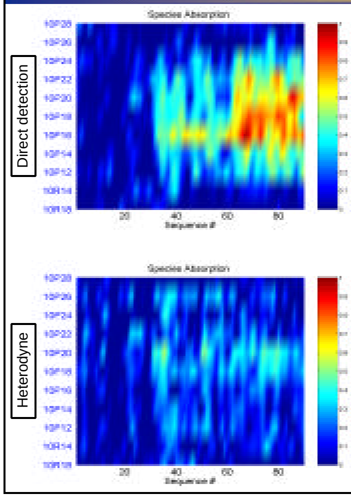

	Sequences [Time (hh:mm:ss)]	Measured CL (ppm-m)	Measured Dp (psi)	Expected Dp (psi)
Reference	10 – 25 [1:00:13 – 1:00:32]	0.17 ± 0.97 (DD) 0.11 ± 1.62 (HD)	–	–
Insertion #1	40 – 55 [1:00:52 – 1:01:11]	5.39 ± 0.80 (DD) 2.10 ± 1.01 (HD)	2.4 (DD) 0.9 (HD)	3.0
Insertion #2	70 – 85 [1:01:31 – 1:01:50]	11.04 ± 1.31 (DD) 2.37 ± 0.91 (HD)	4.8 (DD) 1.0 (HD)	6.0

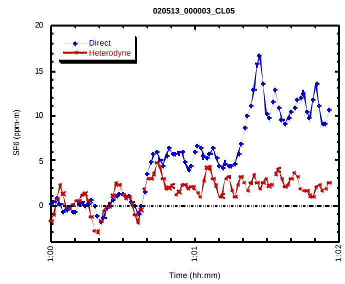

HD/DD DIAL Comparison Test 020513_000001 (4KS BB)

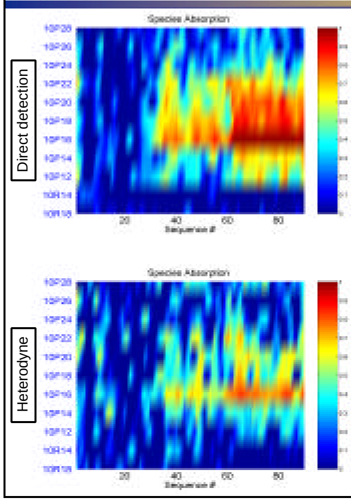

	Sequences [Time (hh:mm:ss)]	Measured CL (ppm-m)	Measured Dp (psi)	Expected Dp (psi)
Reference	10 – 25 [1:00:13 – 1:00:32]	0.29 ± 1.12 (DD) -0.02 ± 1.85 (HD)	–	–
Insertion #1	40 – 55 [1:00:52 – 1:01:11]	9.63 ± 1.72 (DD) 5.56 ± 1.92 (HD)	4.2 (DD) 2.4 (HD)	3.0
Insertion #2	70 – 85 [1:01:31 – 1:01:50]	18.38 ± 1.15 (DD) 8.07 ± 1.40 (HD)	8.0 (DD) 3.5 (HD)	6.0

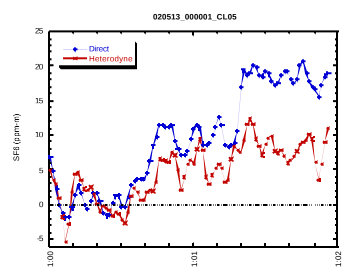

Appendix C. MATLAB Programs

Appendix C Contents

C1. DATREDUC.m - Direct Detection Data Reduction


```
%-------------------------------------------------------------------------------
%
%   Matlab program DATREDUC.M
%
%   Created from ENERGY.M 30 Sep 96 by D.C. Senft
%
%   Computes reduced data parameters from N-ABLE digitized waveform data
%     (U, Vpk, tpk, dteff, Vrms, Vref)
%
%   Modifications -
%   24 Oct 96 -  Transferred from Senft PMac to GLAPS
%   09 Jan 97 -  Plotted signal and reference windows on overlay plot, rather
%                than on average plot
%   07 May 97 -  Corrected Vpk calculation to be referenced from Vref baseline,
%                rather than 0 V
%   07 Jun 97 -  Corrected tpk calculation to be referenced from start of
%                data window, rather than start of signal window
%
%   Arrays work in Matlab-preferred column format, not row format
%     . n is pulse # (varies horizontally)
%     . i is sample # (varies vertically)
%     . data(i-row,n-column)
%
%   i   tau     intra-pulse (sampling) time
%       t       pulse time
%   l   lambda  wavelength, laser line
%   n   Npulse  pulse number
%   m   Nseq    sequence number
%-------------------------------------------------------------------------------
%
%   ---   Processing   ---
%

%fprintf('    \n')                                                     ;
%fprintf(' Nseq   = %d\n',Nseq)                                        ;
%fprintf(' Nlines  = %d\n',Nlines)                                     ;
%fprintf(' Npulses  = %d\n',Npulses)                                   ;
%fprintf(' Nsamples = %d\n',Nsamples)                                  ;

t = tsample                                                            ;
tmin = min(t)                                                          ;
tmax = max(t)                                                          ;

for n=1:Npulses                                                        ;
  Np(n)=n                                                              ;
end                                                                    ;

for m=1:Nseq                                                           ;
  Nm(m)=m                                                              ;
end                                                                    ;

%   <<<  Convert from digitizer units to voltage  >>>
```

```
fprintf          ('   \n')                                          ;
fprintf          ('Digitizer units to voltage conversion \n' )      ;
fprintf          ('  N-ABLE (*(1/4096)-0.100)  [N] \n' )            ;
fprintf          ('  LARS   (*(2/4096)-1.000)  [L] \n' )            ;
fprintf          ('  HP-DAS (+1)               [H] \n' )            ;
fprintf          ('  Kolmar (+1)               [K] \n' )            ;
data2volt = input('  Brimrose (-1)             [B]: ','s')          ;

if     ((data2volt=='N')|(data2volt=='n'))                          ;
  data=data.*(1/4096)-0.100                                         ;
elseif ((data2volt=='L')|(data2volt=='l'))                          ;
  data=data.*(2/4096)-1.000                                         ;
elseif ((data2volt=='H')|(data2volt=='h'))                          ;
  data=data                                                         ;
elseif ((data2volt=='K')|(data2volt=='k'))                          ;
  data=data                                                         ;
elseif ((data2volt=='B')|(data2volt=='b'))                          ;
  data=-data                                                        ;
end                                                                 ;

%----------------
%  -----<<<  Average pulses for each laser wavelength  >>>-----

avgdata = zeros(Nsamples,Nlines)                                ;
for l=1:Nlines                                                  ;
  for m=1:Nseq                                                  ;
    n=(m-1)*Nlines+l                                            ;
    avgdata(:,l)=avgdata(:,l)+data(:,n)                         ;
  end                                                           ;
  avgdata(:,l)=avgdata(:,l)/Nseq                                ;
end                                                             ;

%   -----<<<  Plot overlayed pulses  >>>-----

Nrows = 4                                                       ;
Nfrows= Nrows                                                   ;
Ncols = fix((Nlines-1)/Nrows)+1                                 ;
Nfcols = Ncols                                                  ;
if(Nlines==1)                                                   ;
  Nfrows=2                                                      ;
  Nfcols=2                                                      ;
end                                                             ;
if(Ncols<2)                                                     ;
  Nfcols=2                                                      ;
end                                                             ;
%%%figure('Position',[10,40,300*Nfcols,225*Nfrows])              ;

%----------------

NlinesCh = Nlines                                                       ;
for lch=1:NlinesCh                                                      ;
```

```
  ChLine(lch)=lch                                                  ;
end                                                                ;

if(Nlines>20)                                                      ;
  clear ChLine                                                     ;
  while(1)                                                         ;

    disp('   ')                                                    ;
    disp(' ***  Choose lines to be diplayed  ***' )                 ;
    disp(' ***        <ret> to continue      ***' )                 ;
%   disp('   ')                                                    ;

    LineUsage=zeros(1,99)                                          ;
    LineUsage=LineUsage-1                                          ;
    LineIndex0 = rem(LineIndex,100)                                ;

    for l=1:Nlines                                                 ;
      LineUsage(LineIndex0(1,l))=0                                 ;
    end                                                            ;

    LineChoice                                                     ;
    pause                                                          ;

    NlinesCh = 0                                                   ;
    for l=1:Nlines                                                 ;
      if(LineUsage(LineIndex0(1,l))==1)                            ;
        NlinesCh = NlinesCh + 1                                    ;
        ChLine(NlinesCh)=l                                         ;
      end                                                          ;
    end                                                            ;

    if(NlinesCh==0)                                                ;
      disp('   ')                                                  ;
      disp(' ***  No lines chosen for display  ***' )               ;
      disp(' ***        <ret> to continue      ***' )               ;
      disp('   ')                                                  ;
      pause                                                        ;
    elseif(NlinesCh>20)                                            ;
      disp('   ')                                                  ;
      disp(' ***  Maximum of 20 lines may be chosen  ***' )         ;
      disp(' ***           <ret> to continue         ***' )         ;
      disp('   ')                                                  ;
      pause                                                        ;
    else                                                           ;
      break                                                        ;
    end                                                            ;

  end                                                              ;
end                                                                ;

%---------------
```

```
if(batchflg==0)                                                  ;
  for lch=1:NlinesCh                                             ;
    figure('Position',[30+40*(lch-1),500-40*(lch-1),500,400])    ;
  end                                                            ;
end                                                              ;

sigref='N'                                                       ;
if(batchflg==0)                                                  ;
  TilePlot                                                       ;
end                                                              ;

surfdispflg = 'N'                                                ; % Surface plot?
disp(' ')                                                        ;
surfquery=input('Surface plot (Y/[N]): ','s')                    ;
if ((surfquery=='Y')|(surfquery=='y'))                           ;
  SURFDISP_B                                                     ;
  while(1)                                                       ;
    fprintf('   \n')                                             ;
    fprintf(    'New surface plot       [S] \n' )                ;
    fprintf(    'Print (B&W)            [P/BW] \n' )             ;
    fprintf(    'Print (color)          [C]' )                   ;
    query=input('Continue               [ ]): ','s')             ;

    if((query=='S')|(query=='s'))                                ;
      SURFDISP_B                                                 ;
    elseif((query=='P')|(query=='p'))                            ;
      print                                                      ;
    elseif((query=='BW')|(query=='bw'))                          ;
      print                                                      ;
    elseif((query=='C')|(query=='c'))                            ;
      print -dpsc -Pcolor                                        ;
    else                                                         ;
      break                                                      ;
    end                                                          ;
  end                                                            ;
end                                                              ;

if(batchflg==0)                                                  ;
  if(surfdispflg=='Y')                                           ;
    delete(Nlines+1)                                             ;
  end                                                            ;
end                                                              ;

%%%OverlayPlot                                                    ;
SigRefQuery                                                      ;
for lch=1:NlinesCh                                               ;
  figure(lch)                                                    ;
  PlotSigRef                                                     ;
end                                                              ;
Query                                                            ;

while(sigref=='Y')                                               ; % Plot loop
```

```
  if(batchflg==0)                                           ;
    TilePlot                                                ;
%   PlotSigRef                                              ;
  end                                                       ;
  Query                                                     ;
end                                                         ;

if(batchflg==0)                                             ;
  for lch=1:NlinesCh                                        ;
    delete(lch)                                             ;
  end                                                       ;
end                                                         ;

clear NlinesCh ChLine                                       ;

if(batchflg==0)                                             ;
  figure('Position',[10,40,567,405])                        ;
end                                                         ;

%   -----<<<  Begin integrated signal calculations  >>>-----

Nt_s1 = t_s1/delt                                           ;
Nt_s2 = t_s2/delt                                           ;

Nt_r1 = t_r1/delt                                           ;
Nt_r2 = t_r2/delt                                           ;

if Nt_s1 <= 0                                               ;
  Nt_s1=1                                                   ;
end                                                         ;

if Nt_s2 > Nsamples                                         ;
  Nt_s2 = Nsamples                                          ;
end                                                         ;

if Nt_r1 <= 0                                               ;
  Nt_r1=1                                                   ;
end                                                         ;

if Nt_r2 > Nsamples                                         ;
  Nt_r2 = Nsamples                                          ;
end                                                         ;

Nt_s  = Nt_s2-Nt_s1+1                                       ;
Nt_r  = Nt_r2-Nt_r1+1                                       ;

%---------------

Usig = zeros(Nseq,Nlines)                                   ;
Uref = zeros(Nseq,Nlines)                                   ;
Vref = zeros(Nseq,Nlines)                                   ;
U    = zeros(Nseq,Nlines)                                   ;
```

```
fprintf('\n')                                                   ;
for l=1:Nlines                                                  ;
  fprintf('  Reducing laser line %d of %d (Step 1/3) \r' ,l,Nlines)   ;
  for m=1:Nseq                                                  ;
    n=(m-1)*Nlines+l                                            ;
    meandat=sum(data(Nt_r1:Nt_r2,n))/Nt_r                       ;
    Uvar=0.0                                                    ;
    for i=Nt_r1:Nt_r2                                           ;
      Uref(m,l)=Uref(m,l)+data(i,n)*delt                        ;
      Uvar=Uvar+(data(i,n)-meandat)*(data(i,n)-meandat)*delt    ;
    end                                                         ;
    Vref(m,l)=Uref(m,l)/(Nt_r*delt)                             ;
    Vrms(m,l)=sqrt(Uvar/(Nt_r*delt))                            ;
  end                                                           ;
end                                                             ;

% fprintf('\n')                                                 ;
for l=1:Nlines                                                  ;
  fprintf('  Reducing laser line %d of %d (Step 2/3) \r' ,l,Nlines)   ;
  for m=1:Nseq                                                  ;
    n=(m-1)*Nlines+l                                            ;
    [Vpk(m,l),pkindex]=max(data(Nt_s1:Nt_s2,n))                 ;
    Vpk(m,l)=Vpk(m,l)-Vref(m,l)                                 ;
%   tpk(m,l)=tsample(pkindex)                                   ;
    tpk(m,l)=tsample(pkindex+Nt_s1-1)                           ;
    for i=Nt_s1:Nt_s2                                           ;
      Usig(m,l)=Usig(m,l)+data(i,n)*delt                        ;
    end                                                         ;
  end                                                           ;
end                                                             ;

% fprintf('\n')                                                 ;
for l=1:Nlines                                                  ;
  fprintf('  Reducing laser line %d of %d (Step 3/3) \r' ,l,Nlines)   ;
  for m=1:Nseq                                                  ;
    n=(m-1)*Nlines+l                                            ;
    U(m,l)=Usig(m,l)-(Nt_s*delt)*Vref(m,l)                      ;
    effwid(m,l)=U(m,l)/Vpk(m,l)                                 ;
  end                                                           ;
end                                                             ;
fprintf('\n')                                                   ;

Uavg=sum(U)/Nseq                                                ;
Usdev=std(U)                                                    ;

if(batchflg==0)                                                 ;
  first = 1                                                     ;
  while(1)                                                      ;
    if (first==1)                                               ;
      plot(Nm,U*10^9)                                           ;
      if(Nlines==1)                                             ;
```

```
        title([TRtype,' File = ',file,'   Average = ',num2str(Uavg*10^9), ...
        '  (nV.s)      ','SDev = ',num2str(100*Usdev/Uavg),' (%)']) ;
      else                                                             ;
        title([TRtype,' File = ',file])                                ;
      end                                                              ;
      xlabel('Pulse Number')                                           ;
      ylabel('U  (nV.s)')                                              ;
      av=axis ; xmn=av(1) ; xmx=av(2) ; ymn=av(3) ; ymx=av(4)          ;
      if(TRtype=='Tx')                                                 ;
        axis([xmn xmx min(0,ymn) ymx])                                 ;
      end                                                              ;
      first = 0                                                        ;
    end                                                                ;
    replot=input('Rescale plot (Y/P/[N]): ','s')                       ;
    if((replot=='P')|(replot=='p'))                                    ;
      print                                                            ;
    elseif((replot=='BW')|(replot=='bw'))                              ;
      print                                                            ;
    elseif((replot=='C')|(replot=='c'))                                ;
      print -dpsc -Pcolor                                              ;
    elseif((replot~='Y')&(replot~='y'))                                ;
      break                                                            ;
    else                                                               ;
      xmin=input('Enter new X min: ')                                  ;
      xmax=input('Enter new X max: ')                                  ;
      ymin=input('Enter new Y min: ')                                  ;
      ymax=input('Enter new Y max: ')                                  ;
      axis([xmin xmax ymin ymax])                                      ;
    end                                                                ;
  end                                                                  ;
end                                                                    ;

%Eplot = input('Convert to energy (Y/[N]): ','s')                     ;
%if((Eplot=='Y')|(Eplot=='y'))                                        ;
%  Rv=input('Enter conversion factor (V/W or V.s/J): ')                ;
%  first = 1                                                          ;
%  while (1)                                                          ;
%    if (first)                                                       ;
%      plot(Nm,U/Rv)                                                  ;
%      title([TRtype,' File = ',file,'   Average = ',num2str(Uavg/Rv), ...
%        '  (J)      ','SDev = ',num2str(100*Usdev/Uavg),' (%)'])    ;
%      xlabel('Pulse Number')                                         ;
%      ylabel('Energy  (J)')                                          ;
%      first = 0                                                      ;
%    end                                                              ;
%    replot=input('Rescale plot (Y/[N]): ','s')                       ;
%    if((replot~='Y')&(replot~='y')) break; end                       ;
%    xmin=input('Enter new X min: ')                                  ;
%    xmax=input('Enter new X max: ')                                  ;
%    ymin=input('Enter new Y min: ')                                  ;
%    ymax=input('Enter new Y max: ')                                  ;
%    axis([xmin xmax ymin ymax])                                      ;
```

```
%  end                                                            ;
%end                                                              ;

%-------------------------------------------------------------------------------

%rect = [500,40,567,405]                                          ;
%LARSHist=figure('Position',rect)                                 ;

%hist(U/Uavg,100)                                                 ;
%title([TRtype,' File = ',file,'   U Histogram (',num2str(Npulses), ...
%  ' pulses total) '])                                            ;
%xlabel('Normalized Signal')                                      ;
%ylabel('Number of Occurrences')                                  ;

%while(1)                                                         ;
%  ascout=input('Write ASCII file for histogram (Y/[N]):','s')    ;
%  if((ascout~='Y')&(ascout~='y')) break; end                     ;
%  [frequ uuu]=hist(U/Uavg,100)                                   ;
%  frequ=frequ/Npulses                                            ;
%  save uuu.asc uuu -ascii -double                                ;
%  fprintf('    \n')                                              ;
%  fprintf('    Files frequ.asc and uuu.asc written ')            ;
%  break; end                                                     ;
%end                                                              ;

%-------------------------------------------------------------------------------

if(batchflg==0)                                                   ;
  delete(1)                                                       ;
% delete(2)                                                       ;
end                                                               ;

%-------------------------------------------------------------------------------
```

C2. DATREDUC_HD_X3..m - Heterodyne Detection Data Reduction


```
%-------------------------------------------------------------------------------------------
%
%  DATREDUC_HD_X3
%
%  Created by DCS from DiegoProcessing_DCS, originally written by
%  Diego Pierrottet, Dan Eckelkamp-Baker, and Dan Senft
%
%  14 Nov 02 - Changed computation of CNRx1 to use Welch periodograms with equal signal
%              and noise windows in order to match resolutions for normalization
%              (division).  Renamed CNRx3.
%
%-------------------------------------------------------------------------------------------

% Demultiplexing the raw data into its respective wavelength.
% No header file is used for this version.
% Wavelength sequence assumed to be standard 13 wavelengths,
% starting with 10R18,10P10,10P12,...,10P30

%DS close all
%DS clear all
%DS pack

Tstart = cputime                                                  ;

disp('   ')                                                       ;
sa     = input('   Enter sampling frequency (Hz) [1e9] : ' ) ;
delt   = 1/sa                                                     ;
PRF    = input('   Enter PRF (Hz) [10]                 : ' ) ;
Nseq   = input('   Enter Nseq [101]                    : ' ) ;
Nlines = input('   Enter Nlines [13]                   : ' ) ;
disp('   ')                                                       ;
SigRefQuery1                                                      ; % t_s1,t_s2,t_r1,t_r2 (sec)
Nt_s1 = round(t_s1/delt)+1                                        ;
Nt_s2 = round(t_s2/delt)                                          ;
Nt_r1 = round(t_r1/delt)+1                                        ;
Nt_r2 = round(t_r2/delt)                                          ;

%-------------------------------------------------------------------------------------------

TestFlg = 0                                               ; % Normal (0) or test (1) read-in

if(TestFlg==0)                                            ; % Normal read-in

  disp('   ')                                             ;
  disp('  Reading in TestHDDD.txt ')                        ;
  disp('   ')                                             ;

  load TestHDDD.txt                                       ;
  %DS pickfile                                            ;
  %DS load (together)                                     ;

  TotalPoints=length(TestHDDD)                            ;
```

```
  PointsPerShot=TotalPoints/Nseq/Nlines                ;
  %PointsPerShot=20004                                 ;

% keyboard                                             ;

  %Form data array: data(point,shot,line)
  data=zeros(PointsPerShot,Nseq,Nlines)                ;
  for mm = 1:Nseq                                      ;
    for ll = 1:Nlines                                  ;
      Npt1=round(((mm-1)*Nlines+ll-1)*PointsPerShot+1)       ;
      Npt2=round(((mm-1)*Nlines+ll)*PointsPerShot)           ;
      data(:,mm,ll)=TestHDDD(Npt1:Npt2,1)              ;
%     if(Npt1~=round(Npt1));BBflg=1;keyboard;end       ;
%     if(Npt2~=round(Npt2));BBflg=2;keyboard;end       ;
    end                                                ;
  end                                                  ;

%------------------------------------------------------------------------------------------

  while(0)   ;%^^^^^^^^^^^^^^^^^^^^^^^^^^^^^^^^^^^^^^^^^^^
  Nseq=Nseq-1                                          ;
  data=zeros(PointsPerShot,Nseq,Nlines)                ; % 030828_T2A manual correction
  for mm = 1:Nseq                                      ;
    for ll = 1:Nlines                                  ;
      nn=(mm-1)*Nlines+ll                              ;
      if(nn>= 1056); nn=nn+1; end                      ;% skip bad pulse (#1056)
      Npt1=round((nn-1)*PointsPerShot+1)               ;
      Npt2=round(nn*PointsPerShot)                     ;
      data(:,mm,ll)=TestHDDD(Npt1:Npt2,1)              ;
    end                                                ;
  end                                                  ;
  end        ;%^^^^^^^^^^^^^^^^^^^^^^^^^^^^^^^^^^^^^^^^^^^

%------------------------------------------------------------------------------------------

  clear TestHDDD                                       ;
  pack                                                 ;

else                                                   ; % Test read-in

  load TestMHDDD                                       ;
  data = xdata                                         ;
  clear xdata                                          ;
  Nseq = 10                                            ;

end                                                    ;

time=1/sa:1/sa:PointsPerShot/sa                        ;

%------------------------------------------------------------------------------------------

disp('   ')                                            ;
```

```
disp('  Starting Noise PSD calculation loop' )           ;
disp('    ')                                             ;

Npts = max(Nt_s2-Nt_s1+1,Nt_r2-Nt_r1+1)                 ;
NFFTbase = ceil(log2(Npts))                              ;
NFFT = 2^NFFTbase                                        ;

for mm = 1:1:Nseq                                        ;
  for ll = 1:1:Nlines                                    ;
    noise=data(Nt_r1:Nt_r2,mm,ll)                        ;
%    [Pnn,fn]=pwelch(noise,[],[],NFFT,sa)                ;
    [Pnn,fn]=periodogram(noise,[],NFFT,sa)               ; % use pdgrm for more accur spur calc
    NoisePSD(:,mm,ll)=Pnn                                ;
  end                                                    ;
end                                                      ;

disp('  Done Noise PSD calculation loop' )               ;
disp('    ')                                             ;

%------------------------------------------------------------------------------------------
%  Rearrange data into correct wavelength sequence order

disp('  Starting spur frequency loop' )                          ;
disp('    ')                                                     ;

del_fn = fn(2)                                                   ; % find spur frequencies
N_fn1 = round((75.0e6-fn(1))/del_fn)                             ;
N_fn2 = round((81.0e6-fn(1))/del_fn)                             ;

for mm = 1:Nseq                                                  ;
  for ll = 1:Nlines                                              ;
    [YY,Nindex(mm,ll)] = max(NoisePSD(N_fn1:N_fn2,mm,ll))        ;
    SpurFreq(mm,ll) = fn(Nindex(mm,ll)+N_fn1+1)                  ;
    SF_Index(mm,ll) = mm + (ll-1)/Nlines                         ;
  end                                                            ;
end                                                              ;

qqspur = median(SpurFreq)                                        ;

figure('Position',[ 50 400 400 300])                             ;
plot(SF_Index,SpurFreq/1e6, '.-')                                ;
title('Spur Frequencies (MHz)' )                                 ;
av=axis ; xmn=av(1) ; xmx=av(2) ; ymn=av(3) ; ymx=av(4)          ;
axis([0 Nseq+1 ymn ymx])                                         ;

figure('Position',[500 400 400 300])                             ;
plot(qqspur/1e6)                                                 ;
hold on                                                          ;
plot(qqspur/1e6, 'bx')                                           ;
title('Median Spur Frequency (MHz)' )                            ;

disp('  Arranging data into correct wavelength order' )          ;
```

```
disp('   ')                                                    ;

%  Rearrangement assumes first wavelength in sequence is always lowest wavelength, and
%  therefore highest spur frequency
%  Throw out pulses prior to first occurrence of maximum spur frequency, will cause loss
%  of one sequence

[YY,maxIndex] = max(qqspur)                            ;

for mm1=1:Nseq-1                                       ;
  for ww1=1:Nlines                                     ;
    nn0=(mm1-1)*Nlines+ww1+maxIndex-1                  ;
    mm0=floor((nn0-0.5)/Nlines)+1                      ;
    ww0=nn0-(mm0-1)*Nlines                             ;
    data(:,mm1,ww1)=data(:,mm0,ww0)                    ;
  end                                                  ;
end                                                    ;

data(:,Nseq,:) = 0                                     ; % Clear remainder of orig last seq

Nseq = Nseq-1                                          ;

query=input('  Enter <ret> to continue       : ','s');
delete(1:2)                                            ;

clear NoisePSD                                         ;
pack

%-----------------------------------------------------------------------------------------
%  Calculate PSDs

disp('   ')                                                    ;
disp('  Starting PSD calculation loops' )                      ;
disp('   ')                                                    ;

Nt_s = Nt_s2-Nt_s1+1                                           ;
Nt_r = Nt_r2-Nt_r1+1                                           ;

if(Nt_s<Nt_r)                                                  ;
  disp('  **  Nt_s < Nt_r  **  ')                              ;
  keyboard                                                     ;
end                                                            ;

Npts = Nt_r                                                    ;
NFFTbase = ceil(log2(Npts)+1)                                  ;
NFFT = 2^NFFTbase                                              ;

% NLen = NFFT                                                  ;% for periodograms
NLen = NFFT/4                                                  ; % for Welch periodograms

NoisePSD  = zeros(NLen/2+1,Nseq,Nlines)                        ;
SignalPSD = zeros(NLen/2+1,Nseq,Nlines)                        ;
```

```
NormPSD   = zeros(NLen/2+1,Nseq,Nlines)                    ;

for mm = 1:Nseq                                            ;
  fprintf('  Sequence #:  %d \n',mm)                       ;
  for ll = 1:Nlines                                        ;
    noise=data(Nt_r1:Nt_r2,mm,ll)                          ;
    [Pnn,fn]=pwelch(noise,[],[],NLen,sa)                   ; % X3
%   [Pnn,fn]=periodogram(noise,[],NLen,sa)                 ;% X2
    NoisePSD(:,mm,ll)=Pnn                                  ;
    if(NoisePSD(1,mm,ll)==0)                               ; % eliminate divide by zeros
      NoisePSD(1,mm,ll)=NoisePSD(2,mm,ll)                  ;
    end                                                    ;
    if(NoisePSD(NLen/2+1,mm,ll)==0)                        ; % eliminate divide by zeros
      NoisePSD(NLen/2+1,mm,ll)=NoisePSD(NLen/2,mm,ll)      ;
    end                                                    ;

    Npdgms=ceil(Nt_s/Nt_r)                                 ;
    SigPSD=zeros(NLen/2+1,Npdgms)                          ;
    for Npd = 1:Npdgms                                     ;
      extra=round((Npdgms*Npts-Nt_s)/(Npdgms-1))           ;
      N1=Nt_s1+(Npd-1)*(Npts-extra)                        ;
      N2=N1+Npts-1                                         ;
      signal=data(N1:N2,mm,ll)                             ;
      [Pnn,fn]=pwelch(signal,[],[],NLen,sa)                ; % X3
%     [Pnn,fn]=periodogram(signal,[],NLen,sa)              ;% X2
      SigPSD(:,Npd)=Pnn                                    ;
    end                                                    ;
    SignalPSD(:,mm,ll)=mean(SigPSD')                       ;

    NormPSD(:,mm,ll)=SignalPSD(:,mm,ll)./NoisePSD(:,mm,ll)  ;

%   for qq=2:NFFT/2                                        ;% X2 3-pt smoothing for norm
%     nz3=(NoisePSD(qq-1,mm,ll)+NoisePSD(qq,mm,ll)+NoisePSD(qq+1,mm,ll))/3          ;
%     NormPSD(qq,mm,ll)=SignalPSD(qq,mm,ll)/nz3                                      ;
%   end                                                                              ;
%   nz3=(NoisePSD(1,mm,ll)+NoisePSD(2,mm,ll)+NoisePSD(3,mm,ll))/3                    ;
%   NormPSD(1,mm,ll)=SignalPSD(1,mm,ll)/nz3                                          ;
%   nz3=(NoisePSD(NFFT/2-1,mm,ll)+NoisePSD(NFFT/2,mm,ll)+NoisePSD(NFFT/2+1,mm,ll))/3 ;
%   NormPSD(NFFT/2+1,mm,ll)=SignalPSD(NFFT/2+1,mm,ll)/nz3                            ;

  end                                                      ;
end                                                        ;

disp('   ')                                                ;
disp('  Done PSD calculation loops')                       ;
disp('   ')                                                ;

%-----------------------------------------------------------------------------------------
%  Plot time series, signal and noise spectra, and normalized signal spectrum

Y0 = 400                                                   ;
scl = 1                                                    ;
```

```
sc2 = 1                                                   ;
if(Nlines>=30)                                            ;
  Y0 = 700                                                ;
  sc1=1/2                                                 ;
  sc2=2/3                                                 ;
end                                                       ;

tmn = time(1)                                             ;
tmx = ceil(time)                                          ;

for mm=1:Nseq                                             ;
  fprintf('  Sequence #:  %d \n',mm)                      ;
  for ll=1:Nlines                                         ;

  figure('Position',[25+25*(ll-1)*sc1,Y0-20*(ll-1)*sc1,800*sc2,700*sc2])          ;
% figure('Position',[25+25*(ll-1)*sc1,Y0-25*(ll-1)*sc1,800*sc2,300*sc2], ...
%        'Name',LineName(LineIndex(1,ll),:))              ;
% text(xmx-0.15*(xmx-xmn),ymx-0.05*(ymx-ymn), ...
%   LineName(LineIndex(1,ll),:),'Color',[0 1 1])          ;

  subplot(4,1,1)                                      ; % Time series
  plot(time*1e6,data(:,mm,ll))                        ;
  set(gca,'FontSize',[9])                             ;
% set(gca,'YTickLabel',[])                            ;
  title('Time Series')                                ;
  av=axis ; xmn=av(1) ; xmx=av(2) ; ymn=av(3) ; ymx=av(4)   ;
  axis([0 20 -1.0 1.0])                               ;
  hold on                                             ;
  PlotSigRef1                                         ; % display sig and ref windows

  subplot(4,1,2)                                          ; % Signal (Rx) and noise PSDs
  plot(fn/1e6,NoisePSD(:,mm,ll), 'r-')                    ;
  hold on                                                 ;
  plot(fn/1e6,SignalPSD(:,mm,ll), 'g-')                   ;
% plot(fn,NormPSD(:,mm,ll),'b-')                          ;
  set(gca,'FontSize',[9])                                 ;
% set(gca,'YTickLabel',[])                                ;
  title('Rx and Nz PSDs')                                 ;
  av=axis ; xmn=av(1) ; xmx=av(2) ; ymn=av(3) ; ymx=av(4)   ;
  axis([0 200 min(0,ymn) ymx])                            ;
  hold on                                                 ;

  subplot(4,1,3)                                          ; % Signal PSD
  plot(fn/1e6,SignalPSD(:,mm,ll)-NoisePSD(:,mm,ll))       ;
% plot(fn,NormPSD(:,mm,ll),'b-')                          ;
  set(gca,'FontSize',[9])                                 ;
% set(gca,'YTickLabel',[])                                ;
  title('Signal PSD')                                     ;
  av=axis ; xmn=av(1) ; xmx=av(2) ; ymn=av(3) ; ymx=av(4)   ;
  axis([0 200 min(0,ymn) ymx])                            ;
  hold on                                                 ;
```

```
  subplot(4,1,4)                                          ; % Normalized PSD
  plot(fn/1e6,NormPSD(:,mm,ll))                           ;
  set(gca,'FontSize',[9])                                 ;
% set(gca,'YTickLabel',[])                                ;
  title('Normalized PSD')                                 ;
  av=axis ; xmn=av(1) ; xmx=av(2) ; ymn=av(3) ; ymx=av(4) ;
  axis([0 200 min(0,ymn) ymx])                            ;
  hold on                                                 ;

  end                                                     ;

  fprintf    ('   Enter <ret> to continue \n' )           ;
  query=input('   Enter <s> to stop displays      : ','s') ;
  delete(1:Nlines)                                        ;
  if((query=='S')|(query=='s')); break; end               ;

end                                                       ;

%-------------------------------------------------------------------------------------------

disp('   ')                                               ;
disp('  Starting CNR calculation loops' )                 ;
disp('   ')                                               ;

%-------------------------------------------------------------------------------------------
%  *** CNRt1 ***

RR    = zeros(Nseq,Nlines)                                ;
NN    = zeros(Nseq,Nlines)                                ;
CNRt1 = zeros(Nseq,Nlines)                                ;

%  Compute DC for p(t) in signal and noise windows

for mm=1:Nseq                                             ;
  for ll=1:Nlines                                         ;
    DCsig(mm,ll) = mean(data(Nt_s1:Nt_s2,mm,ll))          ;
    DCnz(mm,ll)  = mean(data(Nt_r1:Nt_r2,mm,ll))          ;
  end                                                     ;
end                                                       ;

%  Compute return power, noise power, (signal power), and CNRt1

for mm=1:Nseq                                             ;
  for ll=1:Nlines                                         ;
    RRt1(mm,ll)=   ...
     sum((data(Nt_s1:Nt_s2,mm,ll)-DCsig(mm,ll)).*(data(Nt_s1:Nt_s2,mm,ll)-DCsig(mm,ll)));
    NNt1(mm,ll)=   ...
     sum((data(Nt_r1:Nt_r2,mm,ll)- DCnz(mm,ll)).*(data(Nt_r1:Nt_r2,mm,ll)- DCnz(mm,ll)));
    CNRt1(mm,ll) = (RRt1(mm,ll)/(((Nt_s2-Nt_s1+1)/(Nt_r2-Nt_r1+1))*NNt1(mm,ll)))-1      ;
  end                                                     ;
end                                                       ;
```

```
%-----------------------------------------------------------------------------------------
%  *** CNRf1 ***

for mm=1:Nseq                                                ;
  for ll=1:Nlines                                            ;
    RRf1(mm,ll)  = sum(SignalPSD(:,mm,ll))                   ;
    NNf1(mm,ll)  = sum( NoisePSD(:,mm,ll))                   ;
    CNRf1(mm,ll) = RRf1(mm,ll)/NNf1(mm,ll)-1                 ;
  end                                                        ;
end                                                          ;

%-----------------------------------------------------------------------------------------
%-----------------------------------------------------------------------------------------
%-----------------------------------------------------------------------------------------
%  *** CNRx3 - Point-by-point frequency normalization ***

% ExcessNzFactor = 0.1785                    ;% approx CNRx1 random noise div factor
% ExcessNzFactor = 0.750                     ;% approx CNRx2 random noise div factor
ExcessNzFactor = 0.150                       ; % approx CNRx3 random noise div factor
SNR = sum(NormPSD-1-ExcessNzFactor)          ;
for mm = 1:Nseq                              ;
  for ll = 1:Nlines                          ;
    CNRx3(mm,ll)=(1/(NFFT/2+1))*SNR(1,mm,ll) ; % scale factor is only approximate
  end                                        ;
end                                          ;

%-----------------------------------------------------------------------------------------
%  *** Display CNRs ***

%  Smooth CNRs to reduce effects of single point nonlinearities in scale factors

Tsmooth = 10                                 ; % set smoothing extent (sec)

for mm=1:Nseq                                ; % create pulse time for Hanning_TSmooth
  for ll=1:Nlines                            ;
    nn=(mm-1)*Nlines+ll                      ;
    tpulse(mm,ll)=(nn/PRF)/3600              ; % approximate pulse time (hh.ddd)
  end                                        ;
end                                          ;

Hdata = CNRt1                                ;
Hanning_TSmooth                              ;
qq_t1 = Hdata                                ;

Hdata = CNRf1                                ;
Hanning_TSmooth                              ;
qq_f1 = Hdata                                ;

Hdata = CNRx3                                ;
Hanning_TSmooth                              ;
qq_0 = Hdata                                 ;
```

```
Scl_f1t1 = mean(qq_f1./qq_t1)                    ;
Scl_0t1  = mean(qq_0./qq_t1)                     ;

%----------

for ll=1:Nlines                                             ;

  figure('Position',[25+25*(ll-1)*sc1,Y0-20*(ll-1)*sc1,600*sc2,700*sc2])        ;

  subplot(4,1,1)                                           ;  % Scaled CNRs overlay
  plot(CNRt1(:,ll),'k-')                                    ;
  hold on                                                  ;
  plot(CNRf1(:,ll)./Scl_f1t1(1,ll), 'g-')                   ;
  plot(CNRx3(:,ll)./Scl_0t1(1,ll), 'r-')                    ;
  set(gca,'FontSize',[9])                                  ;
% set(gca,'YTickLabel',[])                                 ;
  title('Overlayed Scaled CNRs')                            ;
  av=axis ; xmn=av(1) ; xmx=av(2) ; ymn=av(3) ; ymx=av(4)  ;
  axis([xmn xmx min(0,ymn) ymx])                           ;
% hold on                                                  ;

  subplot(4,1,2)                                           ;  % CNRt1
  plot(CNRt1(:,ll))                                        ;
  set(gca,'FontSize',[9])                                  ;
% set(gca,'YTickLabel',[])                                 ;
  title('CNRt1')                                           ;
  av=axis ; xmn=av(1) ; xmx=av(2) ; ymn=av(3) ; ymx=av(4)  ;
  axis([xmn xmx min(0,ymn) ymx])                           ;
% hold on                                                  ;

  subplot(4,1,3)                                           ;  % CNRf1
  plot(CNRf1(:,ll))                                        ;
  set(gca,'FontSize',[9])                                  ;
% set(gca,'YTickLabel',[])                                 ;
  title('CNRf1')                                           ;
  av=axis ; xmn=av(1) ; xmx=av(2) ; ymn=av(3) ; ymx=av(4)  ;
  axis([xmn xmx min(0,ymn) ymx])                           ;
% hold on                                                  ;

  subplot(4,1,4)                                           ;  % CNRx3
  plot(CNRx3(:,ll))                                        ;
  set(gca,'FontSize',[9])                                  ;
% set(gca,'YTickLabel',[])                                 ;
  title('CNRx3')                                           ;
  av=axis ; xmn=av(1) ; xmx=av(2) ; ymn=av(3) ; ymx=av(4)  ;
  axis([xmn xmx min(0,ymn) ymx])                           ;
% hold on                                                  ;

end                                                        ;

%-----------------------------------------------------------------------------------------
```

```
disp('  Done CNR calculation loop');
disp('   ');

%-----------------------------------------------------------------------------------------
%  *** Save CNRs ***

save HDDD CNRt1 CNRf1 CNRx3

disp('  HDDD.mat saved');
disp('   ');

Tend = cputime-Tstart                                       ;
% Tend

fprintf    ('   Enter seq # to display \n')                  ;
query=input('   Enter <0> to stop       : ')                ;
delete(1:Nlines)                                            ;
% delete(1)                                                 ;

%-----------------------------------------------------------------------------------------
%  Plots for selected sequences

while(query~=0)                                             ;

  mm = query                                                ;

  Y0 = 400                                                  ;
  sc1 = 1                                                   ;
  sc2 = 1                                                   ;
  if(Nlines>=30)                                            ;
    Y0 = 700                                                ;
    sc1=1/2                                                 ;
    sc2=2/3                                                 ;
  end                                                       ;

  tmn = time(1)                                             ;
  tmx = ceil(time)                                          ;

%---------------

% fprintf('  Sequence #:  %d \n',mm)                        ;
  for ll=1:Nlines                                           ;

  figure('Position',[25+25*(ll-1)*sc1,Y0-20*(ll-1)*sc1,800*sc2,700*sc2])        ;
% figure('Position',[25+25*(ll-1)*sc1,Y0-25*(ll-1)*sc1,800*sc2,300*sc2], ...
%        'Name',LineName(LineIndex(1,ll),:))                ;
% text(xmx-0.15*(xmx-xmn),ymx-0.05*(ymx-ymn), ...
%   LineName(LineIndex(1,ll),:),'Color',[0 1 1])            ;

  subplot(4,1,1)                                        ;  % Time series
  plot(time*1e6,data(:,mm,ll))                          ;
  set(gca,'FontSize',[9])                               ;
```

```
% set(gca,'YTickLabel',[])                          ;
  title('Time Series')                              ;
  av=axis ; xmn=av(1) ; xmx=av(2) ; ymn=av(3) ; ymx=av(4)    ;
  axis([0 20 -1.0 1.0])                             ;
% axis([0 100 -1.0 1.0])                            ;
  hold on                                           ;
  PlotSigRefl                                       ; % display sig and ref windows

  subplot(4,1,2)                                         ;  % Sig (rcv) and noise PSDs
  plot(fn/1e6,SignalPSD(:,mm,11), 'g-')                  ;
  hold on                                                ;
  plot(fn/1e6,NoisePSD(:,mm,11), 'r-')                   ;
% plot(fn,NormPSD(:,mm,11),'b-')                         ;
  set(gca,'FontSize',[9])                                ;
% set(gca,'YTickLabel',[])                               ;
  title('Rx and Nz PSDs')                                ;
  av=axis ; xmn=av(1) ; xmx=av(2) ; ymn=av(3) ; ymx=av(4)    ;
% axis([0 200e6 min(0,ymn) ymx])                         ;
  axis([0 500 min(0,ymn) ymx])                           ;
  hold on                                                ;

  subplot(4,1,3)                                         ;  % Signal PSD
  plot(fn/1e6,SignalPSD(:,mm,11)-NoisePSD(:,mm,11))      ;
% plot(fn,NormPSD(:,mm,11),'b-')                         ;
  set(gca,'FontSize',[9])                                ;
% set(gca,'YTickLabel',[])                               ;
  title('Signal PSD')                                    ;
  av=axis ; xmn=av(1) ; xmx=av(2) ; ymn=av(3) ; ymx=av(4)    ;
% axis([0 200e6 min(0,ymn) ymx])                         ;
  axis([0 500 min(0,ymn) ymx])                           ;
  hold on                                                ;

  subplot(4,1,4)                                         ;  % Normalized PSD
  plot(fn/1e6,NormPSD(:,mm,11))                          ;
  set(gca,'FontSize',[9])                                ;
% set(gca,'YTickLabel',[])                               ;
  title('Normalized PSD')                                ;
  av=axis ; xmn=av(1) ; xmx=av(2) ; ymn=av(3) ; ymx=av(4)    ;
% axis([0 200e6 min(0,ymn) ymx])                         ;
  axis([0 500 min(0,ymn) ymx])                           ;
  hold on                                                ;

  end                                                    ;

  disp('   ')                                            ;
  fprintf    ('   Enter seq # to display \n')            ;
  query=input('   Enter <0> to stop       : ')           ;
  delete(1:Nlines)                                       ;

end                                                      ;

%------------------------------------------------------------------------------------------
```

C3. HDPulseSim..m - Heterodyne Pulse Simulation (Optical Field Based)

```
8/26/04 3:38 PM  C:\LROS\Models\Heterodyne Pulse Simulation\HD...\HDPulseSim.m     1 of 10

%-----------------------------------------------------------------------------------------
%
%   Matlab program HDPulseSim.m
%
%   Program to simulate modelocked laser pulse in both temporal and frequency space
%
%   Created 14 Mar 03 by D.C. Senft
%
%   Modifications
%     dd mmm yy  -  xxx
%
%-----------------------------------------------------------------------------------------

clear                                           ;
pack

warning off                                     ; % use only on 5.x

% UserID = 'LAPS      '                         ;
% UserID = 'GLAPS     '                         ;
% UserID = '765SCIF_PC'                         ;
% UserID = 'Senft_NTPC'                         ;
  UserID = 'Senft_LT  '                         ;

xxx = computer                                  ;
platform = xxx(1:4)                             ;
clear xxx                                       ;

rand('state',sum(100*clock))                    ; % initialize random # generator
randn('state',sum(100*clock))                   ; % initialize Gaussian random # generator

%-------------------------------
%  Constants (physical and system)

qe_det      = 0.67              ; % detector quantum efficiency
qq          = 1.6e-19           ; % charge of electron
hh          = 6.6256e-34        ; % Planck's constant
cspeed      = 2.998e8           ; % speed of light (m/s)

wvl         = 10.591e-6         ; % wavelength (C12-O16 10P20)
Tsam        = 1e-9              ; % DAC sampling interval
BW_DAC      = 1/(2*Tsam)        ; % data collection bandwidth
LL          = 3.5               ; % cavity length (m)
delf_IF     = 13.7e6            ; % freq offset between Rx and LO (Hz, actually random)

%-------------------------------
%  Create modelocked temporal pulse

TT      = 20e-6                                 ; % time window
dt      = 0.2*1e-9                              ; % time point spacing
Nt      = TT/dt                                 ; % number of temporal points
Dt      = 1e-9                                  ; % actual system sampling interval
```

```
N_Dt    = TT/Dt                              ; % actual number of sample points

tt      = zeros(1,Nt)             ;
tt1     = zeros(1,Nt)             ;
tt_Dt   = zeros(1,N_Dt)           ;
gg      = zeros(1,Nt)             ;
aa      = zeros(1,Nt)             ;
pp      = zeros(1,Nt)             ;
G1      = 1                       ;
sig1    = 0.4e-6                  ; % width param of first Rician
G2      = 0.15                    ;
sig2    = 2.0e-6                  ; % width param of second Rician
siga    = 1.30e-9                 ; % width of Gaussian temporal modes (~3 ns FWHM)
dt_a    = 2*LL/cspeed             ; % spacing between Gaussian temporal modes
Nt_a    = dt_a/dt+1               ; % number of points in single interval

for ii=1:N_Dt                     ; % actual time samples
  tt_Dt(ii)=(ii-1)*Dt             ;
end                               ;

for ii=1:Nt                       ;
  tt(ii)=(ii-1)*dt                ;
  tt1(ii)=tt(ii)-7e-6             ; % shift to start at 7 us to match real data
  if(tt(ii)<=7e-6)                ;
    gg(ii)=0.0                    ;
  else                            ;
    gg(ii)=G1*(tt1(ii)/1e-6)*exp((-tt1(ii)*tt1(ii))/(2*sig1*sig1)) + ...
      G2*(tt1(ii)/1e-6)*exp((-tt1(ii)*tt1(ii))/(2*sig2*sig2))       ;
  end                             ;
end                               ;

for ii=1:Nt                       ; % create sequence of Gaussians
  tta=mod(tt(ii),dt_a)-dt_a/2     ;
  aa(ii)=exp((-tta*tta)/(2*siga*siga))  ;
end                               ;

pp = gg.*aa                       ; % create ml pulse train with temporal envelope
                                  ; % pp is instantaneous power, square of field uu
%----------------

figure('Position',[50 600 550 400])          ;
plot(tt/1e-6,gg)                             ;
hold on                                      ;
plot(tt/1e-6,aa,'r-')                        ;
plot(tt/1e-6,pp,'g-')                        ;
ylabel('Optical Power Components (Modelocked) (W)' )      ;
ylabel('Time (us)')                          ;
ylabel('Optical Power (W)')                  ;
av=axis ; xmn=av(1) ; xmx=av(2) ; ymn=av(3) ; ymx=av(4) ;
axis([0 TT/1e-6 ymn ymx])                            ;
hold off                                     ;
```

```
%-------------------------------
%  Compute frequency spectrum for modelocked temporal pulse

NFFTbase = ceil(log2(Nt))                         ;
NFFT = 2^NFFTbase                                 ;
Fp       = zeros(1,NFFT)                          ;
Fpp      = zeros(1,NFFT)                          ;
freq     = zeros(1,NFFT)                          ;
ppI      = zeros(1,NFFT)                          ;
ttI      = zeros(1,NFFT)                          ;

Fp       = fft(pp*dt,NFFT)                        ;
Fpp      = fftshift(Fp)                           ;
df       = 1/(NFFT*dt)                            ;
BW       = 1/(2*dt)                               ;

for jj=1:NFFT                                     ;
  freq(jj)=(jj-NFFT/2-1)*df                       ;
end                                               ;

figure('Position',[700 500 550 600])              ;
subplot(3,1,1)                                    ;
plot(freq/1e6,abs(Fpp))                           ;
title('Optical Power Frequency Spectrum |Fpp|' ) ;
xlabel('Frequency (MHz)')                         ;
ylabel('Frequency Spectrum')                      ;
subplot(3,1,2)                                    ;
plot(freq/1e6,real(Fpp))                          ;
title('Optical Power Frequency Spectrum (Real(Fpp))' )        ;
xlabel('Frequency (MHz)')                         ;
ylabel('Frequency Spectrum')                      ;
subplot(3,1,3)                                    ;
plot(freq/1e6,imag(Fpp))                          ;
title('Optical Power Frequency Spectrum (Imag(Fpp))' )        ;
xlabel('Frequency (MHz)')                         ;
ylabel('Frequency Spectrum')                      ;

ppI = ifft(Fp*NFFT*df)                            ;
for ii=1:NFFT                                     ;
  ttI(ii)=(ii-1)/(NFFT*df)                        ;
end                                               ;

figure('Position',[50 50 550 400])                ;
plot(ttI/1e-6,ppI)                                ;
hold on                                           ;
plot(tt/1e-6,pp,'g:')                             ;
title('Optical Power (IFFT) (W)')                 ;
xlabel('Time (us)')                               ;
ylabel('Optical Power (W)')                       ;
av=axis ; xmn=av(1) ; xmx=av(2) ; ymn=av(3) ; ymx=av(4) ;
axis([0 TT/1e-6 ymn ymx])                                  ;
```

```
%-------------------------------
%  Compute scale factor to normalize to received energy (integrated instantaneous power)

Epp = sum(pp)*dt                             ;

%-------------------------------
%  Create quasi-cw LO waveform

pp_LO       = zeros(size(pp))                ;
pp_LOac     = zeros(size(pp))                ;
Fp_LO       = zeros(size(Fp))                ;
Fpp_LO      = zeros(size(Fpp))               ;
ppI_LO      = zeros(size(ppI))               ;
Fp_LOac     = zeros(size(Fp))                ;
Fpp_LOac    = zeros(size(Fpp))               ;
ppI_LOac    = zeros(size(ppI))               ;

disp(' ')                                                ;
s77     = input('  Enter 1st spur scale factor [0.8e-3]: ' ) ;
s154    = input('  Enter 2nd spur scale factor [1.2e-3]: ' ) ;

phi77   = 2*pi*rand                     ; % arbitrarily chosen phase
phi154  = 2*pi*rand                     ; % arbitrarily chosen phase
% s_nz  = 1.0e-12                       ;% noise level for LO spectrum
delf_LO = 77e6                          ; % spacing between LO main mode and spurs (Hz)
% sigLO = 85e3                          ;% spectral width of LO frequency modes (Hz)

for ii=1:Nt                                  ;
  pp_LO(ii) = 1 + s77*cos(2*pi*delf_LO*tt(ii)+phi77) +  ...
    s154*cos(2*pi*(2*delf_LO)*tt(ii)+phi154)     ;
  pp_LOac(ii) =    s77*cos(2*pi*delf_LO*tt(ii)+phi77) +  ...
    s154*cos(2*pi*(2*delf_LO)*tt(ii)+phi154)     ;
end                                          ;

Fp_LO       = fft(pp_LO*dt,NFFT)             ;
Fpp_LO      = fftshift(Fp_LO)                ;
ppI_LO      = ifft(Fp_LO*NFFT*df)            ;

Fp_LOac     = fft(pp_LOac*dt,NFFT)           ;
Fpp_LOac    = fftshift(Fp_LOac)              ;
ppI_LOac    = ifft(Fp_LOac*NFFT*df)          ;

figure('Position',[700 300 550 600])         ;
subplot(3,1,1)                               ;
plot(freq/1e6,abs(Fpp_LO))                   ;
hold on                                      ;
plot(freq/1e6,abs(Fpp_LOac), 'r-')           ;
title('LO Frequency Spectrum |Fpp_LO|' )     ;
xlabel('Frequency (MHz)')                    ;
ylabel('Frequency Spectrum')                 ;
subplot(3,1,2)                               ;
plot(freq/1e6,real(Fpp_LO))                  ;
```

```
hold on                                              ;
plot(freq/1e6,real(Fpp_LOac), 'r-')                  ;
title('LO Frequency Spectrum (Real(Fpp))')           ;
xlabel('Frequency (MHz)')                            ;
ylabel('Frequency Spectrum')                         ;
subplot(3,1,3)                                       ;
plot(freq/1e6,imag(Fpp_LO))                          ;
hold on                                              ;
semilogy(freq/1e6,imag(Fpp_LOac), 'r-')              ;
title('LO Frequency Spectrum (Imag(Fpp))')           ;
xlabel('Frequency (MHz)')                            ;
ylabel('Frequency Spectrum')                         ;

figure('Position',[700 50 550 400])                  ;
plot(ttI/1e-6,ppI_LO)                                ;
hold on                                              ;
plot(tt/1e-6,pp_LO, 'y:')                            ;
plot(ttI/1e-6,ppI_LOac, 'r-')                        ;
plot(tt/1e-6,pp_LOac, 'g:')                          ;
title('LO Optical Power (IFFT) (W)')                 ;
xlabel('Time (us)')                                  ;
ylabel('LO Optical Power (W)')                       ;
av=axis ; xmn=av(1) ; xmx=av(2) ; ymn=av(3) ; ymx=av(4) ;
axis([0 TT/1e-6 ymn ymx])                                   ;

%------------------------------
%  Create Rx and LO optical field variables from optical power terms

uu_r    = sqrt(pp)                                   ;
uu_LO   = sqrt(pp_LO)                                ;

Fu_r    = fft(uu_r*dt,NFFT)                          ;
Fuu_r   = fftshift(Fu_r)                             ;

Fu_LO   = fft(uu_LO*dt,NFFT)                         ;
Fuu_LO  = fftshift(Fu_LO)                            ;

%------------------------------
%  Display field / power temporal / spectral values

disp(' ')                                            ;
disp('  ### Press return to continue ###')           ;
disp(' ')                                            ;
pause                                                ;
disp('  Displaying field / power temporal / spectral values  ')      ;
disp(' ')                                            ;

delete(1:5)

figure('Position',[ 50 600 550 400])                 ; %F1 pp and uu_r temporal display
plot(tt/1e-6,pp)                                     ;
hold on                                              ;
```

```
plot(tt/1e-6,uu_r,'r:')                          ;
title('Optical Power (W)')                       ;
xlabel('Time (us)')                              ;
ylabel('Optical Power (W)')                      ;

figure('Position',[ 50  50 550 400])        ; %F2 Fp and Fu_r spectral display (Fpp,Fuu_r)
subplot(2,1,1)                              ;
plot(freq/1e6,abs(Fpp))                     ;
hold on                                     ;
plot(freq/1e6,abs(Fuu_r),'r:')              ;
title('Frequency Spectrum (Power and Field,|Fp|,|Fu|' )      ;
xlabel('Frequency (MHz)')                        ;
ylabel('Frequency Spectrum')                     ;
subplot(2,1,2)                                   ;
plot(freq/1e6,angle(Fpp))                        ;
hold on                                          ;
plot(freq/1e6,angle(Fuu_r),'r:')                 ;
title('Frequency Spectrum Phase (Power and Field,Fp,Fu' )        ;
xlabel('Frequency (MHz)')                        ;
ylabel('Frequency Spectrum Phase')               ;

figure('Position',[700 600 550 400])             ; %F3 pp_LO and uu_LO temporal display
plot(tt/1e-6,pp_LO)                              ;
hold on                                          ;
plot(tt/1e-6,uu_LO,'r:')                         ;
title('LO Optical Power and Field (W,sqrt(W))' ) ;
xlabel('Time (us)')                              ;
ylabel('Optical Power and Field')                ;


figure('Position',[700  50 550 400])    ; %F4 Fp_LO and Fu_LO spectr disp (Fpp_LO,Fuu_LO)
subplot(2,1,1)                          ;
plot(freq/1e6,abs(Fpp_LO))              ;
hold on                                 ;
plot(freq/1e6,abs(Fuu_LO),'r:')         ;
title('LO Frequency Spectrum (Power and Field,|Fp_LO|,|Fu_LO|' )     ;
xlabel('Frequency (MHz)')                        ;
ylabel('Frequency Spectrum')                     ;
subplot(2,1,2)                                   ;
plot(freq/1e6,angle(Fpp_LO))                     ;
hold on                                          ;
plot(freq/1e6,angle(Fuu_LO),'r:')                ;
title('LO Frequency Spectrum Phase (Power and Field,Fp_LO,Fu_LO' )       ;
xlabel('Frequency (MHz)')                        ;
ylabel('Frequency Spectrum')                     ;

%-------------------------------
%  Check that spectrum of received optical power is convolution of Rx opt field spectrum

icnvflg = 0                                              ; % execute flag
if(icnvflg==1)                                           ;
  disp('  ### Rx convolution check routine ### ')        ;
```

```
  disp('  ### Press return to begin ###')                ;
  disp(' ')                                               ;
  pause                                                   ;
  disp('  Rx convolution check routine started')         ;
  disp(' ')                                               ;
  [aa Nsize] = size(Fuu_r)                                ;
  Nuse = 75000                                            ; % size of convolution
  xFu = Fuu_r(1,(Nsize/2-Nuse/2+1):(Nsize/2+Nuse/2))     ;
  xFp = Fpp(1,(Nsize/2-Nuse/2+1):(Nsize/2+Nuse/2))       ;
  xFc = conv(xFu,xFu)*df                                  ;
  xFc = xFc(1,Nuse/2+1:Nuse+Nuse/2)                       ;
  figure('Position',[800 400 550 400])                    ; % overlay power and conv spectra
  plot(abs(xFp))                                          ;
  hold on                                                 ;
  plot(abs(xFc),'r:')                                     ;
end                                                       ;

%------------------------------
%  Check that spectrum of LO optical power is convolution of LO optical field spectrum

icnvflg = 0                                               ; % execute flag
if(icnvflg==1)                                            ;
  disp('  ### LO convolution check routine ### ')        ;
  disp('  ### Press return to begin ###')                ;
  disp(' ')                                               ;
  pause                                                   ;
  disp('  LO convolution check routine started')         ;
  disp(' ')                                               ;
  [aa Nsize] = size(Fuu_LO)                               ;
  Nuse = 75000                                            ; % size of convolution
  xFu = Fuu_LO(1,(Nsize/2-Nuse/2+1):(Nsize/2+Nuse/2))    ;
  xFp = Fpp_LO(1,(Nsize/2-Nuse/2+1):(Nsize/2+Nuse/2))    ;
  xFc = conv(xFu,xFu)*df                                  ;
  xFc = xFc(1,Nuse/2+1:Nuse+Nuse/2)                       ;
  figure('Position',[800 400 550 400])                    ; % overlay power and conv spectra
  plot(abs(xFp))                                          ;
  hold on                                                 ;
  plot(abs(xFc),'r:')                                     ;
end                                                       ;

%------------------------------
%  Clear unneeded variables

clear aa gg ppI ppI_LO ppI_LOac Fpp Fpp_LO Fpp_LOac uu_r uu_LO Fu_r Fuu_r Fu_LO Fuu_LO  ;

%------------------------------
%  Calculate optical power signal on heterodyne detector

disp('  ### Calculation of optical power signal on heterodyne detector ### ')      ;
disp('  ### Press return to begin ###')                  ;
disp(' ')                                                 ;
pause                                                     ;
```

```
disp('  Calculation started')                          ;
delete(1:4)                                            ;

%--- Receive optical power scaling

disp(' ')                                              ;
Eppin = input('  Enter receive optical power on detector (pJ) [2.0]: ' ) ;
disp(' ')                                              ;
Eppin = Eppin*1e-12                                    ; % convert from pJ to J

pp = pp*(Eppin/Epp)                                    ; % scale received optical power

%--- LO optical power scaling


P_LOin = input('  Enter LO optical power on detector (mW) [0.125]: ' )    ;
disp(' ')                                              ;
P_LOin = P_LOin*1e-3                                   ; % convert from mW to W

pp_LO   = P_LOin*pp_LO                                 ; % scale LO power
pp_LOac = P_LOin*pp_LOac                               ; % scale AC-coupled LO power

%--- Calculate LO shot noise optical power
%-   Calculate for full temporal series, then scale and bandlimit to match DAC BW

sig_sn  = sqrt((2*(hh*cspeed/wvl)*BW_DAC/qe_det)*mean(pp_LO))          ;
pp_sn   = sig_sn*randn(size(pp_LO))                    ;

Fp_sn   = fft(pp_sn*dt,NFFT)                           ;
Fpp_sn  = fftshift(Fp_sn)                              ;

N_BWDAC = round(BW_DAC/df)                             ;
stp_fcn = zeros(1,NFFT)                                ;
stp_fcn(1,1:N_BWDAC) = 1                               ;
stp_fcn(1,NFFT-N_BWDAC+1:NFFT) = 1                     ;

Fp_sn   = Fp_sn.*stp_fcn*sqrt(BW/BW_DAC)               ; % scale to maintain noise power
Fpp_sn  = fftshift(Fp_sn)                              ;

ppI_sn  = ifft(Fp_sn*NFFT*df,NFFT)                     ;

[AA BB] = size(pp_sn)                                  ;
pp_sn   = ppI_sn(1,1:BB)                               ;

%--- Calculate heterodyne optical power on detector
%-   Perform AC-coupling now to avoid errors from sinc distortion in numerical calc

pp_hd   = pp + pp_LOac + 2*cos(2*pi*(delf_IF*tt)).*sqrt(pp.*pp_LO) + real(pp_sn)    ;

Fp_hd   = fft(pp_hd*dt,NFFT)                               ;
Fpp_hd  = fftshift(Fp_hd)                                  ;
```

```
%----------

figure('Position',[100 700 550 400])                  ; %Fig pp_hd temporal plot
plot(tt/1e-6,pp_hd)                                   ;
title('HD Optical Power (W)')                         ;
xlabel('Time (us)')                                   ;
ylabel('Optical Power (W)')                           ;
% av=axis ; xmn=av(1) ; xmx=av(2) ; ymn=av(3) ; ymx=av(4)   ;
% axis([xmn xmx 0 ymx])                               ;

figure('Position',[100 100 550 500])                  ; %Fig pp_hd spectrum
subplot(2,1,1)                                        ;
plot(freq/1e6,abs(Fpp_hd))                            ;
title('Frequency Spectrum (HD Optical Power)')        ;
xlabel('Frequency (MHz)')                             ;
ylabel('Frequency Spectrum')                          ;
subplot(2,1,2)                                        ;
plot(freq/1e6,angle(Fpp_hd))                          ;
title('Frequency Spectrum Phase (HD Optical Power)')  ;
xlabel('Frequency (MHz)')                             ;
ylabel('Frequency Spectrum Phase')                    ;

%------------------------------
%  Calculate current (AC-coupled) out of detector (incl bias curr and b.c. shot noise)

I_hd    = (qe_det*qq)/(hh*cspeed/wvl)*pp_hd           ; % includes LO shot noise

%--- Compute bias current and bias current shot noise

disp(' ')                                             ;
I_bias  = input('  Enter bias current (mA) [0.100]: ') ;
disp(' ')                                             ;
I_bias  = I_bias*1e-3                                 ; % convert from mA to A

sig_Ib  = sqrt(2*qq*BW_DAC*I_bias)                    ; % st dev of bias curr shot noise

i_bias  = sig_Ib*randn(size(pp_hd))                   ; % bias current shot noise

Fi_b    = fft(i_bias*dt,NFFT)                         ;
Fii_b   = fftshift(Fi_b)                              ;

Fi_b    = Fi_b.*stp_fcn*sqrt(BW/BW_DAC)               ; % scale to maintain noise power
Fii_b   = fftshift(Fi_b)                              ;

iiZ_b   = ifft(Fi_b*NFFT*df,NFFT)                     ;

[AA BB] = size(i_bias)                                ;
i_bias  = iiZ_b(1,1:BB)                               ;
i_bias  = real(i_bias)                                ; % force i_bias to be real

%--- Compute total AC-coupled current out of detector
```

```
I_det   = I_hd + i_bias                              ;

%-------------------------------
%  Calculate voltage at input to A/D and reduce data to actual system sampling interval
%  Detector -> X74 amp -> 2 MHz high pass -> X22 amp -> 50-ohm A/D

V_AD0   = I_det * 74 * 1.0 * 22 * 50                 ;

V_AD    = interp1(tt,V_AD0,tt_Dt)                    ;

NFFTbaseV   = ceil(log2(N_Dt))                       ;
NFFTV       = 2^NFFTbaseV                            ;
dfV         = 1/(NFFTV*Dt)                           ;

for jj=1:NFFTV                                       ;
  freqV(jj)=(jj-NFFTV/2-1)*dfV                       ;
end                                                  ;

FV_AD   = fft(V_AD*Dt,NFFTV)                         ;
FVV_AD  = fftshift(FV_AD)                            ;

%-----------

figure('Position',[700 700 550 400])                 ; %Fig V_AD temporal plot
plot(tt_Dt/1e-6,V_AD)                                ;
title('Signal at A/D (V)')                           ;
xlabel('Time (us)')                                  ;
ylabel('Signal at A/D (V)')                          ;
% av=axis ; xmn=av(1) ; xmx=av(2) ; ymn=av(3) ; ymx=av(4)    ;
% axis([xmn xmx 0 ymx])                              ;

figure('Position',[700 100 550 500])                 ; %Fig V_AD spectrum
subplot(2,1,1)                                       ;
plot(freqV/1e6,abs(FVV_AD))                          ;
title('Frequency Spectrum (A/D Voltage)')            ;
xlabel('Frequency (MHz)')                            ;
ylabel('Frequency Spectrum')                         ;
subplot(2,1,2)                                       ;
plot(freqV/1e6,angle(FVV_AD))                        ;
title('Frequency Spectrum Phase (A/D Voltage)')      ;
xlabel('Frequency (MHz)')                            ;
ylabel('Frequency Spectrum Phase')                   ;

%-------------------------------
%  Save data as file that can be read into DATREDUC_HD programs (real data analysis)

savdat = V_AD'                                       ;

save HDPS.txt -ascii savdat                          ;

%------------------------------------------------------------------------------------------
```

DISTRIBUTION LIST

DTIC/OCP 8725 John J. Kingman Rd, Suite 0944 Ft Belvoir, VA 22060-6218	1 cy
AFRL/VSIL Kirtland AFB, NM 87117-5776	2 cys
AFRL/VSIH Kirtland AFB, NM 87117-5776	1 cy
Official Record Copy AFRL/DESA/Dan Senft	2 cys
US Army SBCCOM Passive Standoff Detection Team William Loerop AMSSB-RRT-DP Aberdeen Proving Grounds, MD 21010-5424	1 cy